FUNDAMENTALS AND APPLICATIONS OF MACROMOLECULAR TRANSPORT IN HYDROGEL CONTACT LENSES

By

LOKENDRAKUMAR CHAINROOP BENGANI

A DISSERTATION PRESENTED TO THE GRADUATE SCHOOL
OF THE UNIVERSITY OF FLORIDA IN PARTIAL FULFILLMENT
OF THE REQUIREMENTS FOR THE DEGREE OF
DOCTOR OF PHILOSOPHY

UNIVERSITY OF FLORIDA

2013

To my Ma and Papa

ACKNOWLEDGMENTS

Through my life, I have had the good fortune to have excellent guides and friends. This work would never have happened without their presence in my life and I am humbled by their support. I owe a lot to each one and express my earnest gratitude.

First and foremost, I would like to thank my advisor Dr. Anuj Chauhan. He has been an amazing and supportive guide and a good friend. He has taught me how to be a good researcher and he has motivated me to do better each time. This work would not have been possible without his guidance and incessant support. His knowledge, reasoning and analysis have astonished me countless times. He knows the working style of each of his student very well, and allows them the freedom to explore, fail, learn and explore more.

I would like to thank Dr. Sergey Vasenkov, Dr Peng Jiang and Dr. Christopher Batich for their insightfulness and for being able to be part of my doctoral review process. I sincerely thank Dr. Sypros Svoronos for allowing me to his teaching assistant twice and allowing me to work for him for one semester. He is an amazing teacher and he showed me how to be a great teacher. And I express my deepest gratitude to every teacher I have ever had for it is because of them I am where I am and I know what I know. They have been an inspiration to me and I hope one day I can follow in their footsteps.

It has been a pleasure to be in this lab and I have had the good fortune of sharing it with some wonderful members. I begin by thanking Dr. Brett Howell. He is the epitome of an ideal PhD student, an excellent researcher and his passion and discipline set levels almost impossible for others to achieve. I thank Dr. Chhavi Gupta for being a good friend and guiding me through some rough patches. I thank Dr. Cheng Chung

Peng for teaching me proper techniques of research. He is a dedicated researcher and did some remarkable research. I thank Dr. Hyun Jung Jung whose simple presence in lab made the work more fun and created a relaxed atmosphere. She guided me during times when I was down. I have leant a lot from her and her experimental techniques are as close to perfect as they can be. I am thankful for those I mentioned above for being excellent seniors, setting unparalleled benchmarks in research and creating the most wonderful atmosphere in the lab. I thank my current group members Rob Damitz, Samuel Gause, Kuan-Hui Hsu (Vincent) and the latest addition Kristin Conrad. They are quick learners and I have had a great time in lab with them. I hope I have not let down the benchmarks my seniors left.

I would also like to thank the undergrad student I had the good fortune to work with, Jenna Leclerc. She was exceptional with her work and did a lot of the experiments in the Lysozyme Transport section.

Many current and former staff members at the Dept. of Chemical Engineering made my life so much easy. I am thankful for the support by Dennis Vince and James Hinnant who always came through and for Urvashi Shah and Sean Pool for their IT support. I also thank Debbie Sandoval, Carolyn Miller, Shirley Kelly, Sara Wilson and Melissa Fox for their assistance all these years.

I am truly grateful for so many wonderful friends I have had in my time I spent in Gainesville. Our friendships grew such that they became my family. I will cherish my time with them and these memories are my most treasured ones. I thank Nandita for being my best friend, my philosopher and guide. I thank Yi Su for being in my life at the

right time. She has been a source of strength in the last few months and pushed me to do my best.

And at last and most important, I thank all of my family back home. I thank Deepak Bengani for all the support and the fun growing up and for being the most awesome elder brother one can have. I always wanted to copy what he did. I am indebted to my father Chainroop Bengani. He is my source of inspiration and my hero. His values of honesty and hard work are the foundations of my values system and he taught me the important lesson of never giving up. I am thankful for his unwavering support of my every decision. And I am the most indebted to my mom Kusum Bengani for all the hard work and dedication and love and care and sacrifices she made for me. I can never ever repay her and I only hope I have made her proud.

TABLE OF CONTENTS

page

LIST OF TABLES

LIST OF FIGURES

LIST OF ABBREVIATIONS

BAC	Benzalkonium Chloride
CAC	Cetalkonium Chloride
CMC	Critical Micelle Concentration
CYA	Cyclosporine A
DXP	Dexamethasone-21-Phosphate disodium
DI WATER	Deionized water
EAC	Equilibrium Aqueous Content
EWC	Equilibrium Water Content
EGDMA	Ethylene Glycol Dimethacrylate
HEMA	Hydroxyethyl Methacrylate
H30	Hitenol BC-30
N10	Noigen RN-10
N30	Noigen RN-30
ODD	Ocular Drug Delivery
PBS	Phosphate Buffered Saline
PLTF	Pre Lens Tear Film
POLTF	Post Lens Tear Film
P-HEMA	Poly-Hydroxyethyl Methacrylate
PVA	Poly Vinyl Alcohol
PVP	Poly Vinyl Porrolidone
PZSURF	Polymerizable Surfactant

Abstract of Dissertation Presented to the Graduate School
of the University of Florida in Partial Fulfillment of the
Requirements for the Degree of Doctor of Philosophy

FUNDAMENTALS AND APPLICATIONS OF MACROMOLECULAR TRANSPORT IN HYDROGEL CONTACT LENSES

By

Lokendrakumar Chainroop Bengani

August 2013

Chair: Anuj Chauhan
Major: Chemical Engineering.

In their working environment, contact lenses need to interact with various molecules like water, ions and tear film components like proteins. Additionally, drug eluding contact lenses can be very effective ophthalmic drug delivery vehicles but are incapable of releasing drugs for more than a few hours. In this study we propose to modify the properties of the contact lens material by addition of surfactant to aid in extended drug delivery and make the lens wear more comfortable. The aim is to characterize the effects of addition of surfactant on various properties of the hydrogel, evaluate and model drug release in presence of surfactants and explore additionally uses of surfactants.

The interaction of two cationic surfactants: benzalkonium chloride (BAC) and cetalkonium chloride (CAC) with poly-hydroxyethyl methacrylate (p-HEMA) hydrogels has been explored. Addition of CAC to p-HEMA gels creates a charged polymer surface which is able to attenuate the release of an anionc drug dexamethansone-21-phosphate disodium (DXP). The partition coefficient of the drug increases exponentially with surfactant loading in the gel in at least qualitative agreement with the Debye-Hückel

theory. The focus is also on modeling drug transport which is found to be diffusion controlled. The addition of surfactant does not impact transparency of lenses, and has additional benefits of increase in wettability and significant reduction in protein absorption. The surfactant loaded contact lenses provide additional benefits like improved wettability, and reduction in protein binding.

To explore the impact of addition of surfactant, we focus on creating highly wettable lenses by adding polymerizable surfactants (pzsurfs) to the monomer mixture. Excellent surface characteristics have been obtained by addition of pzsurfs while retaining the other important physical properties of a contact lens. Such lenses would potentially ensure a longer pre-lens tear break up time and a consistent pre-lens tear film leading to a more comfortable wear.

Protein binding to hydrogel plays an important role in determining the suitability of such materials in several biomedical applications. Thus tear protein lysozyme uptake and release from p-HEMA gels of various thicknesses has been explored to understand, quantify, and model the transport of lysozyme in the hydrogel.

CHAPTER 1
INTRODUCTION

Hydrogels find extensive utility as biomaterials, with special application in drug delivery [1,2]. An important use of such a hydrogel biomaterial is in the form of a contact lens. Contact lens material is unique as it needs to satisfy several properties like wettability, surface friction (lubricity), modulus, drying or hydration, transparency, ion and oxygen transport and protein and lipid deposition. Each property poses restrictions on the lens composition and structure. A lens material has to have sufficient modulus (crosslinking) to maintain its structural integrity but it should be small enough to allow for a bending motion during blinking. The pore size of the lens material should be less than 100 nm to ensure transparency. Also, when a contact lens is placed in its working environment, it interacts with several biomolecules like proteins. They can adsorb onto or absorb in the hydrogel depending pore size and protein-hydrogel interaction. Thus, it is important to understand how different molecules transport (water, ions, oxygen, protein, lens cleaning agents etc), understand the essential properties of a good contact lens and use this knowledge to develop a material that comes close to fulfilling these requirements. An important application of this knowledge is for ocular drug delivery.

At first glimpse, drug delivery to eye would seem like a problem with a straightforward solution due to the direct accessibility of eyes. However, since the eyes are exposed to the environment, it faces the likelihood of entrance of several unavoidable and potentially detrimental objects or molecules thus creating a need for a multi-fold defense mechanism. Blinking, rapid tear turnover, biochemical action of tear components, a relatively impermeable epithelium of the cornea etc. are among the mechanisms of eye protection which also complicate ocular drug delivery. Although

posterior or intraocular and systemic routes of drug delivery to the eye are used from time to time, they have inherent limitations. Intraocular delivery is usually performed by intravitreal injections which are highly inconvenient while systemic route is limited by blood – retinal barrier and toxicity issues. Hence, direct drug delivery to the anterior segment of the eye resulting in the drug diffusing through the cornea seems most convenient and efficient.

Currently, most of the ocular drug delivery (ODD) formulations are in the form of eye drops, suspensions or ointments and eye drops form more than 90% of commercial ocular compositions [3] even though it is well understood that only a very small fraction of drug delivered through eye drops reaches the target tissue [4]. There are several factors that contribute to the inefficiencies of eye drops. Human tear volume is about 7 µl of fluid [5] and even though it can hold a larger amount after an eye drop instillation, a fraction of the instilled 30 µl eye drop is quickly squeezed out of the eye [4]. The remaining drug mixes within the entire tear volume and then exits through canicular drainage into the nose or transports across the corneal and the conjuctival epithelia. The area of the conjunctiva is about 16-18 times the area of the cornea, and the conjunctiva permeability is also higher than the corneal permeability, and thus the net drug flux into cornea is much lower than that into the conjunctiva [6,7]. A very large fraction of the drug absorbed into the conjunctiva and that drained into the nose enter systemic circulation, leading to the very low corneal bioavailability of less than 5% [4]. The fraction of the delivered drug that enters the systemic circulation escapes the first pass metabolism and enters all major organs, with a potential for side effects [8,9]. The problem of low bioavailability is exacerbated by the short tear film residence time of only

about 2-3 min, leading to a necessity of a frequent dosing regimen [4]. In certain cases, hourly instillations of eye drops are required such for delivery of dexamethasone -21-phosphate disodium (DXP) for anti-inflammatory therapy [10] and delivery of cysteamine for the treatment of corneal crystal formation in nephropathic cystinosis [11]. The high instillation frequency leads to reduced patient compliance, which is also impacted by the difficulties in precisely delivering the eye drop, particularly in elderly patients. The compliance to the eye drop regimen is further affected when multiple medications are recommended, which is common in about 50% of glaucoma patients [12,13] Finally, the stability of eye drop formulations is sometimes limited. For example, the recently released cysteamine eye drop formulation (Cystaran^{TM}) is required to be kept frozen at temperatures < -15^{o}C and after thawing it has a maximum shelf life of a week, even under refrigerated conditions.

The deficiencies of the eye drops has led to considerable research focusing on developing improved ODD formulations like high-viscosity formulations, polymeric gels, mucoadhesive and in-situ forming gels, bioadhesive polymers, biodegradable or non-degradable inserts, punctal plugs, etc [4,14-17]. Also new approaches focusing on driving the drug into the cornea have been explored such as iontophoresis and microneedles [18,19]. Still, eye drops have been the main stay of ocular therapies because most other approaches for ODD also suffered from at least some of the deficiencies of eye drops. It is however clear that eye drops are far from optimal for delivering ophthalmic drugs and a better approach is required for increasing bioavailability, improving patient compliance and reducing the potential for side effects.

The optimal ODD system needs to overcome the deficiencies of eye drops while maintaining all the key requirements regarding physical properties, pharmacokinetics and pharmacodynamics. An ODD system must be highly biocompatible, easy to administer, comfortable, and should not have any adverse effect on vision or normal eye functions like blinking. Also the device should preferably provide extended drug release at therapeutic rates, with increased corneal bioavailability. It is also critical that the drug pharmacokinetics is maintained at least comparable to the eye drop regimen. There are additional factors to consider including costs and the regulatory approval process. For an ODD device to significantly improve the corneal bioavailability, it must be preferentially located closer to the cornea, compared to the conjunctiva, making a contact lens the obvious choice. It is thus natural to explore contact lenses for delivering ocular drugs and several studies focusing on this goal were attempted as early as several decades ago [20,21]. While several studies proved the feasibility of the concept, drug eluding contact lenses never reached the market place mainly because the earliest attempts were conducted with lenses that were not ideally suited for drug delivery.

Contact lenses also fulfill several of the other requirements for ODD such as biocompatibility, ease of insertion, transparency, with minimal effect of ocular functions; at least for the population that wear contact lenses for vision correction. The remaining key requirements are related to the pharmacokinetics and the pharmacodynamics, which are in turn are closely related to the drug transport in the contact lens. It is obvious that the contact lens needs to have a sufficient drug payload to achieve the therapeutic response. The optimal choice of the total drug release duration from the contact lens is however far from clear, and would at least partially depend on the most

common contact lens modality in terms of the wear schedule. Clearly a very short duration of the order of an hour or less is undesirable as that could necessitate multiple contact lenses each day, which would increase cost and reduce patient compliance.

Currently based on the wear schedule, contact lenses can be classified into disposable or frequent replacement. Among the disposable lenses, the daily disposable type are worn just for a day, while the other type are extended wear lenses which can be worn continually for long periods of 1, 2 or 4 weeks depending on the specific lens type, without even taking the lenses off at night. The frequent replacement lenses can last for several weeks but these are worn during the day, taken off and cleaned during the night, and replaced in the eyes in the morning. Since there are several different wearing options, it would be prudent to develop different types of drug eluding contact lenses suited for the various wearing patterns. Thus there appears to be a need to develop contact lenses with controllable release durations ranging from a day to possibly 1-4 weeks. Since the release duration is a key characteristic for the drug eluding contact lenses, researchers have measured the in vitro release profiles from contact lenses for a wide variety of drugs.

Most of the early studies focused on soaking the commercial contact lenses in a drug solution, followed by lens *in vitro* release or insertion in the eye. This method has received the maximum attention from researchers likely due the simplicity of the approach. In addition to the large number of in vitro studies, several animal and human studies have been conducted with the 'soak and release' approach to explore delivery of various molecules to eyes including fluorescein in rabbits [22], pilocarpine in humans [23], dexamethasone phosphate in humans (89 subjects) [24], chloromycetin,

gentamicin, or carbenicillin in humans (466 subjects) [25], gentamicin, kanamycin, tobramycin, ciprofloxacin and floxacin in humans (265 patients) [26], and lomefloxacin in rabbits [27]. The *in vivo* studies clearly proved the feasibility of the concept of using drug eluding contact lenses, while also showing improved efficacy compared to eye drops. The superior performance of a contact lens compared to eye drops suggests an increase in bioavailability due to an increase in the residence time of the drug in the tears. The increase in bioavailability increases the drug concentration in cornea and aqueous humor, which can act as drug reservoirs potentially extending the duration of effect compared to eye drops [28-30]. In spite of the proven benefits of contact lenses, the early studies have not resulted in a commercial product even after five decades. This most likely can be attributed to the short duration of release from the unmodified commercial contact lenses. While the exact release duration depends on both the drug and the lens properties, the release durations are usually only a few minutes to a few hours for all ophthalmic drugs in the size range of 300 to 500 Dalton where majority of the drug is released in an initial burst [31-36]. A contact lens with release duration of 1-2 hours is superior to the eye drops due to increased residence time and biovailability, but the benefits were perhaps not considered sufficient by pharmaceutical companies to invest the large resources necessary to commercialize a new drug delivery device.

The last decade has seen growing interest in developing contact lenses that can provide extended release of ophthalmic drugs. Approaches explored include incorporation of surfactant aggregates [37,38], nanoparticles or nanobarriers [39-41], biomimetic imprinting [42-47], development of new materials [48], Vitamin E barriers

[49-52] etc. There is also a recently concluded Phase III study on release of ketotifen fumarate from contact lenses to develop anti-allergy contact lenses [53].

Addition of additives like surfactants to enhance drug loading and drug release durations by hydrogels is common [54]. There is considerable literature on including surfactants in gels as they can alter solute binding and transport properties [55-59], structure and swelling behavior [60,61] and provide additional benefits such as antibacterial protection [62,63]. However, most of studies mentioned above are focused on gels with less than 10% polymer content and thus with larger pore sizes compared to those in contact lenses. Some recent studies [64,65] focused on incorporation of non-ionic Brij surfactants in p-HEMA contact lenses for extended delivery of hydrophobic drugs such as cyclosporine A(CyA). Brij surfactants form aggregates into which the drug partitions thus resulting in an extended release. Thus it is reasonable to assume that ionic interactions may be the key to increase the release durations of hydrophilic ionic drugs. Researchers have attempted this by incorporation of ionic monomers in the polymer to create charged polymer chains having the potential to increase drug loading and extending drug release of oppositely charged drugs [66-69].

However, addition of ionic molecules prior to polymerization could impact the structure and properties of the lenses. To overcome this limitation, it is proposed to first adsorb a layer of ionic surfactants on the lens matrix, followed by adsorbing the drug on the charged head group of the surfactant. This approach requires a careful choice of the ionic surfactant to optimize the hydrophobic interaction of the tail with the polymer and also the electrostatic interaction of the head with the drug. Essentially, the length of the tail section of the surfactant needs to be sufficiently long to maximize the hydrophobic

interactions, for strong adsorption on the gel matrix with a high packing. If both of these interactions (polymer-surfactant tail and drug-polymer-head) are optimized, it should be possible to design a system that does not release the surfactant into the tear film and also very slowly releases the chosen drug.

One choice for an ionic surfactant is the cationic surfactant with 16 unit tail-cetalkonium chloride (CAC). Benzalkonium chloride (BAC), a commonly used cationic surfactant present in a number of eye care products is a mixture of alkylbenzyldimenthylammonium chlorides with alkyl group primarily being dodecyl and tetradecyl. The surfactant CAC belongs to this family of alkylbenzyldimenthylammonium chlorides with an alkyl group of hexadecyl. Since CAC loaded gels are cationic, these are suitable for extended release of anionic drugs such as DXP. DXP is a corticosteroid which is similar to the natural steroid hormone made by the adrenal glands in the body. Steroids inhibit inflammatory response to provocative agents of mechanical, chemical, or immunological nature. This medication is used to treat various conditions such as severe allergic reactions, arthritis, blood diseases, breathing problems, certain cancers, eye diseases, intestinal disorders, and skin diseases. The drug DXP is used to treat various eye diseases, including persistent macular oedema in retina, which is a major cause of visual disabilities and blindness among individuals with diabetes [70]. As mentioned earlier, the hourly instillation protocol can be uncomfortable for the patient. A system consisting of a daily disposable contact lens with DXP loaded can prove to be very useful in such a case. It will not only eliminate the need for multiple instillations in a day thereby improving patient compliance but also reduce systemic intake. Various groups attempted to delivery DXP from commercial contact lenses by loading DXP

through soaking in drug solutions and examining the release [32,36]. The results showed that DXP release durations were too short to be of any clinical use. Previous transport studies of DXP in p-HEMA gels have revealed very low loading capacities due to its hydrophilic and anionic nature [71].

Accordingly drug transport in surfactant loaded p-HEMA gels, including a p-HEMA based commercial lens has been explored. Additionally the focus has been on understanding and modeling the transport of the drug through the p-HEMA gels. While the main focus is on ophthalmic applications, the results of this study contribute to fundamental understanding of transport of ionic drugs in gels loaded with ionic surfactant, which could find applications in several areas of biomaterials.

The above system is aimed at contact lens wearers. The elderly population represents a large segment of the users of ophthalmic drugs but they may not be suitable for drug therapy by contact lenses because of reduced tear volume and dryness, which can make contact lens use uncomfortable. Other reasons for contact lens wear discomfort include protein deposits and low surface wettability. Thus in order to create a complete ODD system, we need to overcome these challenges.

Almost 50% of the 35 million contact lens wearers in the North America experience some dryness and discomfort, particularly towards the end of the day [72]. Discomfort is in fact the leading cause of contact lens dropouts [73,74]. While the exact mechanisms that cause the dryness and discomfort are complex and not even completely understood, it is known that certain properties of the lenses impact both dryness and discomfort. For instance contact lenses with poor wettability and high water content are considered to have an increased potential for causing dryness [75-77]. The

detrimental effect of the poor wettability can be attributed to the rapid breakup of the tear film on the lens surface leading to increased evaporation. A good wettable lens surface will ensure a stable pre-lens rear film (PLTF) which is necessary to achieve good vision [78] and additionally a stable PLTF will provide a lubricating effect to ease the sliding between the eyelid and lens. Additionally, a continuous tear film between the posterior surface of lens and cornea is a necessary criterion for biocompatibility which would be fulfilled more easily with a wettable lens [79]. The correlation of the dryness symptoms with high water content is surprising but can be rationalized by noting that the higher water content lenses tend to dehydrate more. Researchers have shown that high water content lenses can be comfortable if they are designed to have minimal dehydration thus supporting the hypothesis that the net hydration loss with wear is related to comfort [80-82]. The contact lens discomfort is potentially caused by the interaction of the ocular epithelia with the lens and thus surface lubricity is also expected to also be an important parameter for comfort. The lubricity is typically characterized by measuring the coefficient of friction between the lens and another surface. While some researchers have tried to measure friction between lenses and epithelia mimics, most studies use some reference materials such as glass based on the hypothesis that low friction between the lens and the reference material is evidence of low in vivo friction. Since lubricity and wettability are believed to be two of the main factors impacting dryness and discomfort, significant efforts have been made to improve both of these properties.

Efforts to improve wettability have focused on incorporation of highly hydrophilic monomers, plasma surface treatments, and addition of internal wetting agents such as

poly vinyl alcohol (PVA) or poly vinyl pyrrolidone (PVP) [83]. Extended release of PVA incorporated in Focus DAILIES® (CIBA Vision) into the tears improves comfort [84,85] Incorporation of PVP in Acuvue® Oasys™ with Hydraclear™ Plus lenses (Johnson and Johnson) increases wettability eliminating the need for surface treatment typically required in silicone hydrogel contact lenses. Contrary to the PVA incorporation, the PVP loaded in lenses remains trapped due to the high molecular weight but it is believed to partially diffuse to the surface to increase the wettability [86]. For achieving improvements in comfort, lens modifications have been complemented with efforts for designing better formulations of rewetting drops and lens care solutions to improve the comfort. Both PVA and PVP have been used in artificial tears and rewetting drops for contact lenses [72]. Also addition of surfactants in rewetting drops and lens care solutions has been found to be beneficial most likely due to improved wettability of the surface due to surfactant adsorption [87,88]. The adsorbed and absorbed surfactant however desorbs with time, possibly leading to the reduced end of day comfort [89]. Also, the preservatives included in the formulations can absorb into the lenses and then desorb during lens wear which could lead to patient discomfort and potential toxicity issues [90-93]. Furthermore the desorption of the surfactants into the eye could also cause toxicity. Here we propose a novel idea of covalently attaching surfactants to the lens matrix to increase wettability and lubricity while eliminating the desorption and release into the eye. The covalent attachment is achieved by adding polymerizable surfactants with an ethylenically unsaturated bond to the monomer mixture, followed by UV based lens curing. Polymerized surfactants have been incorporated into materials to modify surface properties but to our knowledge this approach has not been used in

contact lenses [94-96]. The surfactant loaded lenses are characterized by measuring the wettability and lubricity. Additionally some other key lens properties such as modulus, transparency, water content and ion permeability are measured to ensure that surfactant incorporation does not negatively impact any of the bulk properties. Here we focus only on the p-HEMA lenses though the proposed methods could be adapted to silicone hydrogel lenses as well.

Understanding the mechanism of protein transport into/onto hydrogels is important for several reasons, specifically for biomedical applications such as contact lenses. Numerous studies have shown that that protein transport in hydrogels is a function of several properties including water content, surface charge, protein size and charge, and surface roughness [97-102]. Protein deposits on contact lenses originate from tear proteins, and these deposits can cause a number of problems including discomfort, reduced visual acuity, dryness, and reduced lens' life. Additionally, protein deposits may facilitate bacterial adhesion and subsequent infections of the eye, as well as inflammation and adverse immunological response [97-101,103]. Lysozyme is the most abundant protein in tear fluid [103] with normal levels ranging from 0.6 to 2.6 mg/ml [103] thereby comprising about 20-40% of tear proteins. For this reason, as well as the recognized predominance of lysozyme in the adsorbed layer on p-HEMA based hydrogels [99,101], lysozyme is often used as the model protein for in vitro research focusing on protein interactions with contact lenses. Lysozyme is a small (14.7 kDa) [100], compact globular protein with a slightly ellipsoidal shape (45 x 30 x 30 Å) [101] and thus it will likely diffuse into hydrogels with larger pore sizes. Also lysozyme carries

a large net positive charge at physiological pH (isoelectric point = 10.7) [101], and so the electrostatic interactions with contact lenses also likely impact binding and transport.

Several researchers have focused on measuring protein binding to a variety of hydrogels that are common contact lens materials. Soft hydrogel contact lenses have been classified by the FDA into four groups (I-IV) depending on their charge and water content [104]. Group I lenses are non-ionic with low water content, group II lenses are non-ionic with high water content, group III lenses are ionic with low water content and group IV lenses are ionic with high water content. It is widely accepted that group IV Etafilcon lenses, i.e., p-HEMA with copolymer methacrylic acid (MA), deposit substantially more lysozyme than all other hydrogel lens materials [97,98,100-102,105,106]. Higher water content and electrostatic interactions between lysozyme and the negatively charged MA likely drive the large uptake of lysozyme by the Group IV lenses. The group I and II lenses also exhibit significant protein deposition but less compared to Group IV [97], and there is only a limited data on protein uptake by Group III lenses.

The uptake of proteins by contact lenses is likely due to a combination of surface adsorption and absorption followed by adsorption on the polymer chains in the bulk of the lens. Sassi et al. showed that that the mechanism of lysozyme sorption by p-HEMA copolymer hydrogels (HEMA + acrylic acid) was through a combination of surface adsorption and adsorption onto the polymer strands in the hydrogel matrix [99]. Also Okada et al. provided visual evidence for lysozyme binding on the surface, and also in the matrix of group IV contact lenses [103]. However, there are other conflicting reports that show a lack of penetration by lysozyme into some types of contact lenses. For

example, Okada et al. also analyzed lenses belonging to groups I-III, and found no evidence supporting lysozyme binding within the matrix of these lenses. Garrett et al. found that lysozyme penetrates into Etafilcon A and Vifilcon A lenses, whereas almost no penetration of lysozyme occurs in Tefilcon lenses (p-HEMA hydrogels cross-linked and copolymerized with EGDMA) [102]. The lack of protein absorption in certain lenses such as the Group I p-HEMA lenses can likely be attributed to a high degree of crosslinking in the lenses. While increased crosslinking could reduce the detrimental protein binding, it could lead to other undesirable changes in the lens' properties including increased modulus, reduced water content, reduced oxygen permeability, etc. It is thus important to obtain a quantitative understanding of lysozyme uptake in contact lens materials including the effect of degree of crosslinking on transport. Such information will help the lens designers in choosing the optimal crosslinking to impede protein binding with minimal impact on other properties. Also detailed understanding of protein transport will be helpful in designing the cleaning protocols without extensive experimental testing.

Here the focus is on measuring and modeling lysozyme transport in p-HEMA hydrogels, which are a common contact lens material. While lysozyme transport in p-HEMA gels and contact lenses has been explored by several researchers, simultaneous measurements of binding and diffusivity for various crosslinkings and concentrations are not available. Furthermore gel thicknesses utilized in most prior investigations were such that equilibration time for highly crosslinked gels was prohibitively long and so partition coefficients could not be determined. One of unique aspect of our approach is to measure the transport dynamics for gels of different, particularly very small

thicknesses, which allows us first to determine whether diffusion is the rate limiting step and also allows us to explore diffusive transport for highly crosslinked gels within a reasonable time frame. The specific focus is on exploring the dependency of lysozyme binding and transport on the degree of crosslinking, and in particular determine the crosslinking above which protein uptake is negligible. Desorption of the adsorbed protein due to its relevance in contact lens cleaning has also been explored. Protein transport could be controlled by a combination of diffusion and adsorption-desorption of the protein from the gel network, so we conduct transport studies with gels of various thicknesses. Also concentration dependent studies are conducted to understand the transport mechanisms. The modulus and water content of the lens is also measured for various crosslinkings. This data is valuable for contact lens design and could also be utilized by researchers interested in modeling the effect of crosslinking on rheology of the highly crosslinked gels. Finally, theoretical models are utilized to estimate the protein diffusivity and compared with the measured values. Several models have been suggested for solute diffusion in hydrogels [107-113]. These and more models have been extensively reviewed elsewhere [114-116]. The models which use the measured modulus to estimate the mesh size in gel are utilized, and then the mesh size is utilized to estimate the diffusivity. The results of this study will be useful in contact lens design and could also be useful to researchers interested in exploring the effect of crosslinking on partition coefficient and diffusivity of solutes and physical properties such as storage modulus and water content.

Summarizing, in Chapter 2 we have explored in detail the transport of BAC and CAC in water as well as PBS. The effect of concentration of surfactant, solvent (water

and PBS), and hydrogel thickness revel their transport characteristics. In PBS, CAC adsorbs strongly on the polymer chains of creating a charged polymer matrix. The chosen surfactant CAC has a sixteen unit long tail that leads to very strong interactions with the p-HEMA matrix. The strong binding of the surfactant to the tail ensures that negligible surfactant is released into PBS, thus minimizing the possibility of toxicity due to surfactant release in the tear film. The CAC incorporation increases anionic drug loadings significantly as shown in Chapter 3. Here, drug transport in explored as a function of surfactant loading and hydrogel thickness and a detailed model is formulated. We also evaluate the physical and mechanical properties of the hydrogel to ensure that the gels can function as contact lenses.

Even though CAC does not elude out of the lenses, it has the potential for toxicity. Thus it is intuitive to try and add surfactant to the polymer matrix. This can be achieved by adding polymerizable surfactants (pzsurfs) to the monomer mixture. In Chapter 4, we explore how the addition of pzsurfs can affect the surface properties drastically. And finally we explore how lysozyme transports in p-HEMA hydrogels and is a strong function of hydrogel crosslinking. The results of this study can be applied to understand protein adsorption to contact lenses and to design optimum lens care solutions and protocols.

CHAPTER 2
IONIC SURFACTANT TRANSPORT IN P-HEMA HYDROGELS

To understand the effects of surfactant on the properties of hydrogels, it is imperative to understand the interactions between them as well as study the transport of surfactants under different conditions. To do so, surfactants need to be incorporated in hydrogels which can be done by:

- Soaking in a surfactant solution
- Direct entrapment during polymerization

Soaking in a surfactant solution allows us to study the surfactant loading dynamics and make the equilibrium curve. Experiments with direct entrapment enable us to measure release dynamics directly as function of initial loading since loading by soaking in solution is restricted by equilibrium and saturation. Here, cationic surfactant systems of BAC and CAC are being studied. The rate of uptake and release of surfactants for different concentrations and loadings have being investigated and two solvents namely DI water and phosphate buffered saline (PBS) were utilized. Gels of varying thicknesses (240, 100 μm) were used in order to assess the transport mechanism the system.

2.1 Materials and Methods

2.1.1 Materials

2-Hydroxyethyl methacrylate (HEMA), ethylene glycol dimethacrylate (EGDMA), Benzalkonium chloride (BAC), benzyldimenthylhexadecylammonium chloride (CAC, mol. wt. 396) and Dulbecco's phosphate buffered saline (PBS) were purchased from Sigma-Aldrich Chemicals (St Louis, MO).

2.1.2 P-HEMA Hydrogel Synthesis

P-HEMA hydrogels were synthesized by free radical solution polymerization of the monomer with chemical initiation. The monomer (HEMA, 2.7ml), crosslinker (EGDMA, 10 µl i.e. 0.0025 mol / mol HEMA) and DI water (2ml) were mixed together. The solution was then degassed by bubbling nitrogen for 15 minutes to remove any dissolved oxygen present in the mixture. 0.006 gm of the initiator (Darocur, TPO) was added and the solution was stirred at 900 rpm for 5 minutes to ensure complete dissolution of the initiator. Resulting solution was poured in between two glass plates that were separated from each other by a spacer 240, 100 or 15 µm in thickness. The mold was then placed on Ultraviolet transilluminiator UVB-10 (UltraLum, Inc.) and the gel was cured by irradiating UVB light (305 nm) for 40 min.

The gels were removed from the glass plates and cut into small circles of approximately 1 cm diameter. These cut gels were utilized to serve as controls for release dynamics experiments. To utilize these gels for measuring uptake dynamics, unreacted monomer and initiator were extracted by soaking the gels in boiling DI water for 120 minutes with a change of DI water after 40 and 80 minutes. These gels were then dried in air overnight, weighed and used. The thickness of gels was measured after being dried in air.

2.1.3 Surfactant Detection and Measurement

In the surfactant uptake and release experiments, the absorbance of the surfactant solution was measured as a function of time in a UV-Vis spectrophotometer for wavelengths ranging from 235-275 nm.

2.1.4 CMC and Working Range

Based on the calibration curve of UV-spectra, a working range was established for both the surfactants. In order to ascertain the effect of critical micelle concentration (CMC) on dynamics, conductivity measurements were carried out to find CMC of BAC and CAC.

2.1.5 Uptake from Surfactant Solutions

Extracted and dried 100 and 240 µm gels were soaked in surfactant solutions for uptake experiments. These experiments were carried out in DI water and PBS. Volume of solution was chosen such that its ratio (V_f) to volume of gel (V_g) was similar to the ratio of volume of tears produced in a day to the volume of a contact lens. The UV-spec was measured at specific time intervals till equilibrium was established. Every experiment was carried out in triplicate. The UV spectra of the solutions were directly used along with the calibration curve to determine the surfactant concentration and thus the uptake dynamics.

2.1.6 Release of Surfactants

P-HEMA gels of different thicknesses were synthesized with different amounts of CAC entrapped in the polymerization mixture. These gels were soaked in water and the release profiles of the surfactants were measured. When surfactant is loaded directly into the polymerization mixture, the gels cannot be extracted. When these gels are soaked in solvent for surfactant release, unreacted monomer and unused initiator also releases. The absorbance spectra of the unreacted monomer and initiator partially overlap with that of the surfactants and thus an absorbance measurement at a single wavelength is not sufficient to obtain the concentration of the surfactants (Figure 2-1). It was decided to monitor the absorbance at a range of wavelength since if the

absorbance of the sample is measured at a range of wavelengths, the absorbance spectra can be assumed to be a linear superposition of the spectra of p-HEMA and the surfactant. By using a two parameter fit the absorbance contributed by p-HEMA and that by the surfactant can be obtained and this can be then converted to surfactant concentration by using a calibration curve. The separate absorbance of just p-HEMA was obtained from the control gels (no surfactant). The measured absorbance spectra was thus deconvoluted by expressing the measured absorbance as

$$\text{Abs} = \alpha \times \text{surfactant} + \beta \times \text{Control} \quad (2\text{-}1)$$

where Abs is the measured absorbance spectra from 250 to 270 nm, surfactant is the absorbance spectra of the surfactant in the same wavelength range at some arbitrary concentration, Control is the absorbance spectra of the solution in which p-HEMA gel without any surfactant was soaked, and α and β are constants. These constants were obtained by finding best fit values minimizing the error between measured absorbance and calculated absorbance according to Eq. (2-1) using the function 'fminsearch' in MATLAB. The concentration of surfactant was finally obtained by multiplying α to the concentration corresponding to surfactant. The above procedure assumes that the absorbencies of these components are simply additive and linear in concentration, and this was verified by conducting several experiments.

2.2 Results and Discussion

2.2.1 CMC and Working range

CMC of the surfactants were found to be 0.21% and 0.019% respectively (Fig 2-2). For BAC, since CMC was sufficiently high, the uptake tests were carried out at concentrations both below and above the CMC. For CAC, due to low CMC, it was decided to continue with concentrations above CMC.

2.2.2 BAC Uptake from Water

Figure 2-3 shows the uptake dynamics of BAC in 100 µm gels at different concentrations of BAC (indicated in the legend). A few of these concentrations were also used for uptake experiments with 240 µm gels the results of which are shown in the Figure 2-4 (concentrations indicated in legend). A critical equilibrium concentration was observed. Below that concentration, the amount of BAC uptake is proportional to the equilibrium concentration. But above that concentration, the amount of BAC uptake is independent of concentration of surfactant. From the graph of Equilibrium uptake vs Equilibrium concentration (Figure 2-5) it can be seen that this concentration is very close to CMC of BAC. Thus it can be understood that the gel is in equilibrium not with the actual concentration of BAC but with the free concentration of BAC in the solution. A hypothesis for such a behavior is that the surfactant does not aggregate inside the gel and thus once it establishes equilibrium with the free BAC concentration, no more BAC can be loaded in the gel.

Partition coefficient (K) can be defined as

$$K = \frac{C_{g,f}}{C_{w,f}} = \frac{V_w\left(C_{w,i} - C_{w,f}\right)}{V_g C_{w,f}} \tag{2-2}$$

where Vw and Vg are the volumes of the BAC solution and hydrogel, respectively, and Cg,f, Cw,i, and Cw,f are the equilibrium concentration of BAC in the gel and initial and equilibrium BAC concentrations in water, respectively. Analysis of the dependence of partition of coefficient (K) on $C_{w,f}$ revels an inverse relation between them (Fig 2-6a) and it is seen that the inverse of partition coefficient is liner with $C_{w,f}$ (Fig 2-6b).Such a relation is indicative of a saturation behavior.

2.2.2.1 Mechanism of transport of BAC

To understand the mechanism of transport, the graphs of uptake were re plotted with a scaled axis. The x-axis was scaled as $t*(H_0^2/H^2)$ where H_0 is a reference thickness and H is the actual thickness of the gel. On comparing these plots for two thicknesses i.e. 100 µm and 240 µm (Figure 2-7) it was observed that the graphs overlapped. This indicates that the mechanism of transport of BAK is diffusion since diffusion time is proportional to H^2.

2.2.3 CAC Uptake from Water

Similar experiments were carried out with CAC as BAC. Due to restrictions on range of measurement, the concentrations were above CMC. A similar behavior was observed as BAK in terms of mechanism of transport (Figure 2-8). The transport was diffusion controlled and the uptake was independent of the concentration of CAC in water. The hypothesis is same as that for BAC that there are no aggregates forming in the hydrogel.

Through the technique of loading by soaking in surfactant solution in water, it was not possible to vary the loading of surfactant in gel since loading was independent of the surfactant concentration. Hence in order to perform release tests it was decided to incorporate surfactant in the gels during polymerization to understand the effect of loading.

2.2.4 CAC Uptake from PBS

The above procedure was repeated for CAC uptake from solutions in PBS. Due to the buffering effect, CAC would crystallize out. Hence the gels soaked in solution were kept in an oven at 60^0C so as to estimate the final partition coefficient.

The result of the experiment was that irrespective of the concentration of CAC, all the surfactant present in the solution was taken up by the gel. This was confirmed by release experiments in water. The partition coefficients were found to be similar to those in uptake experiments indicating a reversible uptake.

2.2.5 CAC Release in Water

Fig 2-9 shows the CAC release profiles at different CAC loadings on a scaled time axis for 2 different thicknesses. The overlap indicates that the mechanism of transport is diffusive. A model for surfactant release from hydrogels laden with surfactant aggregates has been proposed earlier [64,65], and it predicts the following equation to describe surfactant release at short times,

$$R_S(\%) = \sqrt{2D_S C^*}\sqrt{\frac{t}{C_p h^2}} \times 100 = \sqrt{2D_S C^*}\,\Theta \times 100 \qquad (2\text{-}2)$$

Where R_s (%) is the percentage release from the system, D_s is the diffusivity, C* is the Critical Aggregation Constant, t is the release time, C_p is the concentration of the surfactant present as aggregates and h is the half thickness of gel. The above equation is valid for diffusion of any solute that is loaded in the gel above the saturation limit and so a fraction of the solute precipitates into aggregates. In case of Cp>>C*, Cp can be approximated as the initial loading concentration. If the loaded surfactant forms aggregates such as micelles or vesicles in the gel, the duration of the surfactant release must increase as the square root of the surfactant loading and the cumulative percentage release of the surfactant at a given time should decrease as the square root of the loading. On the other hand, if the surfactant does not aggregate, the release durations and cumulative percentage release profiles would be independent of the surfactant loading. As seen in fig 2-9, the percentage release profiles for the surfactant

are independent of the surfactant loading at short times, supporting the hypothesis that the loaded surfactant is not forming any aggregates in the gel.

2.2.6 CAC Release in PBS

No surfactant was released in PBS which was consistent with uptake experiments.

2.3 Concluding Remarks

From the surfactant transport studies, it is clear that both BAC and CAC have high partitioning in p-HEMA gels which is exacerbated in PBS. Surfactant transport is diffusion controlled. In water, the gel takes up about 0.05 g/g of BAC and 0.065 g/g of CAC at all concentration above their CMC. This is indicative that the gel is in equilibrium with the free surfactant concentration and it may not be aggregating in the gel.

In PBS, CAC is absorbed in high quantities and is not released. Essentially, the length of the tail section of the surfactant is sufficiently long to maximize the hydrophobic interactions, for strong adsorption on the gel matrix with a high packing. An oppositely charged drug can be strongly adsorbed in these CAC loaded gels. The high packing of CAC will ensure a stronger adsorption of the drug molecules on the charged surface and will also minimize the potential release of the surfactant into the tears after the contact lens is inserted in the eyes. The hydrophobic interactions between the surfactant tail and the polymer increase with increasing tail length but increases is the tail length reduce the total charge for a fixed surfactant loading on weight basis. If both of these interactions (polymer-surfactant tail and drug-polymer-head) are optimized, it should be possible to design a system that does not release the surfactant into the tear film and also very slowly releases the chosen drug.

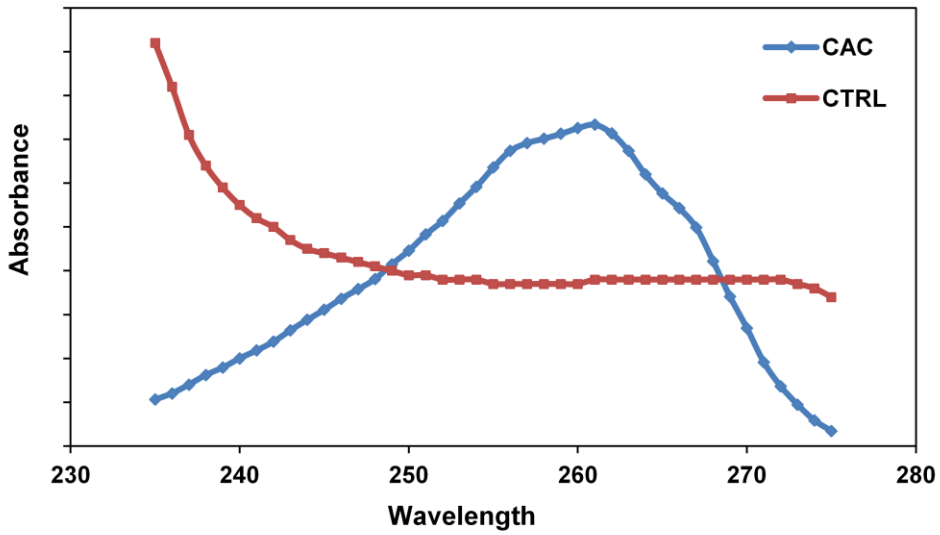

Figure 2-1. Comparison of UV-spectra of CAC and p-HEMA from control gels

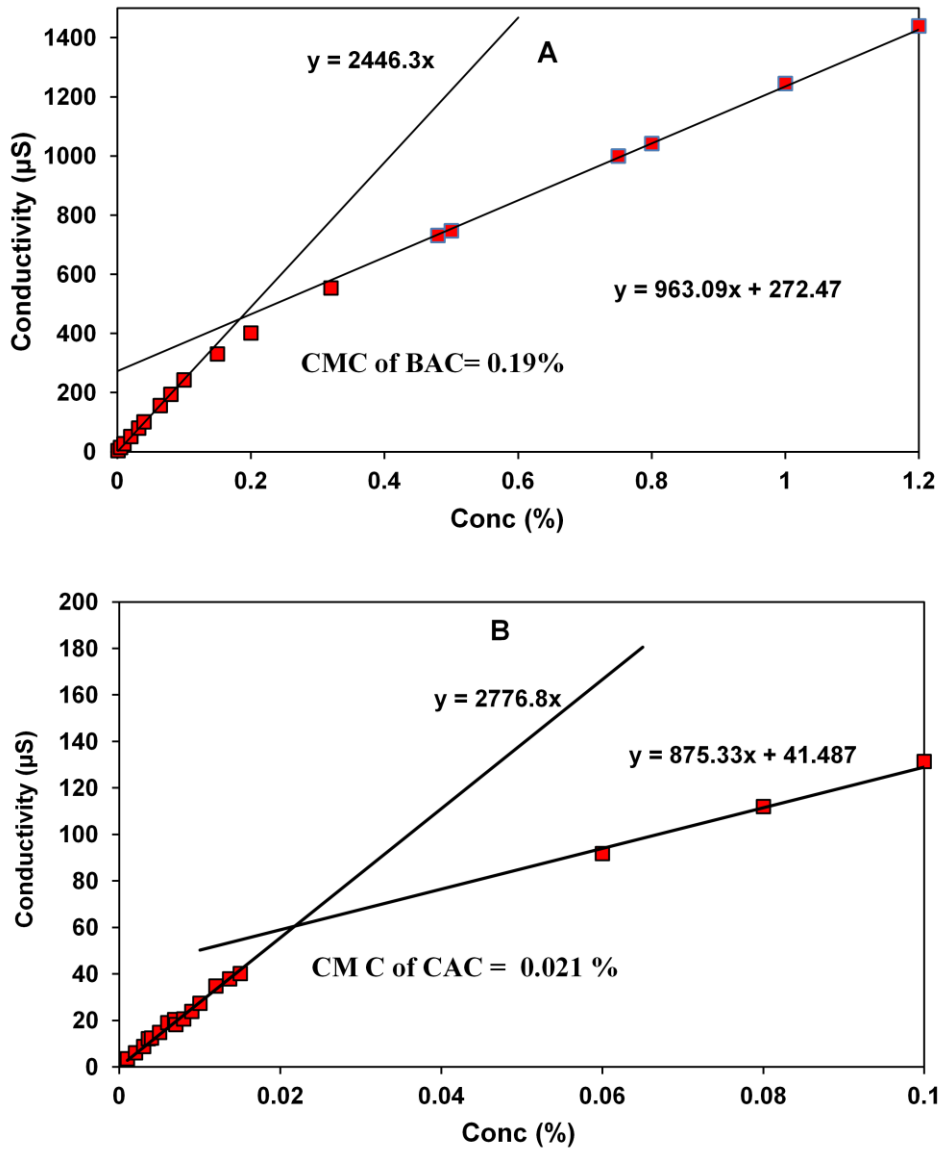

Figure 2-2. CMC of ionic surfactants A) BAC and B) CAC

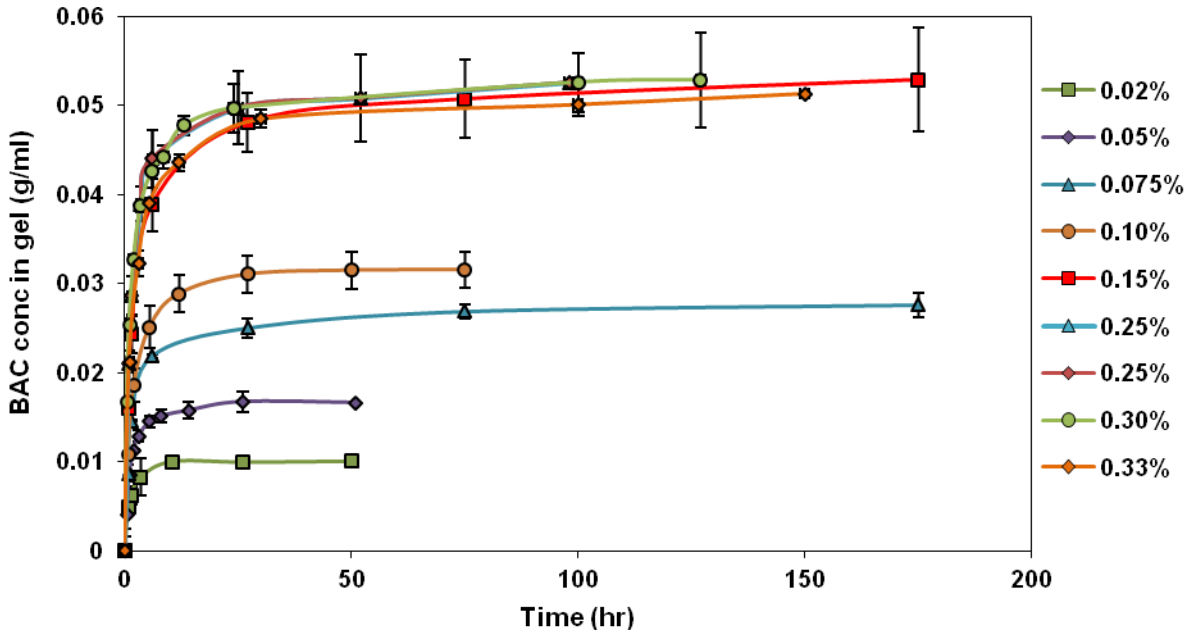

Figure 2-3. BAK Uptake Dynamics in 100 µm p-HEMA gels

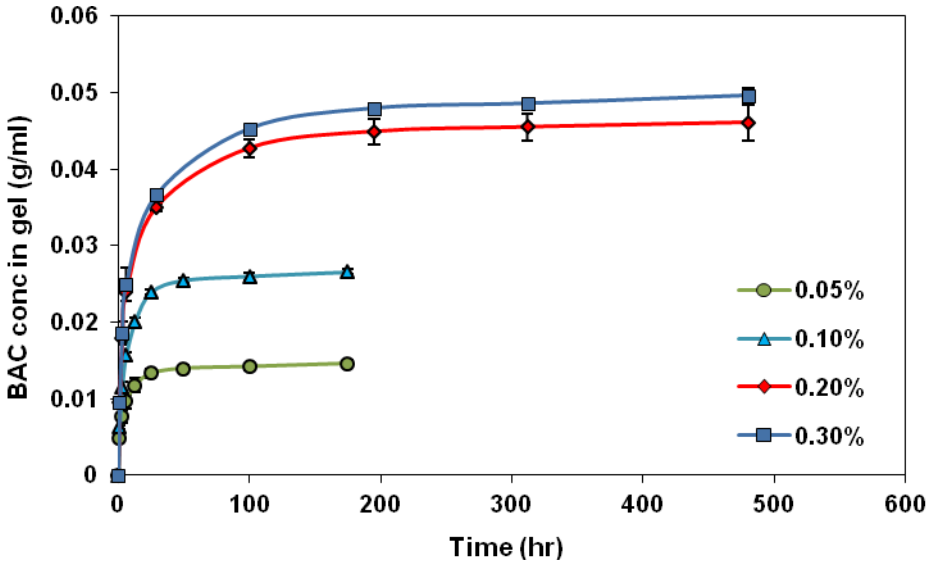

Figure 2-4. BAK Uptake Dynamics in 240 µm p-HEMA gels

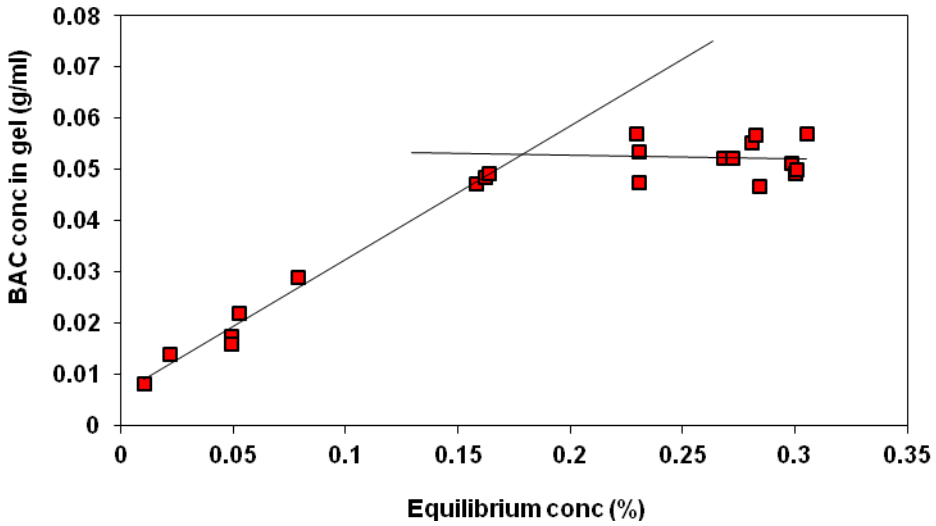

Figure 2-5. Binding isotherm of BAC

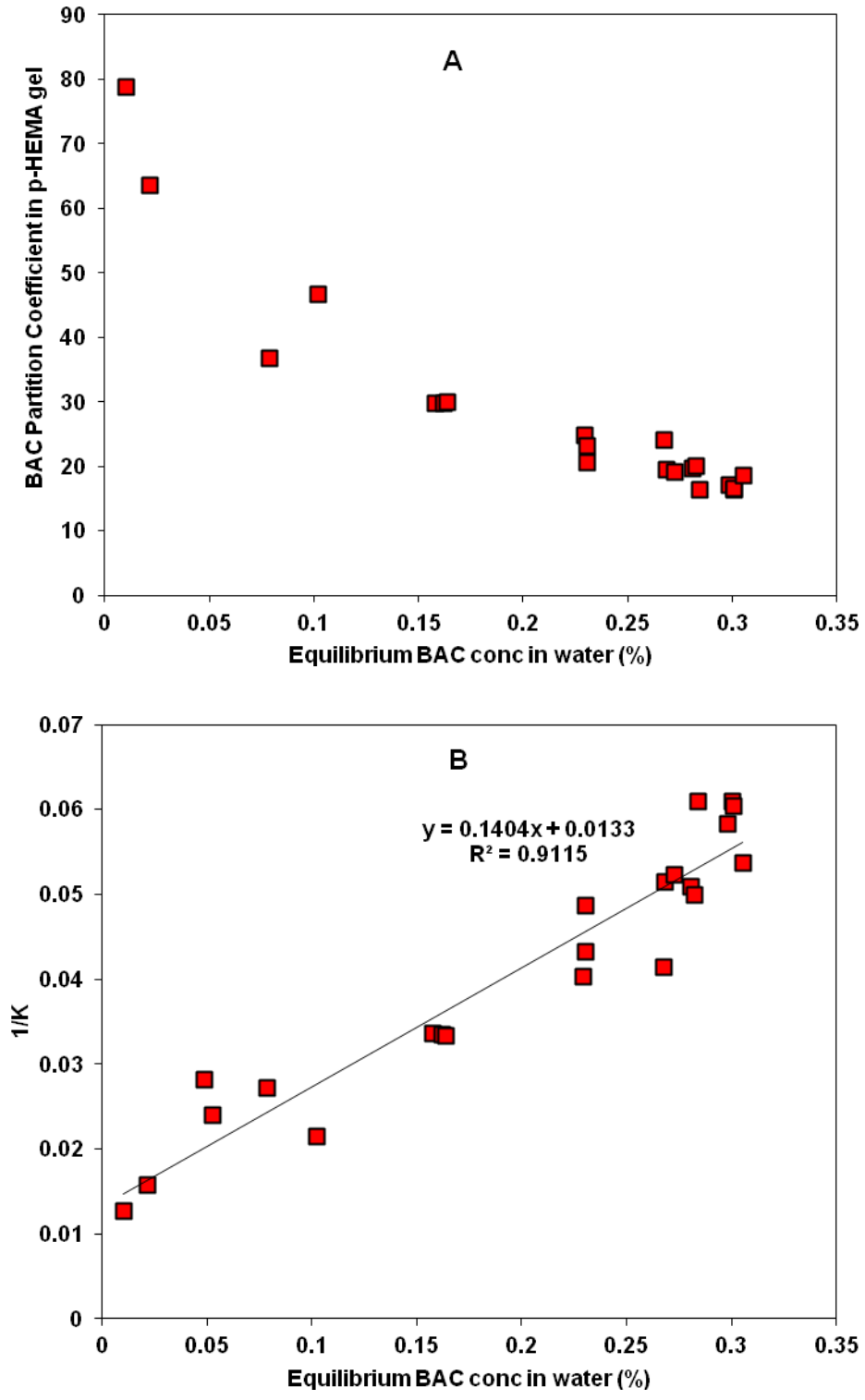

Figure 2-6. Variation of A) Partition coefficient B) Inverse of Partition coefficient with BAC equilibrium

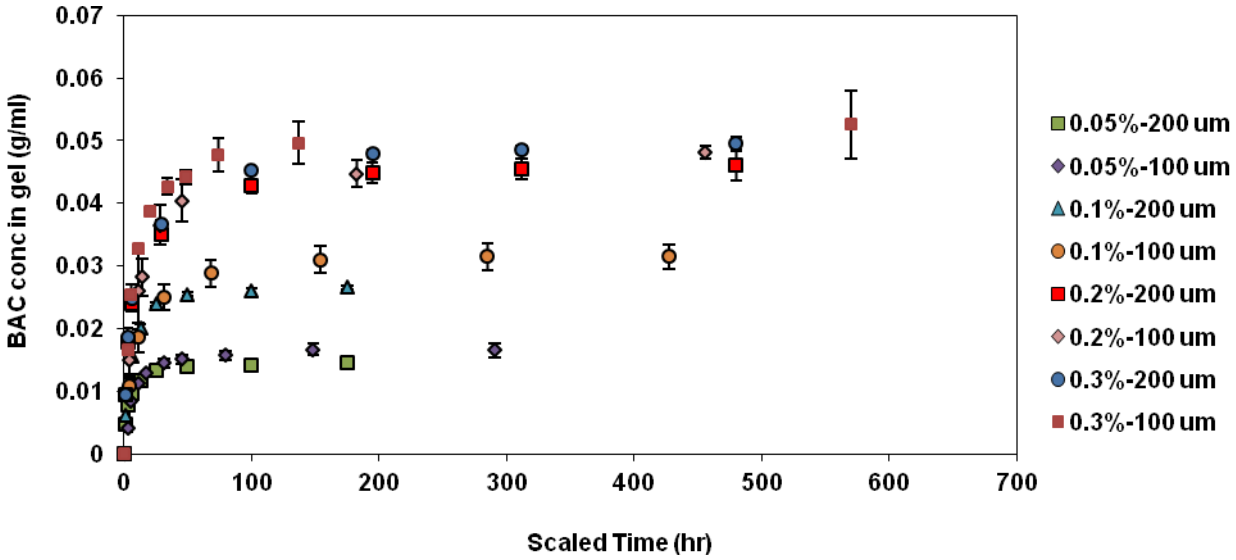

Figure 2-7. BAC Transport Mechanism

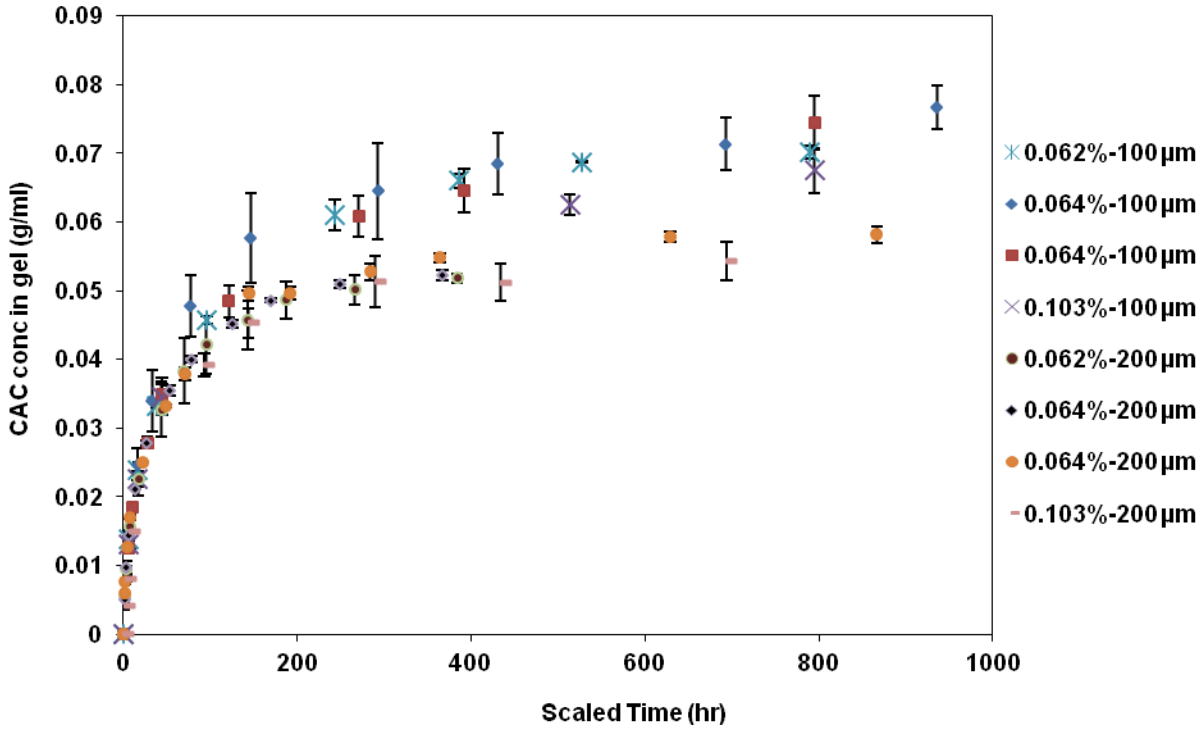

Figure 2-8. CAC Transport Mechanism

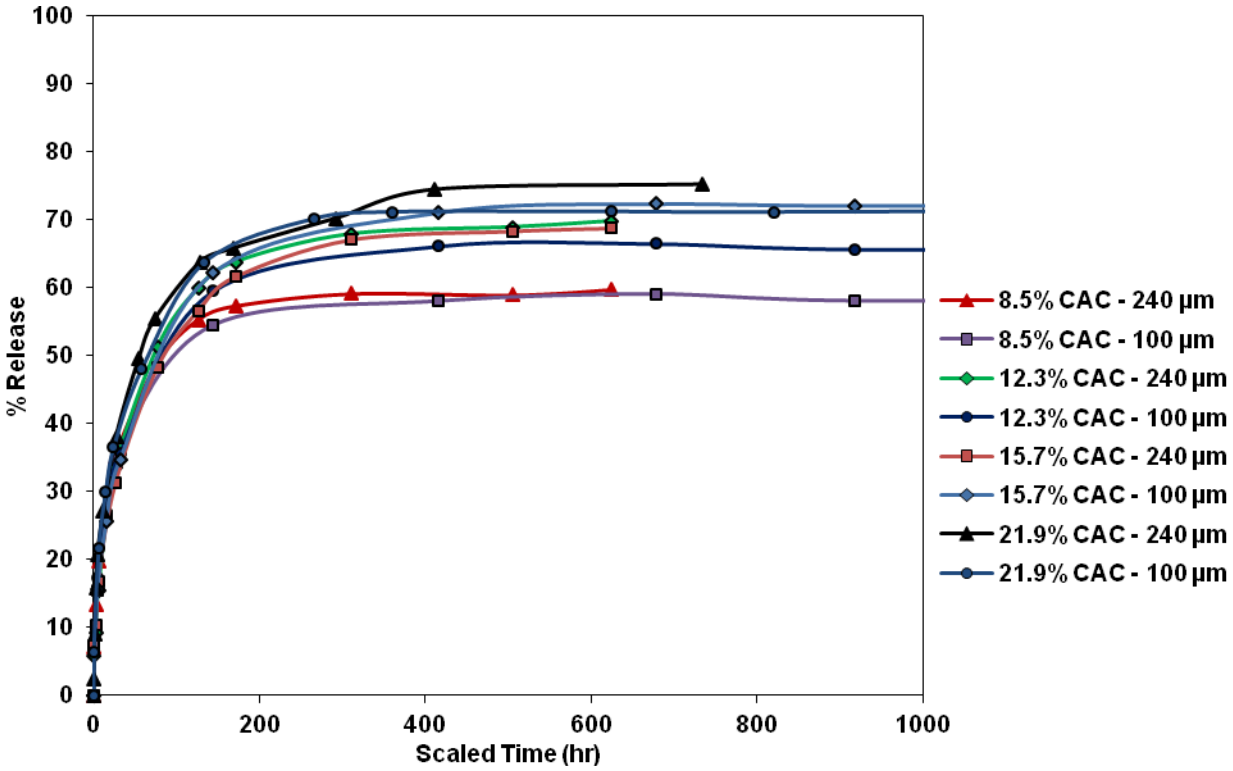

Figure 2-9. % Release of CAC for different surfactant loadings and thicknesses

CHAPTER 3
OCULAR DELIVERY OF A CATIONIC DRUG WITH SURFACTANT LOADED CONTACT LENS

3.1 Materials and Methods

3.1.1 Materials

2-Hydroxyethyl methacrylate (HEMA) monomer, ethylene glycol dimethacrylate (EGDMA), Dulbecco's phosphate buffered saline (PBS), dexamethasone 21-disodium phosphate (DXP), benzyldimenthylhexadecylammonium chloride (CAC, mol. wt. 396) were purchased from Sigma-Aldrich Chemicals (St Louis, MO). 2,4,6-trimethylbenzoyl-diphenyl-phophineoxide (Darocur® TPO) was kindly provided by Ciba (Tarrytown, NY). All the chemicals were reagent grade and were used without further purification.

3.1.2 Preparation of Pure P-HEMA Gels

P-HEMA hydrogels were synthesized as mentioned in section 2.1.2. Here the thicknesses of the hydrogel chosen were 480, 240, 100, 50 and 15 µm. 480, 240 and 100 µm gels were removed from the glass plates and cut into small circles of approximately 1 cm diameter, while the 50 and 15 µm thick gels were cut in strips of variable sizes but with a fixed weight of about 0.02 g.

3.1.3 Preparation of Surfactant Loaded P-HEMA Gels.

Surfactants can be incorporated in hydrogels by either soaking in a surfactant solution or by direct entrapment during polymerization process. To load surfactant by direct addition to the polymerization mixture , the required amount of surfactant (0.01, 0.02, 0.04, 0.07, 0.125, 0.15, 0.2 and 0.3 g/ml of HEMA corresponding 0.9%, 1.8%, 3.6%, 6.1%, 8.5%, 10.5%, 12.3%, 15.7% and 21.9% CAC loadings) was added to the monomer mixture before nitrogen bubbling. The procedures described above were then utilized for gel curing.

Surfactant was also loaded into gels by soaking the gels and contact lenses in a solution of surfactants in PBS since was observed that surfactant absorption into the gels is much higher in PBS as seen in the previous section. As shown earlier, when p-HEMA gels including commercial contact lenses were soaked in a CAC-PBS solution, CAC would partition completely into the gels up to a loading of 25%. Furthermore the loaded CAC was not released from the gels or contact lenses when soaked in PBS. The surfactant loading into gels by soaking in aqueous solutions can be used as a method for incorporation of surfactants into prefabricated contact lenses. This loading approach may be preferable over loading by direct addition to the polymerization mixture prior to polymerization because surfactant loaded in the lenses prior to polymerization could diffuse out of the lenses during processing steps such as unreacted monomer extraction and contact lens sterilization. 8.5% CAC was loaded in p-HEMA gels by soaking the gels in 0.05% CAC-PBS solution of required volume.

3.1.4 Drug Transport Studies.

3.1.4.1 Drug loading

Surfactant loaded gels were soaked in 0.1 mg/ml DXP solution in PBS to load the drug into the gels. Gels of various thicknesses ranging from 15 to 480 µm were utilized, although most experiments focused on 100 and 240 µm. The ratio of gel weight to volume of drug solution was kept constant for gels of different thicknesses and same CAC loading (140 ml solution per g of gel) till a CAC loading of 8.5%. Beyond that, the volume of drug solution was proportionally increased with CAC loading. DXP is photo-labile and so drug solutions were covered with an aluminum foil in a dark chamber, and removed for about a minute for each measurement. The UV absorbance of DXP solution was measured from 220 nm to 270 nm with a peak at 241 nm. Since unreacted

monomer was not extracted before the experiment, it also eluted out during the experiment and its UV spectra was partly overlapping with the spectra of DXP. To distinguish between the absorbance from unreacted HEMA and DXP, the measured absorbance spectra was deconvoluted by technique similar to the employed in surfactant release studies (section 2.1.3)

3.1.4.2 Drug release studies

After equilibrium was established in the drug loading experiments, drug solution was replaced by pure PBS marking the beginning of release experiments. The PBS volume was either 6 ml (for gels with CAC loadings up to 10.5%) or 9 ml (for 12.3% and 15.7% CAC). The dynamic drug concentrations were measured by following the same approach as described above. The model established from loading data was used to predict the drug release and compared to experimental release data.

3.1.5 Equilibrium Aqueous Content (EAC)

The aqueous content of CAC loaded gels was measured by soaking surfactant loaded gels of known weight into PBS and then measuring the fully hydrated weight. The equilibrium aqueous content (EAC) was defined as the mass of PBS uptake per weight of hydrated gel, not including the weight of surfactant, i.e.,

$$\%EAC = \frac{(W_{wet} - W_{dry})}{(W_{wet} - W_{CAC})} \times 100 \qquad (3.1)$$

The aqueous content was also measured after extracting the surfactant from the gels. To extract the surfactant, the gels were soaked in ethanol for 48 hrs and then soaked in DI water at 60^0C for at least another 48 hrs. To make sure all the extractable surfactant has been extracted, these gels were further soaked in pure DI water for another 7 days, and UV spectroscopy was utilized to verify the absence of any eluded

surfactant. These gels were then dried, weighed and soaked in PBS to determine the EAC by using the following formula

$$\%EAC = \frac{(W_{wet} - W_{dry})}{(W_{wet})} \times 100 \quad (3.2)$$

3.1.6 Surfactant and Drug Loading in Prefabricated Contact Lenses

1-Day ACUVUE® contact lenses were removed from their blister packs with a pair of tweezers, soaked in 200 ml of DI water for 1 day and then dried in air. The dry weight of the lenses was found to be 0.018 ± 0.0004 g. The dried contact lenses were soaked in 3.6 ml and 7.2 ml of 0.05% CAC solutions to load 10% and 20% CAC/dry wt. of lens respectively. UV-vis spectroscopy was used to confirm that the entire surfactant has partitioned inside the lens and the amount of surfactant loaded in the lens was simply taken as the amount of surfactant present in the loading solution. These lenses were used for drug loading and release studies using methods identical to those described above for drug transport in p-HEMA gels loaded with surfactant.

3.1.7 Effect of Surfactant Loading on Protein Binding.

To understand the influence of presence of surfactant on protein sorption by commercial contact lenses, a 1 mg/ml lysozyme solution was prepared by adding 50 mg of lysozyme to 50 ml of PBS. The solution was stirred overnight and filtered through a 0.2 μm filter. 1-Day ACUVUE® control lenses and those loaded with 10% CAC were soaked in 3.5 ml of lysozyme solution and the amount of lysozyme that was taken up by the lenses was monitored by UV-vis spectroscopy in the wavelength range 252–320 nm with a peak at 278 nm.

3.2 Results and Discussion

3.2.1. DXP Transport in CAC Loaded P-HEMA Hydrogels.

3.2.1.1. Effect of CAC loading on DXP loading profiles

Figure 3-1 shows the drug (DXP) loading profiles in 240 µm thick CAC loaded p-HEMA gels. The CAC loading in the gels varies from 0 to 21.9% (wt/total dry gel wt), while the starting concentration of DXP in the loading solution was 0.1 mg/ml for each case. The measurements of the dynamic DXP concentration in PBS were utilized in a mass balance to calculate the average DXP concentrations in the gel which are plotted in Figure 3-1 and subsequent figures. The DXP concentration in the gel is actually position dependent, except at equilibrium, and thus the concentrations obtained from the mass balance represent the mean DXP concentrations in the gel. The equilibrium uptake of the drug was utilized to determine the partition coefficient of the drug in the surfactant loaded gels. The partition coefficient K is plotted as a function of the surfactant loading in Figure 3-2. The data clearly shows that increasing surfactant loading in the gel leads to a non-linear increase in the partition coefficient. Additionally the loading duration which is defined as the time required to reach 80% of the equilibrium concentration increases with surfactant loading till a loading of about 10%, with a relatively minor increase with a further increase in surfactant loading (Figure 3-3). It is noted that the surfactant was loaded in the gels by direct addition to the polymerization mixture. The release of surfactant was also monitored in these experiments but there was negligible release of the surfactant in PBS due to very strong binding of the surfactant to the gel in PBS medium. Thus, the surfactant loadings in the gels are constant during the entire experiment.

3.2.1.2. Rate limiting step in DXP transport.

The increase in drug loading amounts and the equilibration time strongly suggests that the drug DXP interacts with the surfactant through ionic forces. The interaction of the drug with the surfactants could increase the release duration through several mechanisms. Firstly, the drug could adsorb to the surfactant aggregates and the time scale for adsorption could be the rate limiting step. Secondly, the drug adsorbed to the surfactants may not be able to diffuse, or diffuse at a slower rate compared to the free drug, thereby slowing down the overall transport. If diffusion is rate limiting the free and the bound drug concentrations are in local equilibrium then an average diffusivity can be determined. To determine whether drug adsorption or diffusion is rate limiting during drug loading into the gels, experiments were conducted with various gel thicknesses. If diffusion is rate limiting, the time scale should vary as the square of the gel thickness, i.e., the data for DXP concentration in gel from experiments with different thicknesses should overlap if it is plotted as a function of the scaled time, which is defined as

$$\text{Scaled Time} = Time\left(\frac{H_o}{H}\right)^2 \quad (3\text{-}3)$$

where H_0 is a reference thickness and H is the actual thickness of the gel. The data for 100 and 240 μm thick gels are compared in Figure 3-4 with H_0 = 240 μm. The loading profiles overlap for both thicknesses at various CAC loadings, indicating that the drug loading is diffusion-controlled for all cases. To further prove that diffusion is rate controlling, the data was fitted to a diffusion control model (described in next section) and the solid lines in Figure 3-4 are the best fits from the model. The good agreement between model fits and the experimental data along with the overlapping of the scaled

data proves that diffusion is rate limiting, and the bound and free drug fractions in the gel can be considered to be local equilibrium.

The diffusion time scale varies as square of the gel thickness, and thus even though diffusion is the rate controlling step for transport in 100 and 240 μm thick gels, adsorption-desorption could potentially become rate limiting for thinner gels. In an attempt to determine the adsorption-desorption rate constants, drug loading was also measured for thinner gels, and scaled profiles are plotted in Figure 3-5(A) for 8.5% CAC loading and in Figure 3-5(B) for 15.7% CAC loading. The scaled plots overlap for thinner gels as well, showing that adsorption-desorption dynamics are very rapid, and experiments with much thinner gels or particles may be needed to determine the adsorption-desorption rate constants.

3.2.1.3. Microstructure of the surfactant loaded in the gels.

The data shown above clearly proves that diffusion through the gel is the rate limiting step in transport, and thus surfactant is attenuating the transport by increasing the fraction of the bound drug. The surfactant loaded in the gel is expected to partition between free surfactant dissolved in the aqueous phase in the gel and bound surfactant that is adsorbed to the polymer. Alternatively, a fraction of the surfactant loaded into the gels could form aggregates in the pores of the hydrogel. The microstructure of the surfactant will have a significant impact on the drug transport. Determining the detailed morphology of the surfactant-loaded gels requires imaging through neutron scattering, but the most likely microstructure could be deduced by analyzing the transport data for the surfactant and the drug. Below we present indirect evidence based on four different types of measurements that all suggest that the surfactant loaded in the gels is not forming aggregates and is instead mainly adsorbing on the p-HEMA polymer.

If the surfactant primarily forms aggregates in the gel, increased surfactant loading should increase the aggregate loading in the gel, without any significant increase in the surfactant packing in each aggregate. In that case, the interaction of a drug molecule with the surfactant aggregates would be relatively independent of the surfactant concentration and thus the number of drug molecules adsorbed to each aggregate would be constant. The increased partition coefficient of the drug would then be simply due to an increase in the number of aggregates, and the increase in partition coefficient would likely be linear in surfactant concentration. On the contrary if the surfactant molecules do not form aggregates but instead primarily adsorb on the p-HEMA polymer chains, the charge density and the potential of the surfactant covered polymer would increase linearly with surfactant concentration. Assuming Debye-Huckel model, the adsorption of the charged drug molecules would increase exponentially with the surface potential, leading to an exponential increase in the partition coefficient. The data in Figure 3-3 clearly shows an exponential dependency and thus it is speculated that the surfactant loaded in the gels is primarily bound to the polymer with the charged group exposed to the bulk.

Additional evidence supporting this speculation was obtained by measuring the rate of release of the surfactant from the gels in DI water. The surfactant has a very high partition coefficient for partitioning between gel and PBS, and thus the loaded surfactant exhibits negligible release in PBS. However the partition coefficients are much smaller in DI water likely due to two reasons. First, the enthalpic penalty due to the interactions of the surfactant tail with the solvent increase as the polarity of the solution increases due to an increase in the ionic strength. Second, the ionic repulsion between the head

groups of adsorbed surfactant molecules is stronger in DI water due to a larger Debye length compared to PBS. The larger repulsion will reduce the packing of the adsorbed surfactant. The release behavior of the surfactant in DI water can indicate the microstructure of the adsorbed surfactant and it was hypothesized in section 2.2.4 that that the loaded surfactant is not forming micelles in the gel.

Further support for the absence of micelles was provided by the effect of the surfactant loading on the aqueous content of the gels (Figure 3-6). The formation of micelles or vesicles, both of which contain aqueous cores will likely increase the water content due to creation of large pores in the gels. However data shows that aqueous content of the gels decrease with increasing surfactant loading. The aqueous content after surfactant extraction is independent of the mass of surfactant initially loaded in the gels, suggesting that surfactant presence does not impact the crosslinking density. The decrease in aqueous content thus must be due to alteration of the polymer-fluid interactions due to surfactant adsorption.

Further evidence in support of the hypothesis of absence of aggregates was provided by comparing drug transport data in gels in which surfactant was loaded by adsorption from PBS solutions with the data from gels with surfactant added to the polymerization mixture. 8.5% CAC was loaded in p-HEMA gels by soaking the gels in 0.05% CAC-PBS solution of required volume. The drug transport was independent of the loading approaches for gels with comparable surfactant loadings (Figure 3-7). Since surfactant adsorbed into preformed gels will unlikely form micelles due to the constrained pores, the surfactant incorporated prior to polymerization also is unlikely to be forming aggregates. While direct imaging is necessary to determine the

microstructure of the surfactant in the gel, all the evidence presented above supports the hypothesis that surfactant is adsorbing to the HEMA polymer and not forming aggregates. The next section on modeling transport data also provides evidence to support this hypothesis.

3.2.1.4. Modeling of drug loading dynamics.

The concentration of drug in the gel C can be separated into the free component C_{free} that is dissolved in the water fraction of the gel and the adsorbed component C_b that is bound to the gel or the surfactant. It is noted that C, C_{free} and C_b are based on the gel volume, which includes both the aqueous and the gel phase. The bound concentration is essentially the product of the true surface concentration of the bound solute and the specific surface area of the gel. The free and the bound fractions can be considered to be in local equilibrium due to the rapid time scales as compared to diffusion. The free and the bound components can both diffuse with respective diffusivities, and thus transport of solute in the gel can be expressed through the following mass balance

$$\frac{\partial C}{\partial t} = D_f \frac{\partial^2 C_{free}}{\partial y^2} + D_b \frac{\partial^2 C_b}{\partial y^2} \tag{3-4}$$

where D_f and D_s are the diffusivities of the free and the bound components. It is noted that the diffusivity of the bound component D_b is the ratio of the surface diffusivity and the specific surface area. It is also noted that if the drug molecules are binding to the micelle surface, D_b would be zero. We can assume that the DXP concentration in the aqueous part of the gel (C_{free}) is same as the DXP concentration in PBS outside the gel (C_f). If f is the fractional aqueous content of the hydrated gel and K is the partition

coefficient between the total DXP concentrations in gel and the DXP concentration in PBS, then

$$C_{free} = fC_f \tag{3-5}$$

$$C_b = (K - f)C_f \tag{3-6}$$

$$C = KC_f \tag{3-7}$$

On assuming local equilibrium between the free and the bound components, Equation (3-4) can be simplified to

$$\frac{\partial C}{\partial t} = \frac{\left(fD_f + (K - f)D_b\right)}{K}\frac{\partial^2 C}{\partial y^2} = D_{eff}\frac{\partial^2 C}{\partial y^2} \tag{3-8}$$

fD_f represents the diffusivity of drug in pure hydrogel matrix in absence of surfactant. The partition coefficient is dependent on the surfactant concentration, which is independent of position and time because the loaded surfactant does not diffuse into the PBS. Based on this model, the presence of surfactant reduces the effective diffusivity only because of the increase in the bound fraction, which diffuses at a slower rate compared to the free unbound molecules. The following mass balance on the aqueous phase, initial condition, and boundary conditions, respectively, are the remaining equations and conditions required to model the drug diffusion:

$$V_f\frac{\partial C_f}{\partial t} = 2A\left(-D_{eff}\frac{\partial C}{\partial y}\right)_{y=H} \tag{3-9}$$

$$C(y, t = 0) = 0 \tag{3-10}$$

$$C(t, y = H) = KC_f \tag{3-11}$$

$$\frac{\partial C}{\partial y}(t, y = 0) = 0 \tag{3-12}$$

where C_f is the DXP concentration in PBS, V_f is the PBS volume, A is the surface area of one face of the hydrogel, and H is the half-thickness of gel. The first boundary condition, Equation (3-11), assumes equilibrium between the drug concentration in the external drug solution and that within the hydrogel, and the second boundary condition, Equation (3-12) assumes symmetry at the center of the gel.

For ease of manipulation, the above equations were non-dimensionalized using the following variables:

$$C^*=C/C_0,\ C_f^*=C_f/C_0,\ y^*=y/H,\ t+= H^2/D_{eff},\ t^*=t/t+,\ A^*2H=V_g \quad (3\text{-}13)$$

where V_g is the volume of gel and C_0 is the initial drug concentration in the fluid.

Substitution of the dimensionless variables into Equations (3-8 to 3-12), and removal of the * signs, gives the following dimensionless equations:

$$\frac{\partial C}{\partial t}=\frac{\partial^2 C}{\partial y^2} \quad (3\text{-}14)$$

$$V_{fg}\frac{\partial C_f}{\partial t}=\left(-\frac{\partial C}{\partial y}\right)_{y=1} \quad (3\text{-}15)$$

$$C(y,t=0)=0 \quad (3\text{-}16)$$

$$C(t,y=H)=K \quad (3\text{-}17)$$

$$\frac{\partial C}{\partial y}(t,y=0)=0 \quad (3\text{-}18)$$

where the new variable $V_{fg} = V_f/V_g$. This new set of equations is no longer dependent on the gel thickness or initial drug concentration.

The drug loading data for gels of different thicknesses and surfactant loading was fitted to Equations (3-14 – 3-18) to determine the best-fit values of the parameters D and K. The differential equations were solved numerically using an implicit finite-

difference scheme. The best-fit values of the parameters were obtained by minimizing the error defined as $E = \sum_{i=1}^{Ne} (C_f - C_{model})^2$, where Ne is total number of data points, and C_f and C_{model} are the dimensionless experimental and model predicted concentrations in fluid, respectively. The minimization was done using the function fminsearch in MATLAB. The model fits are compared with the experimental data in Figs.3-4 and 3-5, and the best-fit values for D_{eff} are given in Table 1. Also K and D_{eff} are plotted as a function of the CAC loading in Figs. 3-2 and 3-8.

As expected the partition coefficient and drug diffusivity are independent of thickness, but showed a strong dependency of the surfactant loading in the gel. The effective diffusivity decreases with increasing surfactant loading due to the increase in the fraction of the bound drug. Assuming constant values of D_f and D_b, and based on the definition $D_{eff} \equiv \frac{\left(fD_f + (K-f)D_b\right)}{K}$ a plot of KD_{eff} and (K-f) should be a straight line of intercept fD_f and slope D_b. From Figure 3-9, D_b and fD_f can be estimated as 5.72 x 10^{-15} m^2/s and 4.3 x 10^{-13} m^2/s. The finite value of D_b further suggests that the drug molecules are adsorbing to the charged surfactant covered HEMA polymer, and thus reaffirms the hypothesis of the absence of aggregates in the surfactant loaded gels.

3.2.1.5. Effect of surfactant loading on drug release dynamics.

The drug loading data demonstrated that the transport of drug is diffusion controlled with partition coefficient that increases with surfactant loading. The main goal of surfactant incorporation is to develop an extended drug delivery device, and so it is important to show that drug loading also increase the release duration. After equilibrium was achieved in the drug loading phase, gels were transferred to fresh PBS and the

dynamic drug concentrations in PBS were measured. Also the dynamic concentrations were predicted based on the diffusion model with the values of D_{eff} determined from the loading phase. The data for the dynamic drug concentrations along with the predicted profiles are shown in Figure 3-10 for drug release from the 240 μm gels. The surfactant concentrations are noted in the legend and the volume of PBS in the release medium was 6 ml. The good agreement between the experimental data and the predictions support the model, and also prove that surfactant incorporation can significantly increase the drug release duration.

3.2.2 Drug Transport in Commercial Contact Lenses Loaded with Surfactant.

1-Day ACUVUE® lenses were loaded with CAC from CAC-PBS solutions and drug loading and release studies were conducted similar to p-HEMA gels. Figure 3-11 shows the drug loading profiles for these contact lenses which are compared to contact lenses with no surfactant. A similar diffusion model was fitted to the loading data and the solid lines in Figure 3-11 represent the best fits of the model. Results were very similar to those of p-HEMA gels. The partition coefficients and uptake durations for DXP loading were greatly enhanced when CAC was loaded in these lenses.

Release experiments were carried out for drug loaded 1-D ACUVUE® contact lenses similar to p-HEMA gels. Figure 3-12 shows the experimental data along with the model prediction based on the diffusivity obtained from fitting the drug uptake data. At equilibrium, due to a high partition coefficient of DXP, significant amount of the drug is still in the lenses. However, in an on-eye situation, the lenses would not be reaching equilibrium but be subjected to near perfect sink conditions which would lead to almost 100% release of the drug. The equations for a release with perfect sink condition would be

$$\frac{\partial C}{\partial t} = D_{eff}\frac{\partial^2 C}{\partial y^2} \tag{3-19}$$

$$C(y, t=0) = 0 \tag{3-20}$$

$$C(t, y=H) = 0 \tag{3-21}$$

$$\frac{\partial C}{\partial y}(t, y=0) = 0 \tag{3-22}$$

This can be analytically solved to give

$$\%\,\mathrm{Re}\,lease = 100 \times (1 - 8\sum_{n=0}^{n=\infty}\frac{1}{[(2n+1)\pi]^2}\exp\left[-\left((2n+1)\frac{\pi}{2h}\right)^2\frac{Dt}{K}\right]) \tag{3-23}$$

The expected release in the perfect sink environment is also shown in Figure 3-12.

Figure 3-13 compares photographs of control and 10% CAC loaded 1-Day ACUVUE® contact lenses containing a drop of water. The photographs clearly show that CAC loading does not affect the transparency of the contact lenses. The images also show that surfactant incorporation increases wettability as the drop of water spreads in the contact lens loaded with the surfactant, while the water is pooled at the bottom in the control lens.

Ocular delivery of DXP via eye drops requires hourly instillation of 1-2 drops of 0.1% solution during the day, with a slightly reduced frequency of once every two hours during the night. Assuming that 50 µl of drug solution is instilled each time, the amount of drug delivered to the eye is about 600 µg of drug for a 12 hr period. As stated before, the bioavailability of dug delivered via contact lenses has been found to be about 10 times greater than that of drug delivered via eye drops. Thus a contact lens loaded with

DXP should able to deliver about 60 µg of drug in 12 hrs. From the data for release of drug from 10% CAC loaded commercial lenses, it is observed that we are able to release about 50 µg of drug and a fairly constant rate (Fig 3-14). Also, the concentration of the drug loading solution was 0.1 mg/ml which is $1/10^{th}$ of concentration the commercial solution which is an added advantage.

Addition of surfactant not only affects the pore size of the gel but also increases ionic and hydrophobic interactions all of which can cause protein sorption to either increase or decrease. The effect of addition of an ionic surfactant to p-HEMA contact lenses on lysozyme sorption is shown in Figure 3-15. At 10% CAC loading, a drastic reduction in lysozyme uptake is observed. This can be beneficial in case of extended wear contact lenses being used for drug delivery.

3.3 Concluding Remarks

The idea of achieving extended delivery of an anionic drug (DXP) by cationic surfactant (CAC) loaded p-HEMA contact lenses has been explored. The chosen surfactant CAC has a sixteen unit long tail that leads to very strong interactions with the p-HEMA matrix. The strong binding of the surfactant to the tail ensures that negligible surfactant is released into PBS, thus minimizing the possibility of toxicity due to surfactant release in the tear film. The CAC incorporation increases drug loadings significantly, while also increasing the release durations. We propose that CAC binds to the gel polymer chains creating a charged surface which then interacts with the charged drug. Surfactant can be incorporated either pre-polymerization or post lens fabrication, thus making it easier to integrate this approach with current lens manufacturing approaches. The loading and release dynamics of drug are diffusion controlled, even for very thin gels showing that the time scale for adsorption and desorption are rapid.

Similar results can be reproduced for commercial p-HEMA contact lenses implying practicality of such a system. For the commercial contact lens loaded with surfactant, in a perfect sink condition, the drug release durations can be increased from less than 2 hrs to more than 50 hrs. Significant reduction of lysozyme (tear protein) sorption in CAC loaded lenses is an additional benefit. Thus, the surfactant loaded contact lenses provide several benefits including extended drug release, improved wettability and reduction in protein binding. The surfactant loading does not impact transparency but its impact on other can properties such as oxygen transport needs to be assessed and furthermore in vitro animal studies are necessary to establish the safety and efficacy of the lenses for drug delivery.

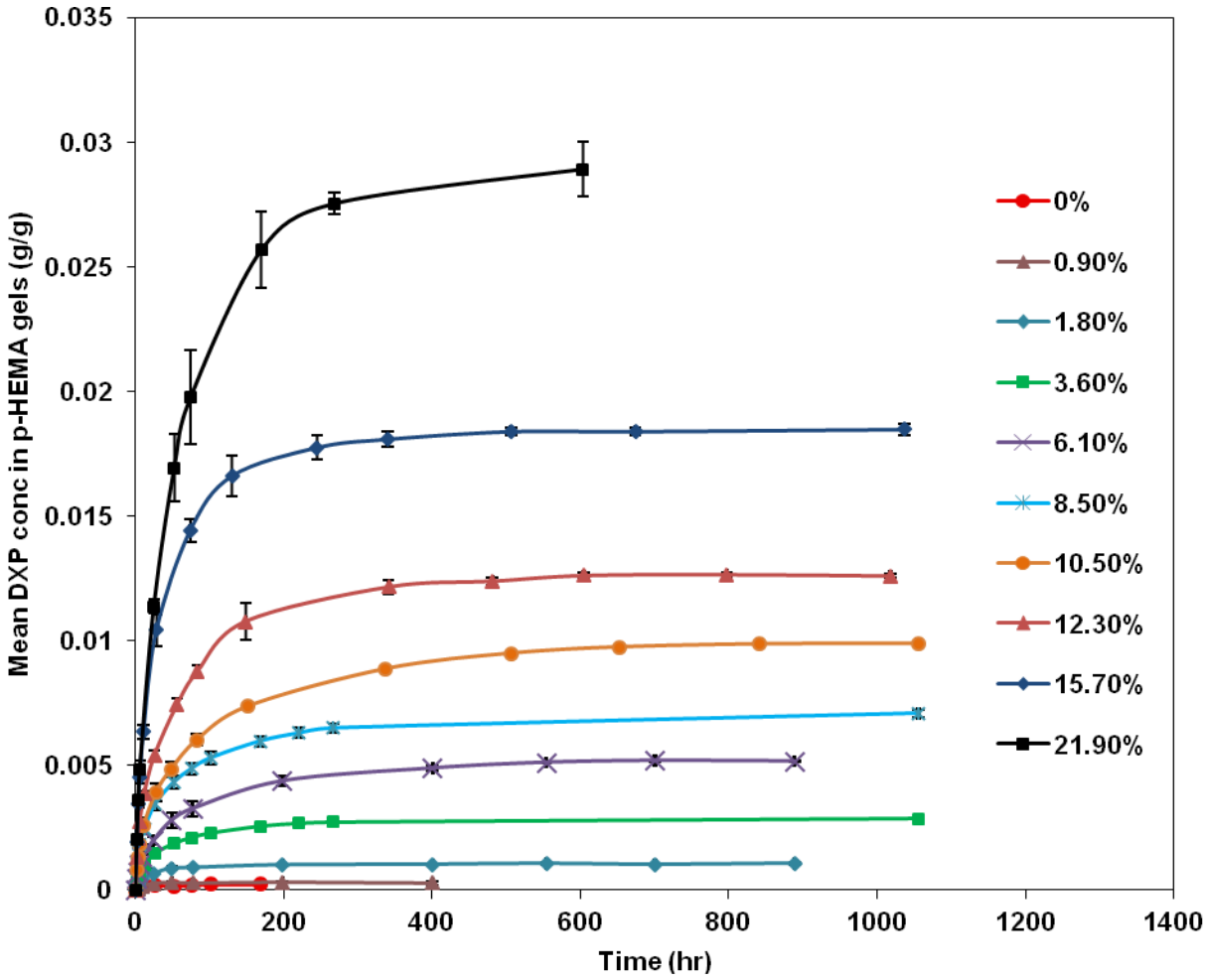

Figure 3-1. DXP loading dynamics for CAC loaded p-HEMA gels of thickness 240 µm soaked in DXP-PBS solution. Legend indicates CAC loading. Data are represented as mean ± S.D. with n = 3.

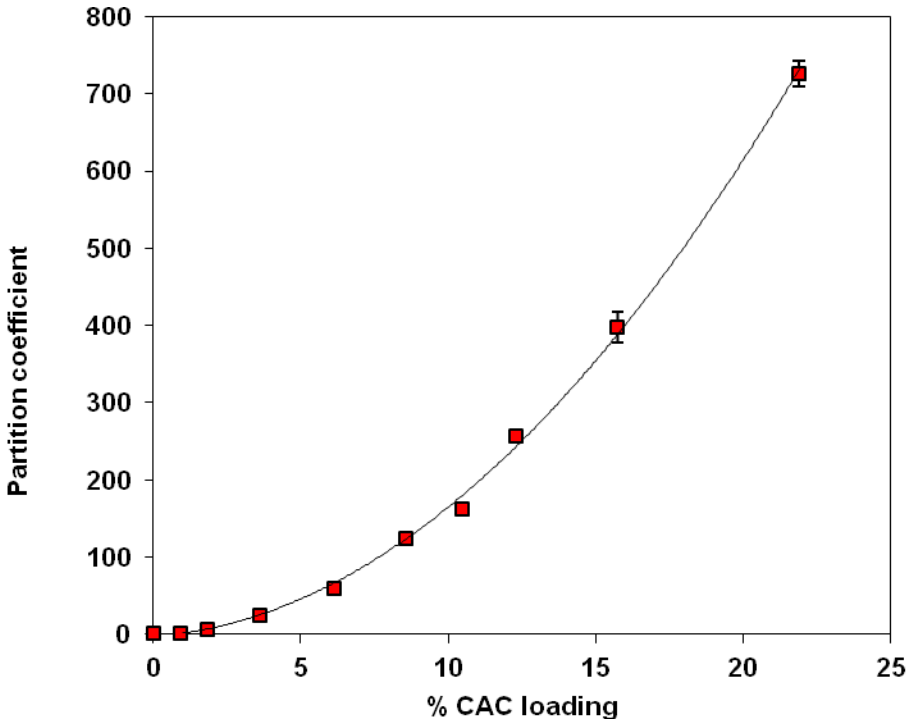

Figure 3-2. DXP partition coefficient as a function of CAC loading. Data are represented as mean ± S.D. with n = 6

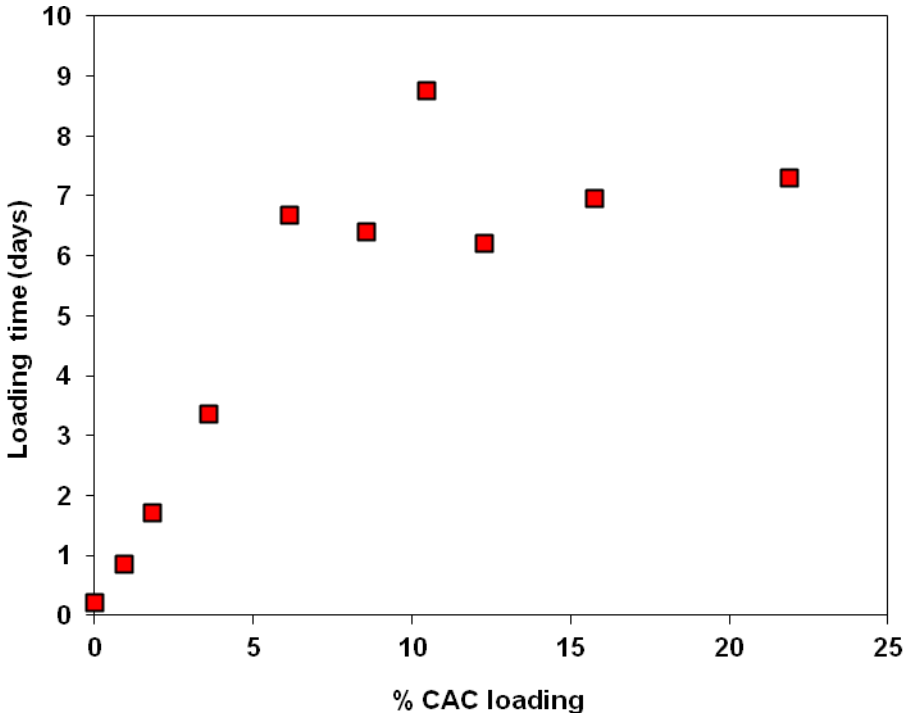

Figure 3-3. Equilibrium time for DXP loading as a function of surfactant concentration in p-HEMA hydrogel.

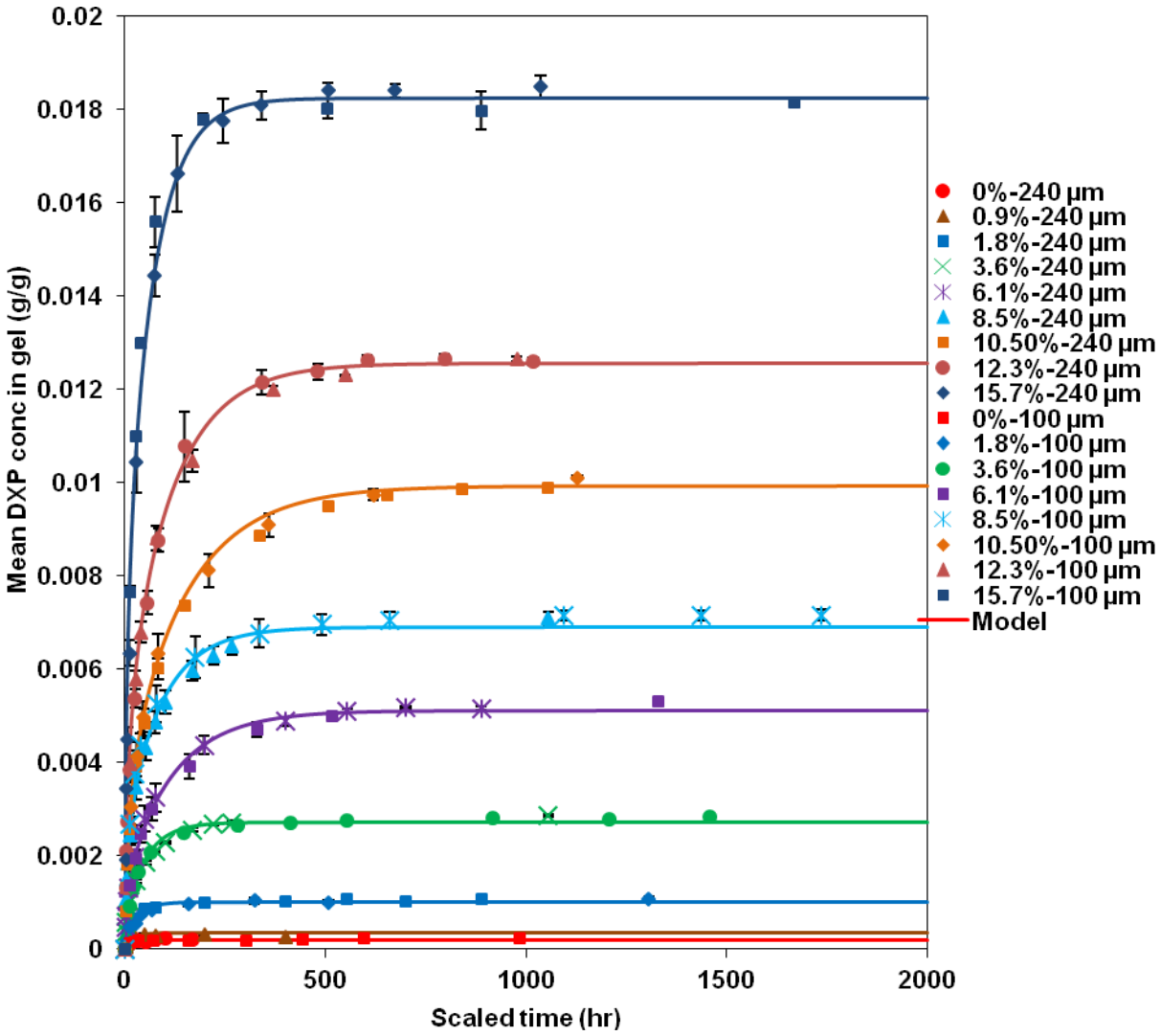

Figure 3-4. DXP loading dynamics for CAC loaded p-HEMA gels of thicknesses 100 and 240 µm soaked in DXP-PBS solution. Legend indicates CAC loading and gel thickness on a scaled time axis where reference thickness is 240 µm (Equation (3-3)). Data are represented as mean ± S.D. with n = 3. The model and experimental data are represented by a solid line and points, respectively.

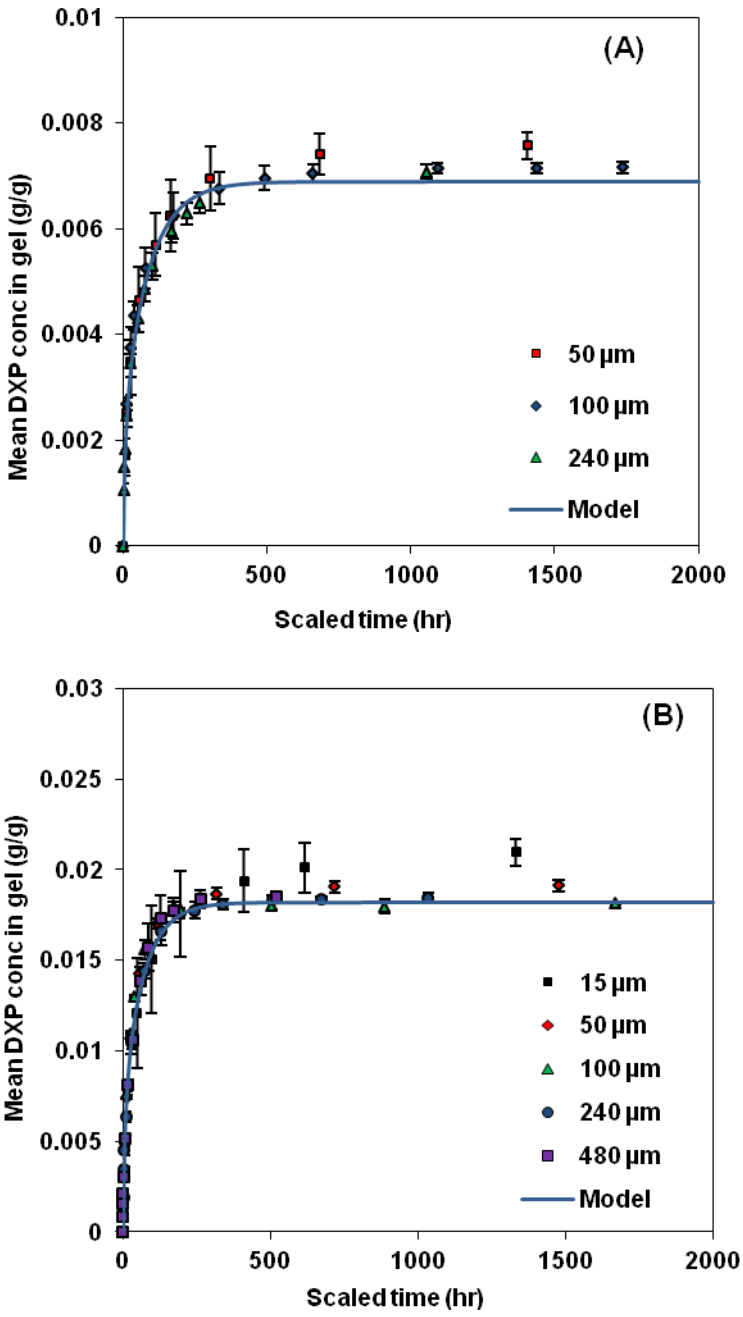

Figure 3-5. DXP loading dynamics by 8.5% CAC loaded gels A) and 15.7% CAC loaded gels. B) on a scaled time axis where reference thickness is 240 µm. Legend indicates gel thickness. Data are represented as mean ± S.D. with n = 3. The model and experimental data are represented by a solid line and points, respectively.

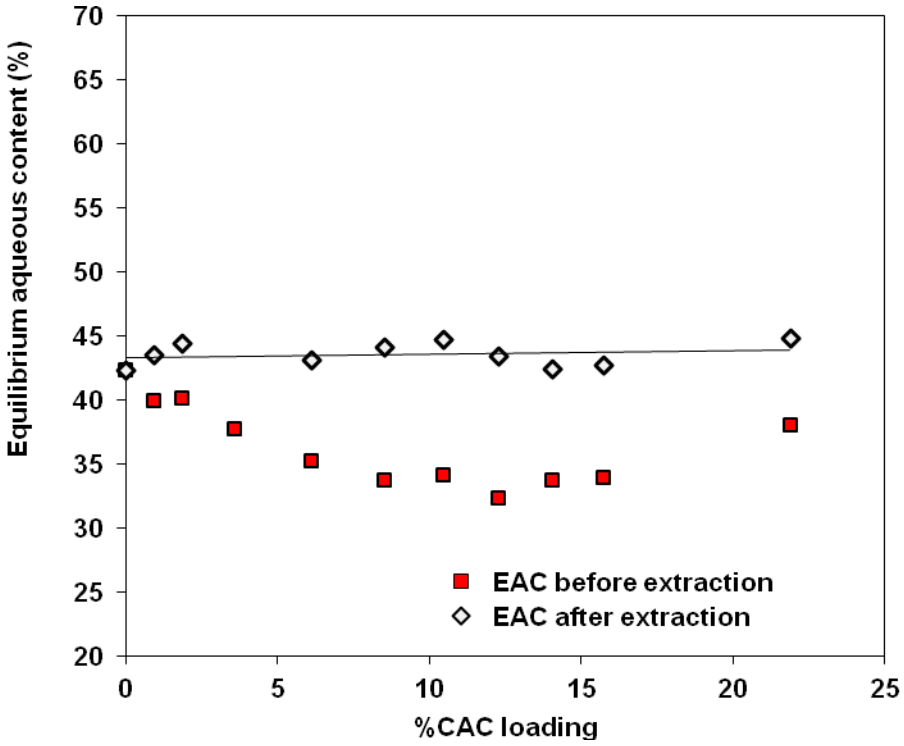

Figure 3-6. EAC of p-HEMA gels before (filled squares) and after surfactant extraction (open diamonds).

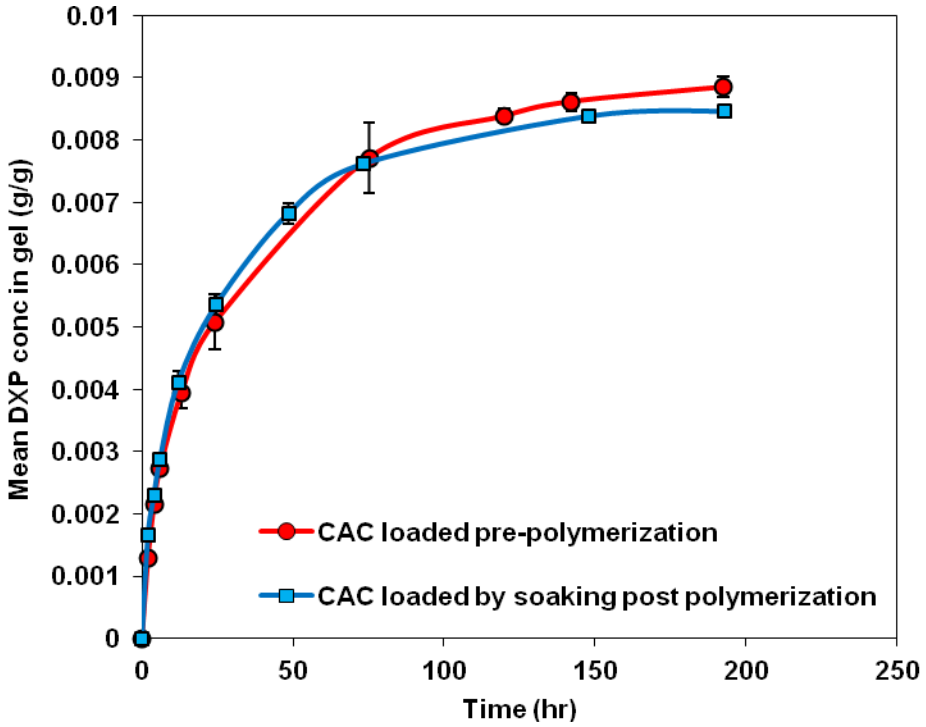

Figure 3-7. Comparison of DXP uptake by 240 µm p-HEMA gels with 8.5% CAC loaded by either direct addition to the polymerization mixture (red circles) followed by curing or by soaking gels in CAC-PBS solution (blue squares).

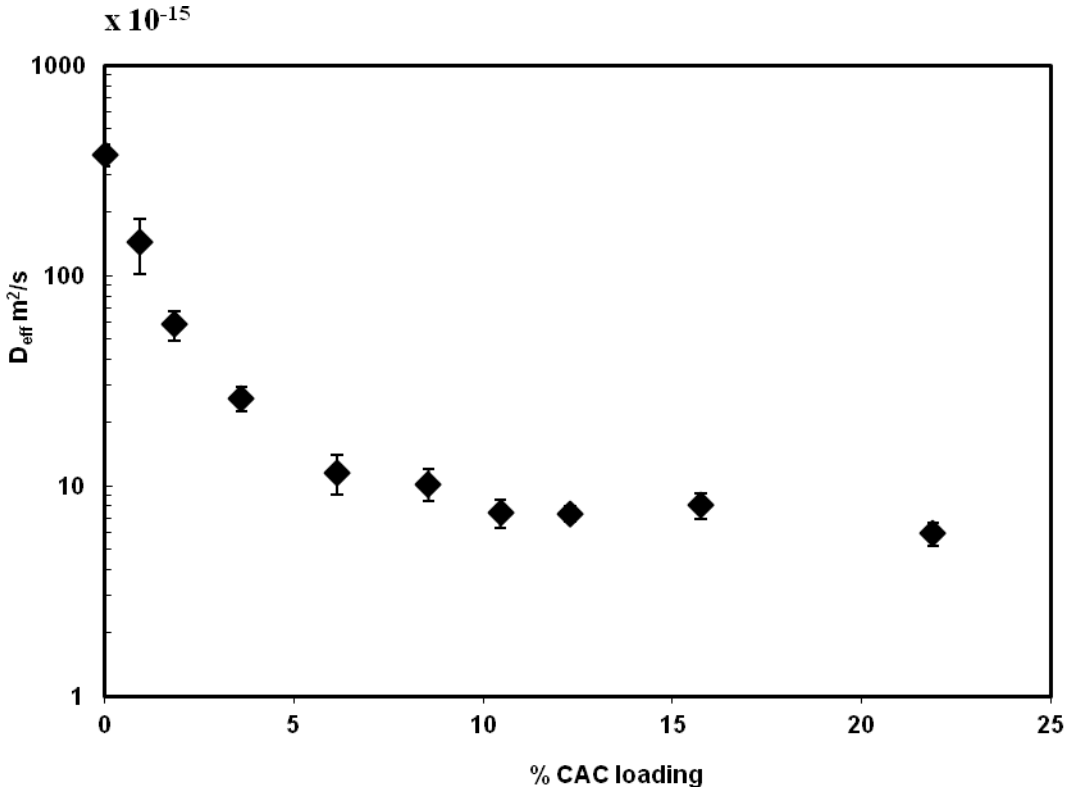

Figure 3-8. Effective Diffusivity of DXP in CAC loaded p-HEMA gels as a function of CAC loading. Data are represented as mean ± S.D. with n = 6

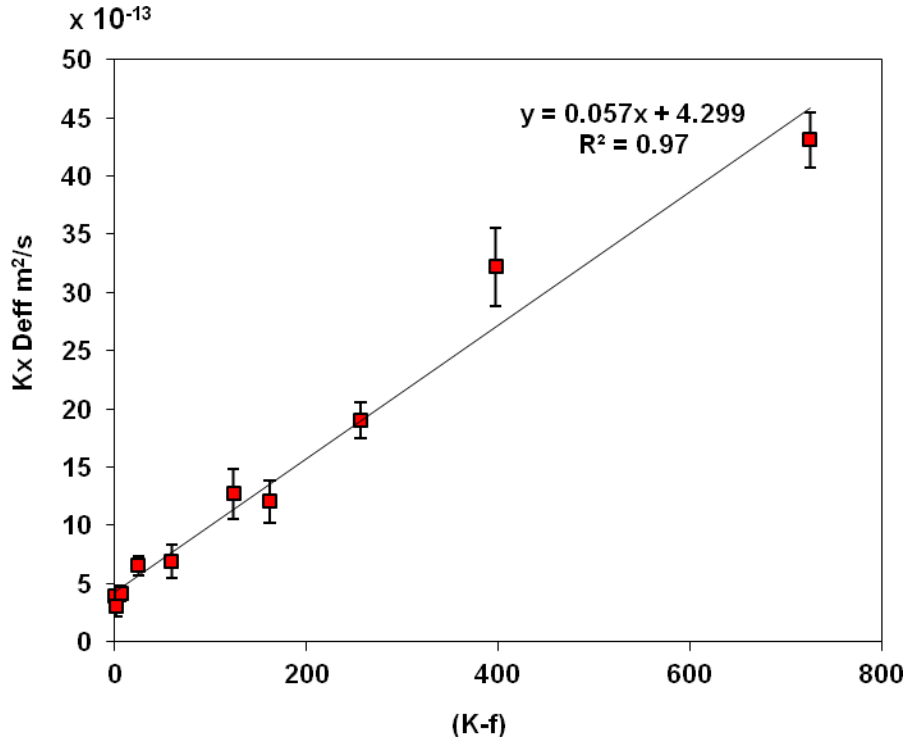

Figure 3-9. K x D_{eff} of DXP in CAC loaded p-HEMA gels as a function of (K-f). Data are represented as mean ± S.D. with n = 6

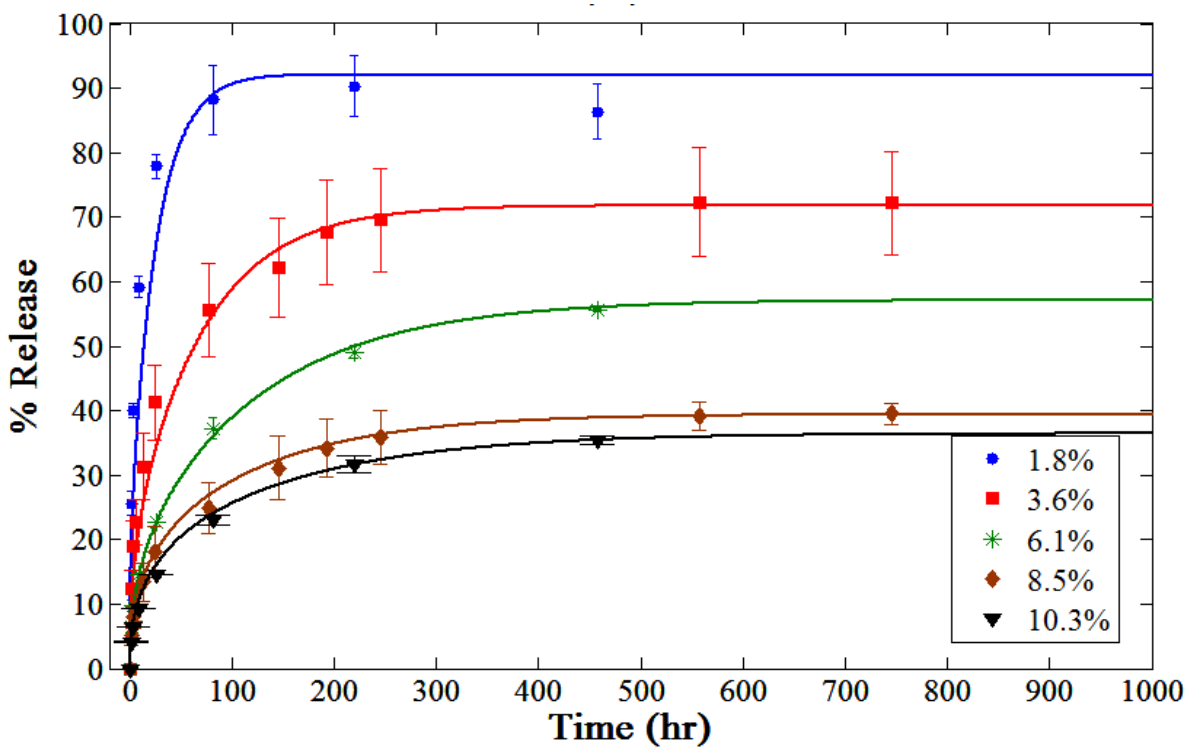

Figure 3-10. Profiles for percentage DXP release from 240 µm gels into 6 ml PBS. The CAC loadings are indicated in the legend. The model and experimental data are represented by a solid line and points, respectively. Data are represented as mean ± S.D. with n = 3.

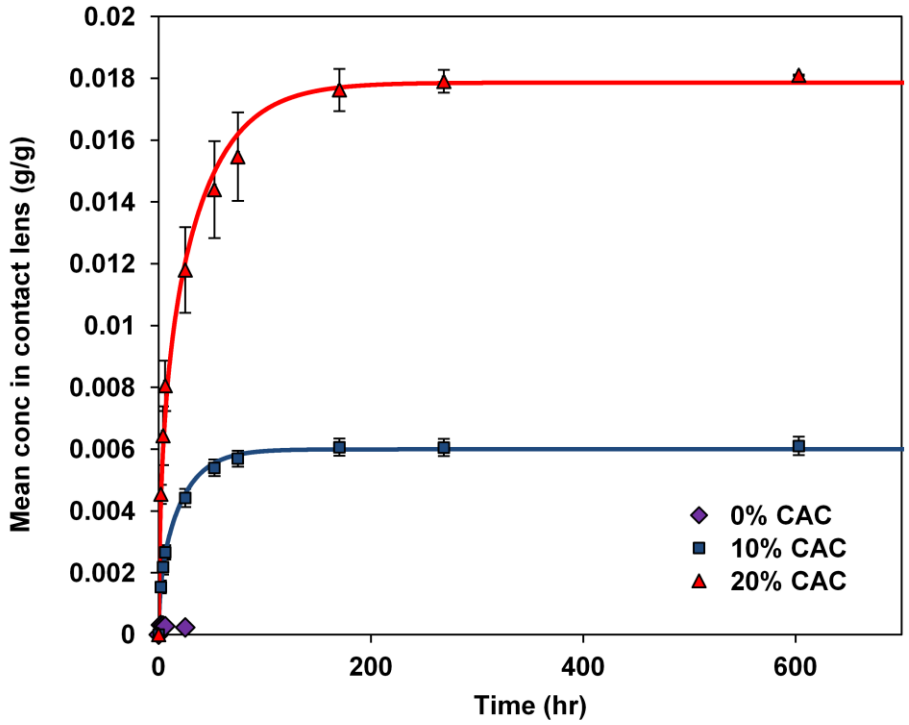

Figure 3-11. DXP loading profiles for commercial HEMA contact lens loaded with CAC. Legend indicates CAC loading. Data are represented as mean ± S.D. with n = 3. The model and experimental data are represented by a solid line and points, respectively.

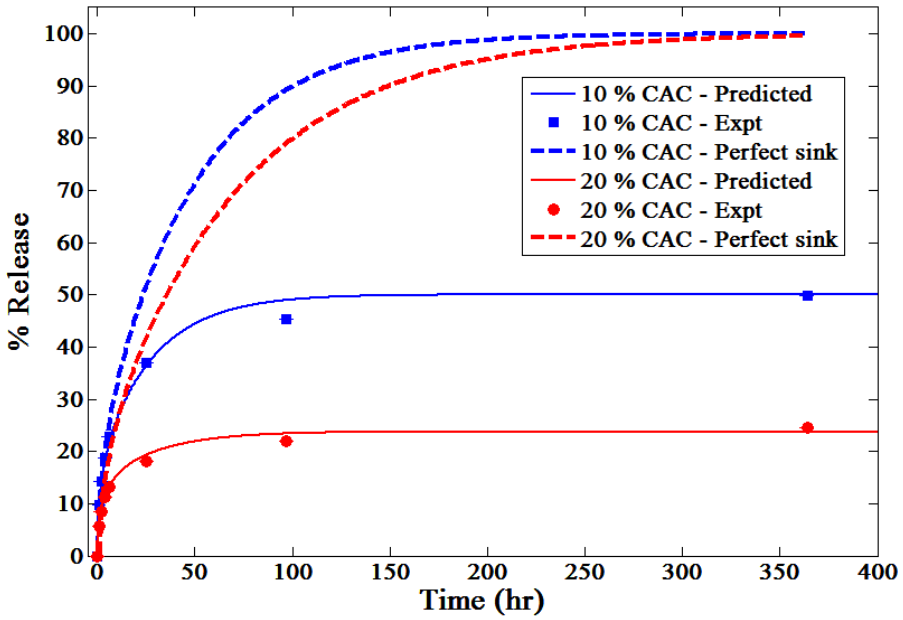

Figure 3-12. DXP release profiles for commercial HEMA contact lens loaded with surfactant. The predicted and experimental data are represented by a solid line and points, respectively. Data are represented as mean ± S.D. with n = 3. Predicted profiles with perfect sink release are shown as dashed lines.

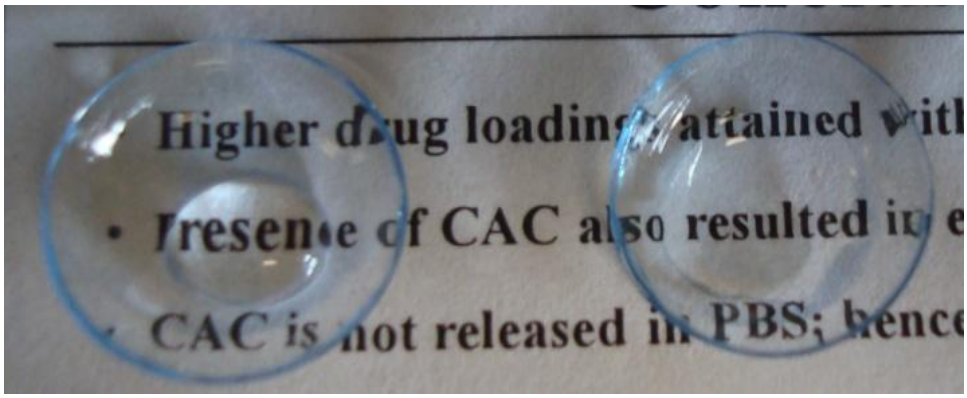

Figure 3-13. Photographs of control (left) and 10 % CAC loaded 1-Day ACUVUE® Contact lenses (right) containing a drop of water (0.1 ml).

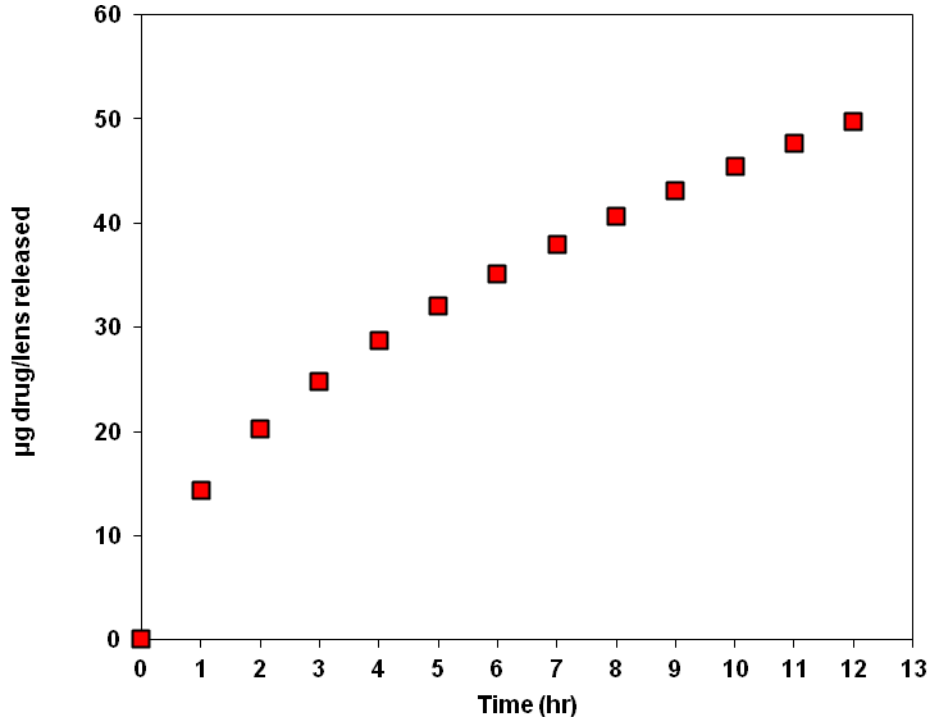

Figure 3-14. Amount of DXP delivered to eye by 10% CAC loaded 1-Day ACUVUE® contact lenses under perfect sink conditions

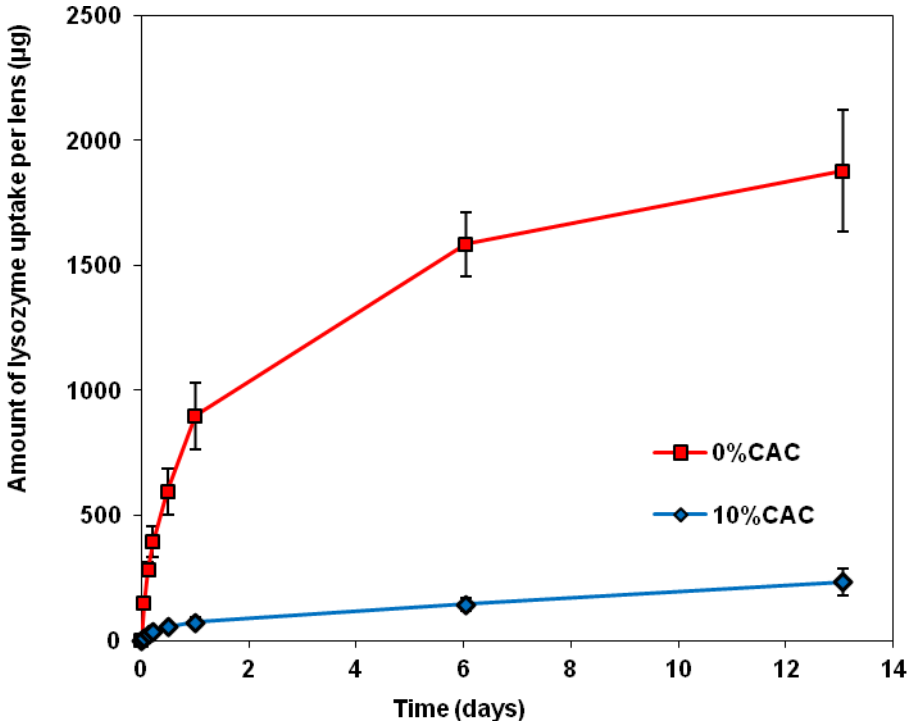

Figure 3-15. Lysozyme sorption in CAC loaded and pure 1-Day ACUVUE® lenses. CAC loading mentioned in legend.

Table 3-1. Effective diffusivity for DXP loading in CAC loaded p-HEMA hydrogels for various thicknesses

CAC %	15 µm	50 µm	100 µm	240 µm	p
0			24.1 ± 349.6	59.3 ± 385.9	0.89
0.9				30.9 ± 143.9	
1.8			8.52 ± 56.45	11.5 ± 60.89	0.52
3.6			2.77 ± 28.33	2.04 ± 23.61	0.16
6.1			2.83 ± 11.04	2.47 ± 11.97	0.7
8.5		3.31 ± 9.01	1.31 ± 12.45	1.35 ± 9.81	0.28
10.5			1.35 ± 6.93	0.95 ± 6.36	0.38
12.3			0.69 ± 7.43	0.59 ± 6.29	0.16
15.7	4.2 ± 8.36	0.92 ± 10.17	1.59 ± 14.47	0.41 ± 9.24	0.34
21.9				0.39 ± 5.94	

*Values shown as mean ± std. dev. (n = 3) x 10^{15} m^2/s. p is probability value for one way ANOVA test for different thicknesses.

CHAPTER 4
P-HEMA HYDROGELS WITH POLYMERIZABLE SURFACTANTS

4.1 Materials and Methods

4.1.1 Materials

2-Hydroxyethyl methacrylate (HEMA) monomer and ethylene glycol dimethacrylate (EGDMA) were purchased from Sigma-Aldrich Chemicals (St Louis, MO). Sodium chloride (99.9+%) was purchased from Fisher Scientific (Fairlawn, NJ). 2,4,6-trimethylbenzoyl-diphenyl-phophineoxide (Darocur® TPO) was kindly provided by Ciba (Tarrytown, NY). Noigen RN-10^{TM} (N10), Noigen RN30 ^{TM} (N30) and Hitenol BC30 ^{TM} (H30) were kindly provided by Montello Inc (Tulsa, OK). All the chemicals were reagent grade and were used without further purification.

4.1.2 Preparation and Purification of P-HEMA gels with Polymerizable Surfactants

The structures of the three polymerizable surfactants used in this study are shown in Figure 4-1. The N10 and N30 belong to the Noigen series with values of 10 and 30 for n, respectively, while H30 belongs to the Hitenol series with n = 30. The surfactant loaded gels were prepared by photo-polymerization of an aqueous solution of the surfactants, monomer (HEMA), crosslinker (EGDMA) and the initiator Darocur® TPO. The masses of HEMA, EGDMA, and the water were kept fixed, while the mass of the surfactant was increased to prepare gels with various surfactant loadings. The exact compositions of the solutions are included in Table 4-1. At higher surfactant loadings, the crosslinker content was increased to compensate the decrease in modulus. The solution was degassed to reduce the concentration of dissolved oxygen by bubbling nitrogen for 15 minutes. 12 mg of the photoinitiator (Darocur® TPO) was then added, accompanied by stirring at 750 rpm for 5 minutes to ensure complete dissolution of the

initiator. The solution was then poured in between two 5 mm thick glass plates that were separated from each other by spacers which were approximately 780, 240 and 100 µm in thickness. The mold was then placed on Ultraviolet transilluminiator UVB-10 (UltraLum, Inc.) and the gel was cured by irradiating UVB light (305 nm) for 40 min. The gels were removed from the glass plates and cut into rectangles pieces of the desired size. The unreacted monomer was removed by soaking the gels in boiling de-ionized (DI) water for 3 hours, and subsequently soaking in fresh DI water for another 20 hours at room temperature.

4.1.3 Hydrogel Characterization

4.1.3.1 Surface characterization

4.1.3.1.1 Contact Angle

The wettability of the gels was characterized by measuring the contact angle between the surface and a sessile water drop with a Drop Shape Analyzer (DSA100, KRUSS) using the Tangent method. A hydrated 240 µm thick gel was placed on a glass slide and the surface was lightly wiped with a Kimwipe® to remove any excess water. A small drop of DI water was then placed on the surface and the volume was slowly increased incrementally, while measuring the contact angle for each drop volume.

4.1.3.1.2 Surface friction

The surface lubricity was characterized by measuring the friction between an iron ball and the surface using an in-house apparatus. A hydrated square piece of gel approx. 1.5 x 1.5 cm was placed on glass slide resting on an inclined plane whose angle could be precisely controlled. A metal ball weighing 0.264 g was placed on the gel and the angle of the inclined plane was gradually increased until the ball started rolling.

The coefficient of friction was calculated as the tangent of the rolling angle. 4 measurements were conducted for each gel and 3 gel samples were utilized with identical composition.

4.1.3.2 Bulk Characterization

4.1.3.2.1 Equilibrium water content (EWC)

After extraction, the gels were dried and weighed to obtain W_{dry}. The gels were then soaked in water for sufficient duration to achieve equilibrium. The final equilibrium weight (W_{wet}) was measured. The surface of the gels was gently wiped with Kimpwipes® before each measurement. The water content of the gels was determined by

$$\%EWC = \frac{(W_{wet} - W_{dry})}{(W_{wet})} \times 100 \quad (4\text{-}1)$$

4.1.3.2.2 Transmittance

The transmittance of 100 μm thick hydrated gels ($T(\lambda)$) was measured using UV-Vis spectrophotometer (Thermospectronic Genesys 10 UV) at wavelengths ranging from 200 nm to 700 nm. The average transmittance from 600 nm to 700 was calculated to characterize the visual clarity. The UV absorbance spectra $A = -\log_{10}(T/100)$ was used to quantify the average concentration of the surfactant in the lens using the Beer Lambert's law, i.e., $A = A_{HEMA} + \varepsilon(\lambda)cl$, where A_{HEMA} is the absorbance of the control HEMA gel, $\varepsilon(\lambda)$ is the molar absorptivity, c is the concentration and l (=100 μm) is the path length. The absorbance spectra of hydrated 100 μm thick p-HEMA gel was measured to obtain A_{HEMA} and the molar absorptivity of the surfactant $\varepsilon(\lambda)$ was

determined by measuring the absorbance of aqueous surfactant solutions at a concentration of 0.01% (w/w) and using the Beer Lambert law with l = 1 cm.

4.1.3.2.3 Mechanical properties

The storage modulus of hydrated rectangular 780 µm thick gels was measured using a dynamic mechanical analyzer (DMA Q800, TA instruments) using a submersion tension clamp at room temperature. A preload force applied 0.01N and force track was 115% used and strain sweep tests were recorded to confirm the linear range at room temperature at 1 Hz. Subsequently, frequency dependent storage modulus and loss modulus was obtained by fixing the strain within the linear range.

4.1.3.2.4 Ion permeability

A circular hydrogel of 1.65 cm diameter was soaked in 3.5 ml of 1 M NaCl solution until equilibrium was achieved. The salt-loaded gel was then transferred into a well-mixed 27.5 ml DI water maintained at room temperature. The conductivity of the solution was periodically measured by Con 110 series sensor (OAKTON®) and the salt concentration was then determined through the calibration curve, which was linear with a slope of 8.58×10^{-6} M/µs. The dynamic salt concentration was fitted to a sink release model to calculate the effective ion diffusivity in the lens.

4.2 Results and Discussion

4.2.1 Transmittance

Figure 4-2 shows the transmittance spectra of hydrated 100 µm thick gels for wavelengths ranging from 200-700. The lenses are identified by the name of surfactant followed by the weight ratio of the surfactant and HEMA in the formulation. The visual clarity was characterized by calculating the average transmittance for 600 – 700 nm range (Table 4-2). Table 4-2 also shows the average transmittance values for UVA

(315-400 nm) and UVB (280-315 nm) radiation. All lenses transmit about 100% of the light in the visible and UVA spectrum. The UVB transmittance decrease significantly on surfactant incorporation, which is an additional benefit because UV radiation has the potential to cause ocular damage. The molar absorptivity of the surfactants was obtained by measuring the absorbance in aqueous solutions at 0.01% (w/w). The surfactant concentration in each gel was then obtained by fitting the absorbance spectra $A(\lambda)$ to the Beer Lambert law, i.e., $A = A_{HEMA} + \varepsilon(\lambda)cl$ using a least square fit. The fitted value of the concentration was used to determine the fractional conversion, i.e, the ratio of the surfactant concentration in the gels after the extraction and the originally loaded concentration. The % conversions reported in Table 4-2 depend strongly on the type of the surfactant. The conversions for the N30 surfactant decrease with increasing surfactant concentration ranging from about 18 to 4% for initial loadings of 1 and 30%, respectively. For the N10 surfactant, the conversion appears to relatively constant at about 29% for initial loadings varying from 3.5 to 15%. It was not feasible to reliably calculate the surfactant concentration in gels with higher loadings because the transmittance increases very rapidly from 0 to 100% over a short wavelength range and the approach of determining the concentration loses sensitivity. The conversions are higher for the N10 compared to the N30 most likely due to the stearic effects of the longer hydrophilic chain. The conversions for the H30 surfactants are even lower than the N30, which shows that the end group capping the hydrophilic chain plays significantly impacts the reactivity of the surfactant monomer. Since the conversions are very low for the H30 gels, these were not included in any of the characterization studies

described below. The low conversions in general suggest that the reactivity of the vinyl group in these surfactants is lower than the reactivity in HEMA.

4.2.2 Contact Angle

The contact angles of a water drop in contact with the gels are listed in Table 4-3 along with the equilibrium water content. Also some representative images of the sessile drops are included in Figure 4-3. The results clearly demonstrate that surfactant incorporation in the lenses significantly reduces the contact angle from 900 for p-HEMA gels to less than 100 for the N10 gels with initial loadings of greater than 30%. For the N10-50% hydrogel, the contact angle could not be measured since the drop of water spread spontaneously into a thin film, implying a contact angle of about zero degree. To compare the effect of various surfactants, the contact angles for the various gels are plotted in Figure 4-4 as a function of the moles of surfactant retained in the gel after the extraction. Since it was not possible to estimate the surfactant remaining for N10-30% gels, 29% conversion was assumed since that was the average conversion for the rest of gels containing N10. The data shows that the contact angle reduction is relatively independent of the surfactant type as the data for all the surfactants collapses on the same curve even though the N10 surfactants have a higher molar concentration due to the smaller molecular weight. The contact angle decreases with increasing surfactant concentration, but the rate of the decrease becomes smaller with increasing loadings, possibly due to saturation of the surface active groups at the surface. The on-eye contact angles are expected to be lower than the in vitro measurements because adsorption of the tear components (lysozyme and lipids) can lead to reduction of contact angle [117,118].

4.2.3 Surface Friction

The coefficient of friction between a metal ball and the hydrated hydrogels are listed in Table 4-3 along with the concentrations of surfactant in the gels and the water content. The coefficient of friction is significantly lower for the surfactant loaded gels compared to the p-HEMA gel. The N30 gel with 0.19% surfactant (2% in the formulation) has a friction coefficient of 0.097 compared to 0.162 for the HEMA gel. The N10 gel with 0.56% surfactant (3.5% in the formulation) also has a significantly smaller coefficient of 0.065. A plot of the friction coefficient and the surfactant concentration in the gel shows that friction decreases rapidly with surfactant incorporation but the rate of decrease becomes smaller at high concentrations (Figure 4- 5). This behavior is similar to the effect of surfactant on the contact angle suggesting that the contact angle and the friction coefficient are correlated. However it is difficult to accurately assess the correlation between the contact angle and friction coefficient because the sensitivity of the friction measurements are low.

4.2.4 Water Content

The water content increases on incorporation of the polymerizable surfactants as shown in Table 4-3. The dynamics of water transport were also measured for a few of the systems and results plotted in Figure 4-6 show that the water transport dynamics are not impacted by surfactant incorporation. The water content in the p-HEMA gels is correlated to the oxygen permeability, and thus increasing water content without impacting the rates of transport is desirable.

4.2.5 Mechanical Properties: Storage Modulus

Incorporation of surfactants is expected to make the contact lenses softer, which could increase comfort but may also make contact lens insertion in the eye very difficult.

It was thus important to measure the effect of surfactant incorporation on modulus. The frequency dependent storage modulus is plotted in Figure 4-7A and B for the N10 and N30 gels, and the zero-frequency intercepts are listed in Table 4-4. The loss modulus was also measured (data not shown). The degree of crosslinking is explicitly included in the lens description because of its strong impact on the moduli. 1X and 3X denote 20 and 60 µl of EGDMA, respectively in the formulation, while keeping amounts of all other components unchanged (Table 4-1). The results in Figure 4-7 and in Table 4-4 show that the modulus slightly decreases with increasing surfactant incorporation likely due to the increased water content. The data also shows that an increase in the degree of crosslinking increases the modulus, and thus it counteracts the effects of increasing surfactant loading.

4.2.6 Ion Permeability

A contact lens needs adequate transport of ions to maintain on-eye movement. An increased crosslinking that is required to counteract the effect of decrease in modulus with surfactant incorporation could potentially reduce the ion permeability. To test this effect the ion permeability was measured for a few illustrative systems. The data in Figure 4-8 shows that both surfactant incorporation and increase in crosslinking have a minor effect on the ion permeability. The change in the ion permeability could be correlated to the change in water content as shown in the inset of the figure.

4.3 Concluding Remarks

The contact angle and coefficient of friction of p-HEMA hydrogels could be significantly reduced by the incorporation of polymerizable surfactants. This decrease will likely improve wettability and lubricity, and thus improve comfort. Both N10 and N30 Noigen surfactants decreased contact angle and friction coefficient, but the N10

surfactant is more suitable because of its higher incorporation into the lens matrix. The surfactant incorporation does not appear to significantly impact any other critical property and so its incorporation into the lenses could improve surface properties without any adverse effect on the bulk properties. Based on this study we conclude that a p-HEMA contact lens with 30% of the N10 surfactant in the formulation is an excellent candidate for further in vitro characterization and in vivo comfort studies.

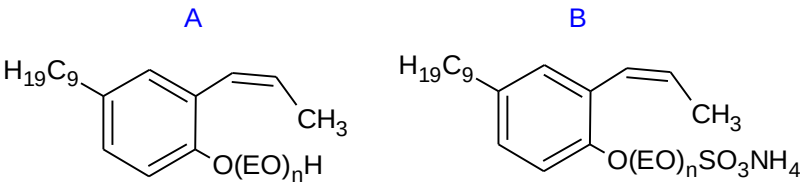

Figure 4-1. Structure of the polymerizable surfaces A: Noigen series and B: Hitenol series.

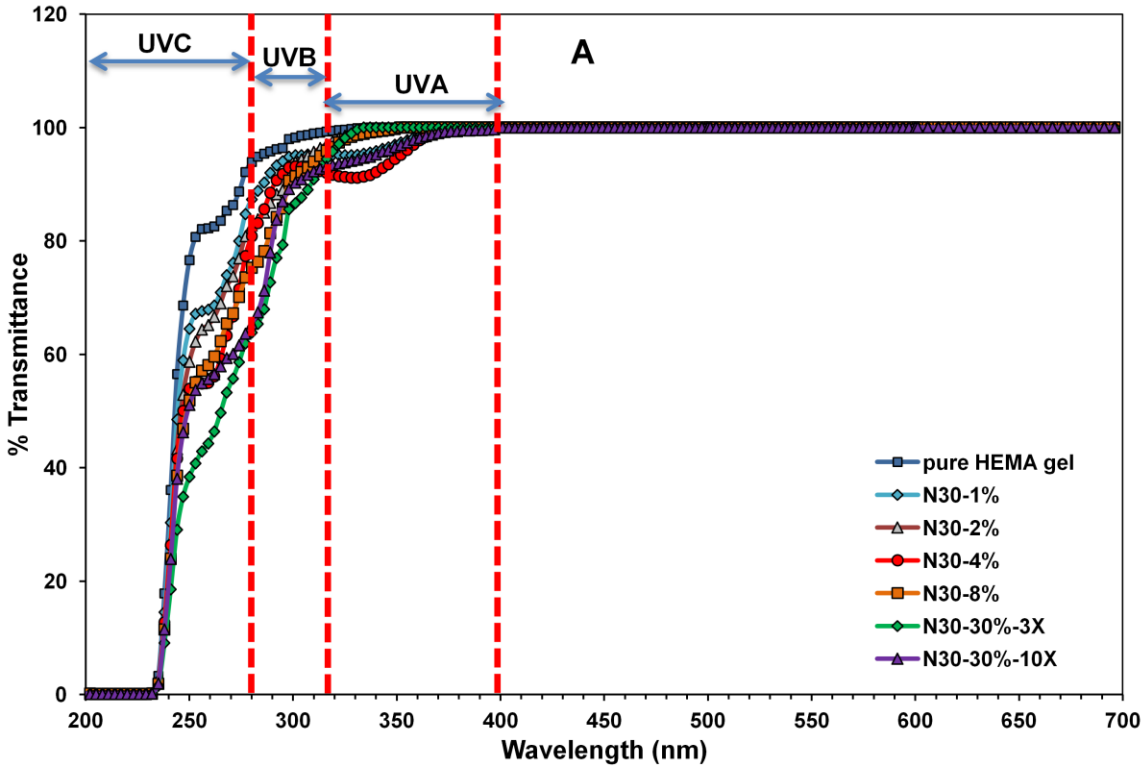

Figure 4-2. Transmittance spectra of p-HEMA gels with different polymerizable surfactants A) N30. B). N10. C) H30

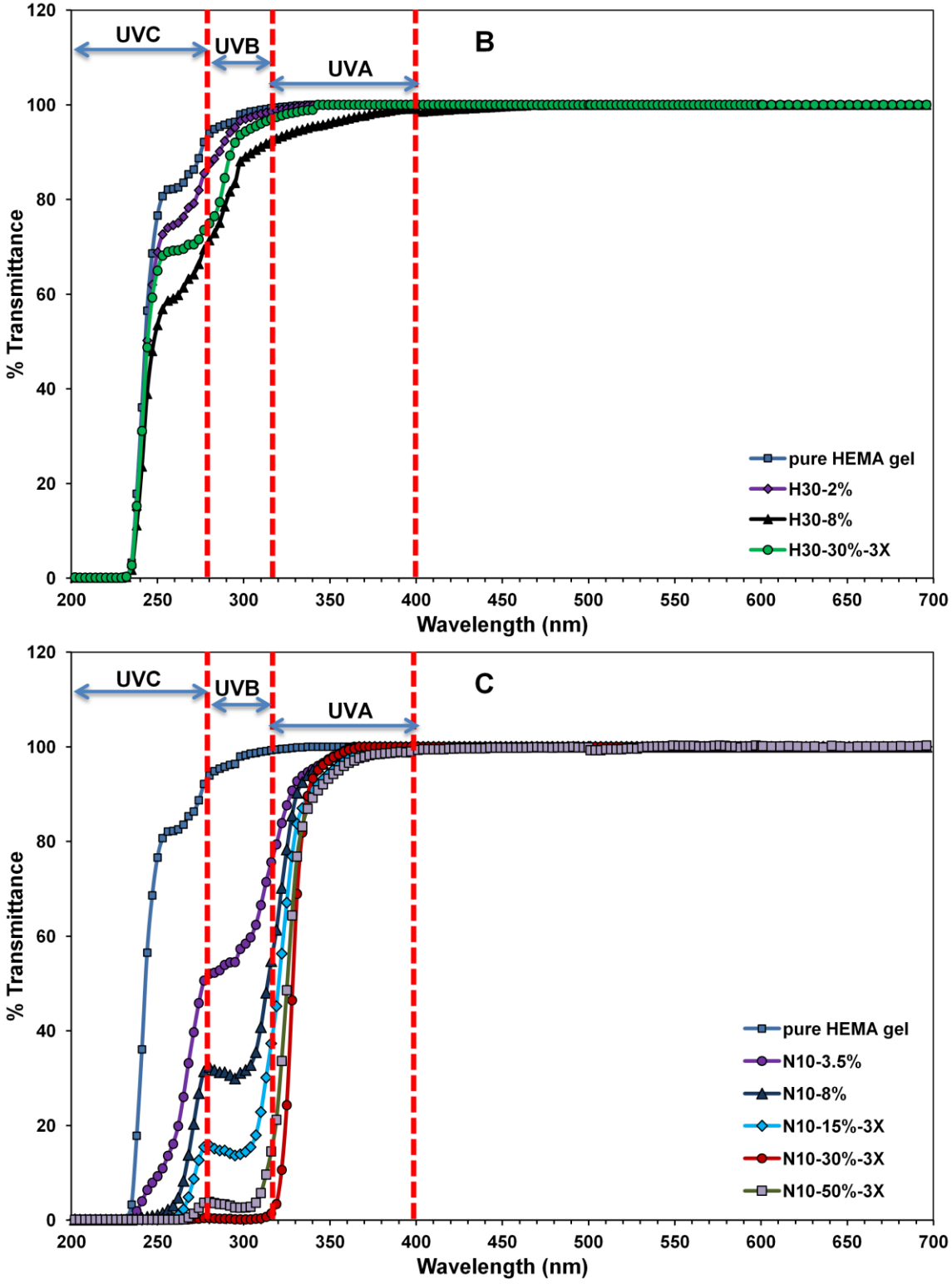

Figure 4-2. Cont.

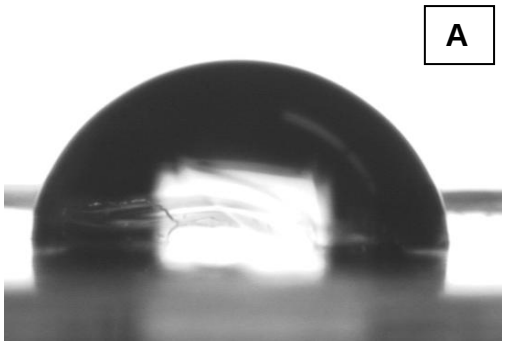

Figure 4-3. Image of a sessile drop on A) p-HEMA hydrogel B) Surfactants loaded gels

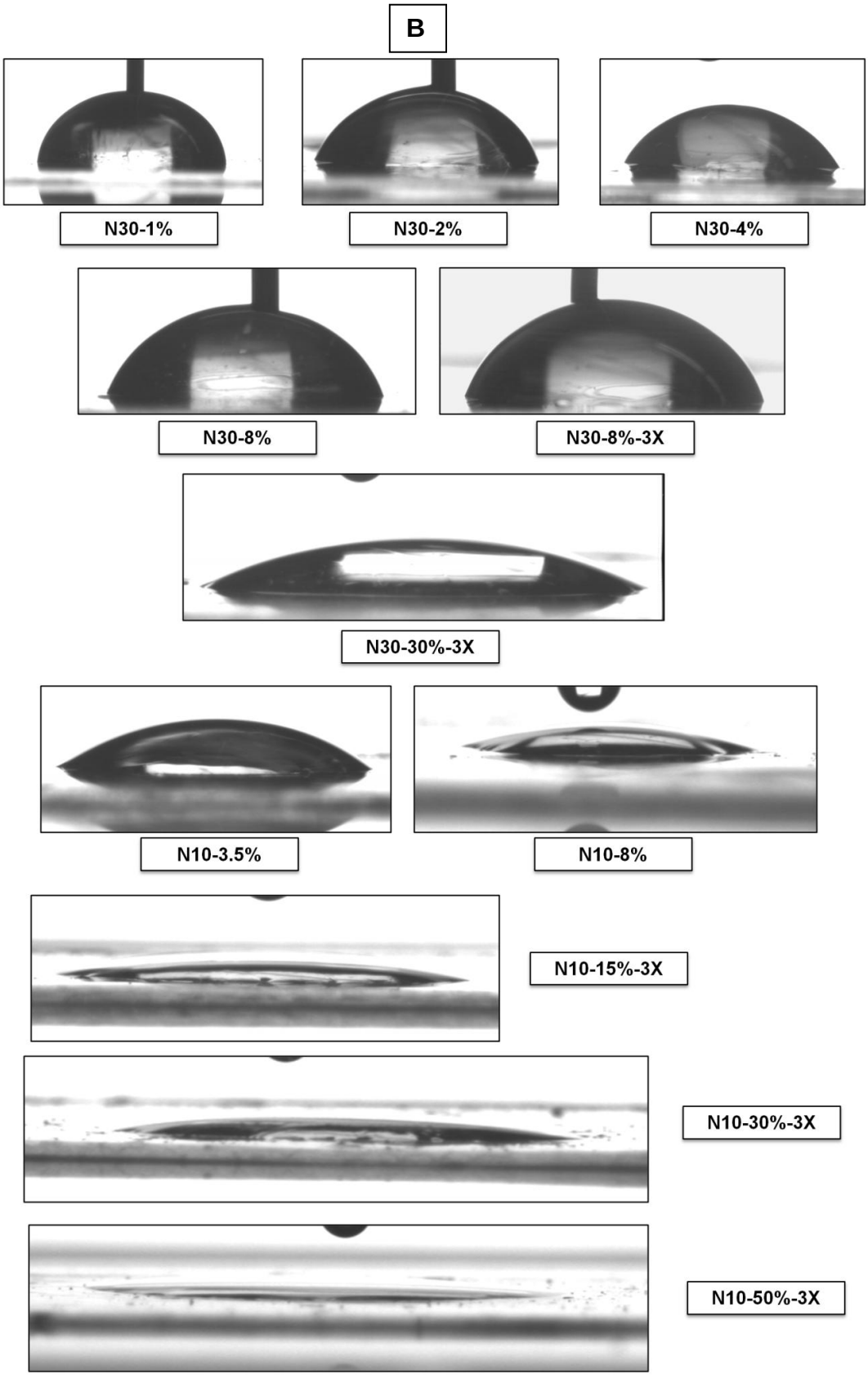

Figure 4-3. Cont.

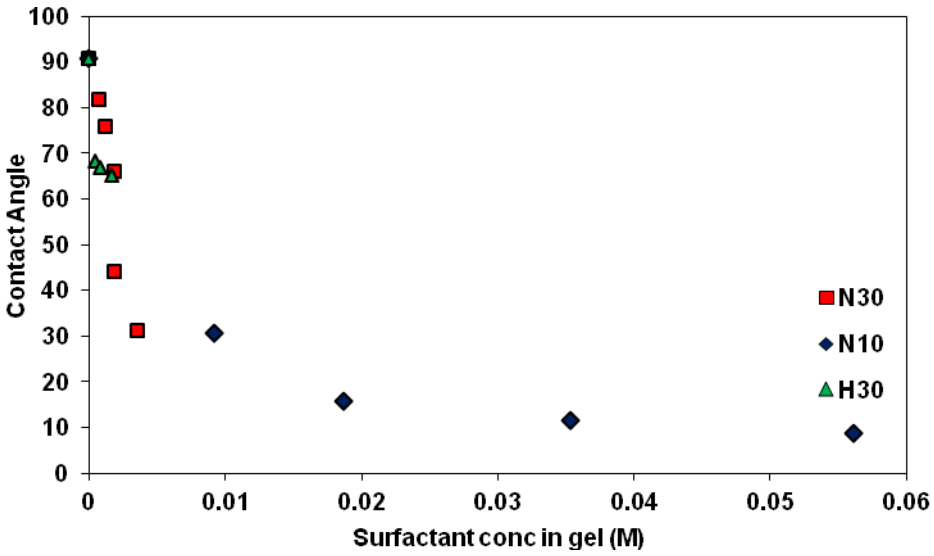

Figure 4-4. Effect of surfactant concentration in the gel on contact angle.

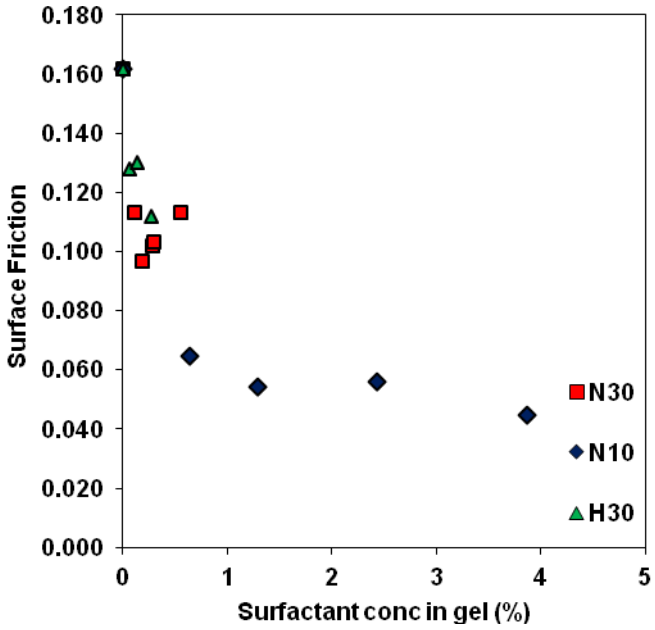

Figure 4-5. Variation of surface friction with surfactant incorporation

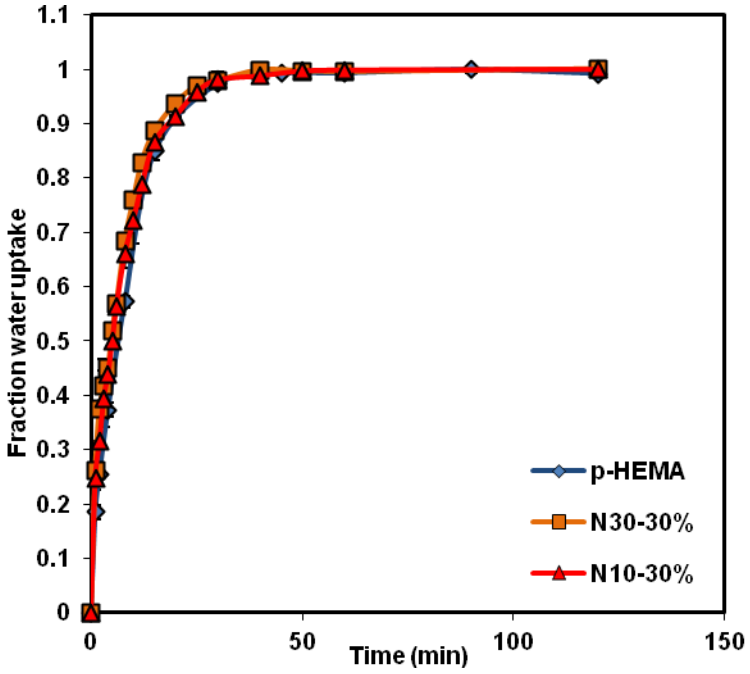

Figure 4-6. Dynamics of water transport in p-HEMA and modified p-HEMA gels. Data represented as mean ± std dev (n=3)

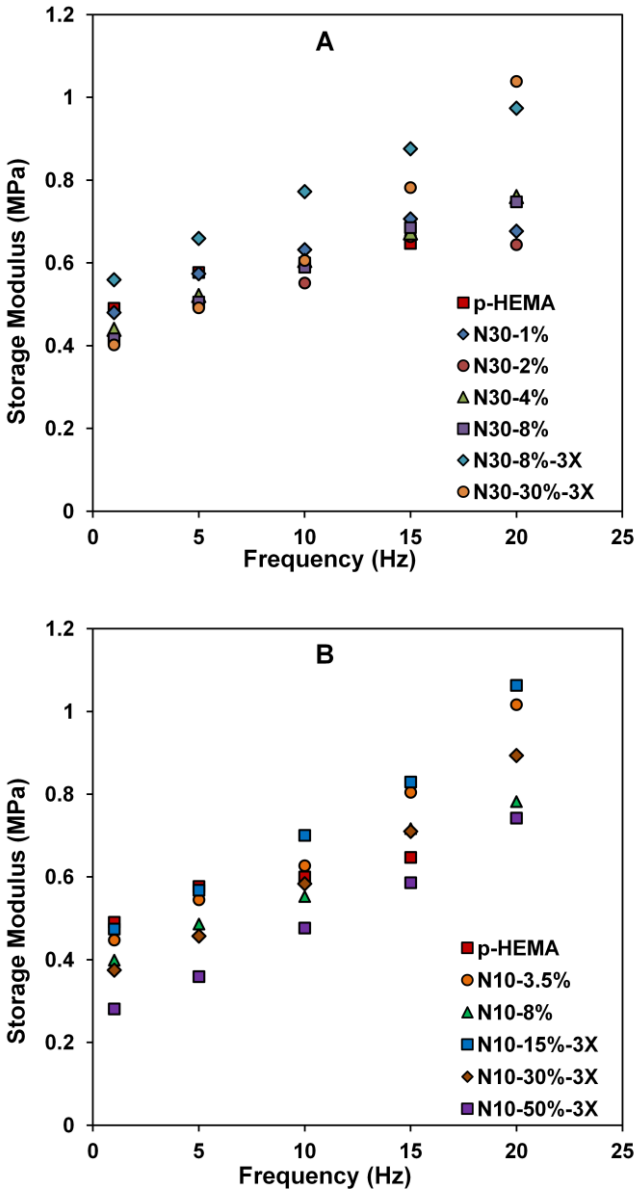

Figure 4-7. Frequency dependent storage modulus for the surfactant loaded gels A) N30. B) N10 gels.

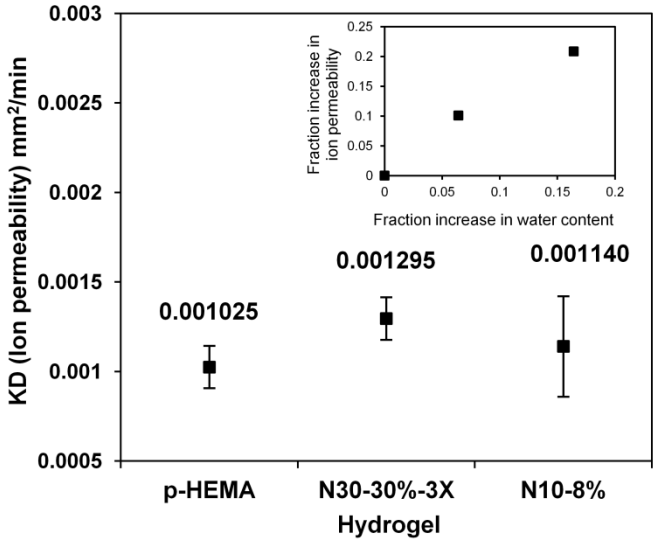

Figure 4-8. Ion permeability of p-HEMA, N30-30%-3X and N10-8% gels

Table 4-1. Composition of the polymerizing solutions

Gel name	Pzsurf	Surfactant / HEMA g/ml	HEMA ml	Water ml	Pzsurf g	EGDMA µl
p-HEMA	None	0	5.4	4	0	20
N30-1%	N30	1	5.4	4	0.054	20
N30-2%	N30	2	5.4	4	0.108	20
N30-4%	N30	4	5.4	4	0.216	20
N30-8%	N30	8	5.4	4	0.432	20
N30-30%-3X	N30	30	5.4	4	1.62	60
N30-30%-10X	N30	30	5.4	4	1.62	200
N10-3.5%	N10	3.5	5.4	4	0.19	20
N10-8%	N10	8	5.4	4	0.432	20
N10-15%-3X	N10	15	5.4	4	0.81	60
N10-30%-3X	N10	30	5.4	4	1.62	60
N10-50%-3X	N10	50	5.4	4	2.7	60
H30-2%	H30	2	5.4	4	0.108	20
H30-8%	H30	8	5.4	4	0.432	20
H30-30%-3X	H30	30	5.4	4	1.62	60

Table 4-2. % Transmittance and % conversion in surfactant loaded gels

Gel	Surfactant loading % * Initial Formulation	Remaining surfactant % ** After Extraction	Conversion %	Mean transmittance			
				Visible	UVA	UVB	UVC
HEMA	0	0		100	100	97.45	38.58
N30-1%	0.637	0.117	18.38	100	98.36	94.67	33.98
N30-2%	1.244	0.189	15.19	100	99.60	90.60	30.98
N30-4%	2.438	0.282	11.58	100	96.79	91.16	28.68
N30-8%	4.652	0.290	6.23	100	98.72	87.35	28.37
N30-30%-3X	13.15	0.556	4.23	100	100	82.43	22.52
N30-30%-10X	14.76	0.316	2.14	100	97.81	86.08	26.55
N10-3.5%	2.165	0.634	29.29	100	97.05	58.92	11.22
N10-8%	4.561	1.290	28.27	100	95.68	36.82	5.18
N10-15%-3X	7.888	2.433	30.85	100	88.38	18.69	2.23
N10-30%-3X	13.32	n/a		100	86.02	0.41	0.20
N10-50%-3X	18.70	n/a		100	83.32	4.82	0.52
H30-2%	1.228	0.065	5.30	100	100	95.18	34.66
H30-8%	4.632	0.275	5.94	100	97.54	86.18	27.84
H30-30%-3X	14.44	0.140	0.97	100	99.23	90.69	32.19

* On hydrated wt. basis assuming 100% conversion for surfactant to polymer

** On hydrated wt. basis

Table 4-3. Effect of surfactant incorporation on contact angle, coefficient of friction and water content

Gel	Water Content %	Contact Angle deg	Surface Friction
p-HEMA	35.96 ± 0.14	90.7 ± 1.3	0.162 ± 0.027
N30-1%	35.67 ± 0.15	81.8 ± 3.2	0.113 ± 0.016
N30-2%	36.56 ± 0.30	75.7 ± 6.2	0.097 ± 0.007
N30-4%	36.60 ± 0.54	66.0 ± 7.1	0.102 ± 0.018
N30-8%	37.20 ± 0.47	44.3 ± 15.8	0.103 ± 0.018
N30-30%-3X	43.02 ± 0.35	31.3 ± 10.8	0.113 ± 0.016
N30-30%-10X	36.03 ± 0.58	28.1 ± 6.8	0.085 ± 0.017
N10-3.5%	35.97 ± 0.50	30.7 ± 7.7	0.065 ± 0.018
N10-8%	38.42 ± 1.16	15.7 ± 3.9	0.054 ± 0.015
N10-15%-3X	39.53 ± 0.25	11.6 ± 3.9	0.056 ± 0.017
N10-30%-3X	42.26 ± 0.22	8.8 ± 2.9	0.045 ± 0.014
N10-50%-3X	43.90 ± 0.28	n/a	0.047 ± 0.015
H30-2%	37.36 ± 0.91	68.3 ± 7.2	0.128 ± 0.025
H30-8%	37.47 ± 0.25	65.2 ± 9.5	0.112 ± 0.020
H30-30%-3X	37.41 ± 0.38	67.0 ± 6.2	0.130 ± 0.023

Table 4-4. Zero-frequency storage modulus for the surfactant loaded gels

Gel	Storage Modulus at 0 Hz
p-HEMA	0.498
N30-1%	0.478
N30-2%	0.409
N30-4%	0.432
N30-8%	0.410
N30-8%-3X	0.546
N30-30%	0.330
N10-3.5%	0.390
N10-8%	0.375
N10-15%-3X	0.420
N10-30%-3X	0.329
N10-50%-3X	0.244

.

CHAPTER 5
TRANSPORT OF LYSOZYME IN P-HEMA HYDROGELS

5.1 Materials and Methods

5.1.1 Materials

2-Hydroxyethyl methacrylate (HEMA) monomer, ethylene glycol dimethacrylate (EGDMA), lysozyme from chicken egg white, and Dulbecco's phosphate buffered saline (PBS) were purchased from Sigma-Aldrich Chemicals (St Louis, MO). 2,4,6-Trimethylbenzoyl-diphenyl-phosphineoxide (Darocur TPO) was kindly provided by Ciba Specialty Chemicals (Tarrytown, NY). All the chemicals were reagent grade, and were used without further purification.

5.1.2 Preparation of P-HEMA Hydrogels

The p-HEMA hydrogels were synthesized by free-radical polymerization with photoinitiation. The monomer solution consisted of 2.7 ml of HEMA, 2 ml of de-ionized water, and 20 µl of crosslinker (EGDMA) which corresponds to 0.0048 mol EGDMA / mol HEMA or 1X crosslinker concentration. The crosslinker concentration was also varied from 0X to 15X in order to measure the effect of degree of crosslinking on p-HEMA hydrogel properties. Even the 0X gels are crosslinked due to residual crosslinker in the HEMA monomer and due to the chain transfer step in polymerization. The mixture was purged with bubbling nitrogen for 15 min to remove dissolved oxygen. After degassing, 6 mg of Darocur® TPO was added and the solution was stirred at 600 rpm for 5 min to completely dissolve the photoinitiator. The mixture was then immediately injected between two 5 mm thick glass plates separated by a plastic spacer of the desired thickness. The spacer thickness was chosen to be 18, 29, or 49 µm. The surfaces of the glass plates were treated with a hydrophobic coating prior to injection to

allow for easy removal of the gels. The mold was then irradiated with UV-B light for 40 min utilizing an ultraviolet transilluminator UVB-10 (UltraLum, Inc.).

5.1.3 Preparation of Lysozyme Solutions

Lysozyme solutions were prepared at various concentrations (0.1, 0.2, 0.5, 0.8, 1.2, 1.5, and 3.0 mg/ml) using PBS, pH 7.4. Each solution was stirred at approximately 150 rpm for 24 h. All solutions were filtered by means of a 0.2 μm filter prior to use.

5.1.4 Lysozyme Uptake Experiments

After polymerization, each gel was removed from the glass mold and cut to a weight of 20 mg. The unreacted monomer was removed by soaking the gels in de-ionized water overnight. The water was subsequently removed and replaced with fresh de-ionized water for an additional soaking period of 30 min. Water was removed prior to the uptake experiments. Following monomer extraction, the gels were soaked in 3.5 ml of a lysozyme-PBS solution until equilibrium was reached. The lysozyme concentration in the fluid was monitored by measuring the absorbance spectrum of the solution over the wavelength range 252-321 nm with a UV–vis spectrophotometer (Thermospectronic Genesys 10 UV). A control experiment without gels was conducted to ensure that lysozyme adsorption to the vials was negligible.

5.1.5 Lysozyme Release Experiments

Once equilibrium was reached in the lysozyme uptake experiments, the lysozyme solution was removed and replaced with 3.5 ml of PBS, marking the beginning of the release experiments. The lysozyme concentration in the PBS was analyzed in the same way as described in the lysozyme uptake experiments.

5.1.6 Gel Physical Properties

5.1.6.1. Equilibrium aqueous content (EAC)

To determine EAC of p-HEMA hydrogels and its dependence on degree of crosslinking, gels of known weights were soaked in water for extended periods of time. Excess water was removed from surface by dabbing the gels with Kimwipes® (Fisher Scientific) before weighing. Three samples were used for each crosslinker concentration. The equilibrium aqueous content (EAC) was determined by the amount of water uptake per weight of hydrated gel, i.e.,

$$\%EAC = \frac{(W_{wet} - W_{dry})}{(W_{wet})} \times 100$$

5.1.6.2. Storage modulus

Storage modulus of the gels was measured using a dynamic mechanical analyzer (DMA Q800, TA instruments). Hydrated rectangular gels 500 μm in thickness were mounted in the submersion tension clamp at room temperature. A preload force applied 0.01N and force track was 115% used. Strain sweep tests were recorded to confirm the linear range at room temperature at 1 Hz. Subsequently, frequency dependent storage modulus was obtained by fixing the strain within the linear range. Shear modulus was measured and plotted as a function of applied frequency (1 Hz – 20 Hz).

5.2 Results and Discussion

5.2.1 Effect of Gel Thickness on Lysozyme Uptake

Figure 5-1(a) shows the profiles of lysozyme uptake for 1X crosslinked gels of three different hydrogel thicknesses (18, 29, 49 μm) for an initial lysozyme concentration of 0.2 mg/ml. The scaled lysozyme concentration in PBS, i.e., the ratio of the transient

concentration and the initial concentration is plotted as a function of time for each of the thickness. Since the ratio of the lysozyme solution to gel volume was kept fixed for all gels, the equilibration time will scale as the square of the gel thickness for a purely diffusion controlled process. On the other hand, if diffusion is very rapid, the lysozyme concentration in gel will be controlled by adsorption of lysozyme onto the polymer, which is a thickness-independent process. The data in Figure 5-1(a) shows a strong dependency on the gel thickness. The uptake profiles suggest that transport is controlled by lysozyme diffusion into the lens. To prove the hypothesis that the uptake is diffusion controlled, the data for the gels in Figure 5-1(a) is plotted again in Figure 5-1(b) except that the scaled lysozyme concentration in gel is plotted as a function of the scaled time, which is defined the same as Equation (3-3). Figure 5-1(b) shows that the scaled uptake profiles overlap within experimental errors for all three thicknesses, indicating that the lysozyme uptake is diffusion-controlled. This was further confirmed later when diffusion coefficient was found to be constant and independent of thickness.

5.2.2 Effect of Lysozyme Concentration on Uptake

Figure 5-2 shows the dynamics of lysozyme uptake into 1X gels for lysozyme-PBS solutions of varying initial lysozyme concentrations (0.1, 0.2, 0.5, 0.8, 1.2, 1.5, and 3 mg/ml). The measurements of the dynamic lysozyme concentration in PBS were utilized to calculate the average lysozyme concentrations in the gel which are plotted in Figure 5-2 and subsequent figures through a simple mass balance. The lysozyme concentration in gel is actually position dependent, except at equilibrium, and thus the concentrations obtained from the mass balance represent the mean lysozyme concentrations in gel. The profiles in Figure 5-2 show a clear dependence on the initial lysozyme concentration.

The equilibrium uptakes in Figure 5-2 were utilized to determine the partition coefficients of lysozyme in the gel, for each set of data, by the following equation:

$$K = \frac{C_{g,f}}{C_{w,f}} = \frac{V_w\left(C_{w,i} - C_{w,f}\right)}{V_g C_{w,f}} \tag{5-1}$$

where V_w and V_g are the volumes of the lysozyme solution and hydrated gel, respectively, and $C_{g,f}$, $C_{w,i}$, and $C_{w,f}$ are the equilibrium concentration of lysozyme in the gel and initial and equilibrium lysozyme concentrations in PBS, respectively. Figure 5-3 shows a plot of the calculated values for the inverse partition coefficients (1/K) as a function of the equilibrium lysozyme concentration in PBS. As shown in Figure 5-3, the inverse of the partition coefficient is linearly related to the equilibrium concentration in PBS.

The relatively small values for the inverse of the partition coefficients, or equivalently, the relatively large magnitude of the partition coefficients indicate the preference of lysozyme to reside within the hydrogel matrix and bind to polymer chains. The reduction in partition coefficient with increasing lysozyme concentration could be attributed to saturation of the binding sites on the polymer.

5.2.3. Effect of Crosslinking

Normal HEMA gels prepared have crosslinker concentration of 0.0048 mol EDGMA/mol HEMA (1X). To understand the effect of crosslinking, HEMA gels were prepared with crosslinker concentrations of 0 (0X), 0.024 (5X) and 0.072 mol EGDMA/ mol HEMA (15X), and all physical properties and lysozyme transport were explored.

5.2.3.1. Effect on partition coefficient

The effect of crosslinking on transport was explored by varying the fraction of crosslinker in the gels. Increasing the crosslinking decreases the mesh size of the

hydrogel, which should result in a reduction in the rate of lysozyme uptake. Figure5-4 shows the effect of crosslinking on the lysozyme concentration within the hydrogel. For the 0X crosslinking, the gels were weak and hence 240 μm gels were used for that study. For comparison with gels with higher degree of crosslinking, the uptake data shown for 0X has been rescaled to 18 μm through Eq. 5-1 by assuming diffusion as the rate limiting process. The equilibrium lysozyme concentration in the gel was utilized to determine the partition coefficients, which are listed in Table 5-1.

Figure 5-4 and Table 5-1 show a significant reduction in lysozyme uptake with increased crosslinking. For a 1X to 5X increase in crosslinking, K decreases by a factor of 6, and for 1X to 15X increase, K decreases by a factor of 20. The effect of crosslinker concentration on the partition coefficient is rather surprising. Increasing crosslinking should reduce diffusivity, but should have minimal impact of the partition coefficient. The partition coefficients in the 0X and 1X gels are indeed similar but further increase in crosslinkings reduce the partition coefficients. It is possible that the stearic repulsion between the protein and the polymer reduces partition coefficients for high degree of crosslinkings. It is also possible that the highly crosslinked gels are heterogeneous and contain regions in the gel which are inaccessible to the protein, thereby reducing the equilibrium uptake. The partition coefficient at the highest crosslinking of 15X is likely due to surface binding only.

5.2.3.2. Effect on p-HEMA hydrogel mesh size

The effect of the degree of crosslinking on the p-HEMA hydrogel mesh size can be estimated using certain gel properties. Mesh size can be related to the gel rheology through the following equation [119]:

$$\xi = l_{c-c}\left(\frac{6C_n\rho_2 RT}{EM_r\phi_2^{1/3}}\right)^{1/2} \quad (5\text{-}2)$$

where l_{c-c} is the length of a covalent carbon – carbon bond in the backbone (1.54 Å), C_n is the Flory characteristic ratio or rigidity factor (6.9 for p-HEMA gels) [119], ρ_2 is the mass density of dry polymer (1.26 g/ml), M_r is the molecular wt. of a repeat unit (130 g/mol in this case) [119], E is the Young's tensile modulus, φ_2 is the polymer fraction in a swollen gel and ξ is gel mesh size, defined as the statistical length between two crosslinks.

Since E = 2G' (1 + v) where G' is storage modulus and we can assume Possion's ratio v = 0.5, then

$$\xi = l_{c-c}\left(\frac{2C_n\rho_2 RT}{G'(\omega=0)M_r\phi_2^{1/3}}\right)^{1/2} \quad (5\text{-}3)$$

G' was determined experimentally as stated before. Measurements were recorded for each of the eight degrees of crosslinking and shown in Figure 5-5. G' (ω = 0) was established by quadratic extrapolation as reported in Table 2 along with their corresponding equilibrium aqueous content (%). Storage modulus was found to be a strong function of degree of crosslinking as seen in Figure 5-6.

Thus for the various degrees of crosslinking ξ was estimated. However, as a simple rule, about 20% of the water phase in these gels is not accessible to the diffusing species [119] which reduces ξ by about 8% and the corresponding estimated values are reported in table 5-2. These are in excellent agreement with those calculated by Peppas et al. [120] for p-HEMA gels with similar EGDMA crosslinking ratios. Comparing these values to size of lysozyme molecule which has dimensions (45 x 30 x 30 Å) and a hydrodynamic diameter of 37.8 Å [121] suggests that lysozyme would diffuse in 1X gels

and be completely excluded from the 15X gels. The partial uptake in the 5X gels is potentially due to heterogeneities in the gel structure and chain fluctuations which allow lysozyme to diffuse into certain regions resulting in absorption into the matrix, but with a reduced partition coefficient.

5.2.4 Model for Lysozyme Transport

The matrix of a hydrogel such as p-HEMA consists of chemically crosslinked polymer chains surrounded by the aqueous phase. The water fraction of the gel determines the mesh size and the 1X p-HEMA gels prepared here have a water content of about 34%. For a solute of size significantly smaller than the mesh size, the absorbed amount can be separated into the free component that is dissolved in the water fraction of the gel and the adsorbed component that is bound to the polymer (Figure 5-7(a)). The free and the bound fractions are typically in equilibrium due to the rapid time scales as compared to diffusion. The free and the bound components can both diffuse with respective diffusivities, and thus transport of solute in the gel can be expressed through the following mass balance

$$\frac{\partial C}{\partial t} = D_f \frac{\partial^2 C_{free}}{\partial y^2} + D_b \frac{\partial^2 C_b}{\partial y^2} \tag{5-4}$$

where C, C_{free} and C_b are the total and the free and the bound concentrations and D_f and D_s are the diffusivities of the free and the bound components. It is noted that the bound concentration is essentially the product of the true surface concentration of the bound solute and the specific surface area of the gel. Similarly the diffusivity D_b of the bound component is the ratio of the surface diffusivity and the specific surface area. We can assume that the lysozyme concentration in the aqueous part of the gel (C_{free}) is same as the lysozyme concentration in PBS outside the gel (C_f). If f is the fractional

aqueous content of the hydrated gel and K is the partition coefficient between the total lysozyme concentrations in gel and the lysozyme concentration in PBS, then

$$C_f = fC_f \tag{5-5}$$

$$C_b = (K - f)C_f \tag{5-6}$$

$$C = KC_f \tag{5-7}$$

On assuming local equilibrium between the free and the bound components, the above equation can be simplified to

$$\frac{\partial C}{\partial t} = \frac{\left(fD_f + (K - f)D_b\right)}{K}\frac{\partial^2 C}{\partial y^2} \tag{5-8}$$

The partition coefficient is treated as independent of concentration in this simple analysis. In the limit of negligible surface diffusion, the effective diffusivity becomes fD_f/K. Thus the diffusion of a solute could be slowed considerably even in very porous gels due to binding of the solute to the polymer.

As described below, the diffusivity of the free solute could be estimated from several theories and the effective diffusivity can be determined by fitting the experimental data to the effective diffusion equation. By comparing the calculated D_f and the measured D_{eff}, one could potentially determine the diffusivity of the bound solute Db. Unfortunately the size of the lysozyme is comparable to the mesh size for all crosslinkings explored here and thus it is not possible to clearly differentiate between free and bound components (Figure 5-7(b)). The mass transfer for such solute could potentially still be described by the following effective equation

$$\frac{\partial C}{\partial t} = D_{eff}\frac{\partial^2 C}{\partial y^2} \tag{5-9}$$

However it is not feasible to split the effective diffusivity into free and bound components. Thus for lysozyme transport the estimated diffusivities and measured diffusivities could potentially not agree. Below we first fit the experimental data to the diffusion equation to obtain the effective diffusivity and then estimate diffusivity based on theoretical models. These values are then compared to determine the validity of the theories for transport of lysozyme in p-HEMA gels. Additionally the experimental data for lysozyme release from the gels is compared to that predicted from the diffusion model to determine whether the adsorbed lysozyme can desorb and diffuse on immersing the lysozyme loaded gels in fresh PBS.

In addition to the governing differential equation (Equation 5-9), Equations (3-9) to (3-12) from section 3.2.1.4 are the remaining equations and conditions required to model the lysozyme diffusion. In these equations, where C_f is the lysozyme concentration in PBS, V_f is the external fluid volume, A is the surface area of one face of the hydrogel, and H is the half-thickness of gel. The first boundary condition, assumes equilibrium between the lysozyme concentration in the external lysozyme solution and that within the hydrogel, and the second boundary condition, assumes symmetry at the center of the gel. For ease of manipulation, the above equations were non-dimensionalized using the following variables:

$$C^* = \frac{C}{C_0}, C_f^* = \frac{C_f}{C_0}, y^* = \frac{y}{H}, t^+ = \frac{H^2}{D_{eff}}, t^* = t/t^+, A^* 2H = V_g \quad (5\text{-}10)$$

where V_g is the volume of gel and C_0 is the initial lysozyme concentration in the fluid.

Substitution of the dimensionless variables, and removal of the * signs, gives the following dimensionless equations:

$$\frac{\partial C}{\partial t} = \frac{\partial^2 C}{\partial y^2} \tag{5-11}$$

$$V_{fg} \frac{\partial C_f}{\partial t} = \left(-\frac{\partial C}{\partial y} \right)_{y=1} \tag{5-12}$$

$$C(y, t=0) = 0 \tag{5-13}$$

$$C(t, y=H) = KC_f \tag{5-14}$$

$$C_f(t=0) = C_{f0} \tag{5-15}$$

$$\frac{\partial C}{\partial y}(t, y=0) = 0 \tag{5-16}$$

where the new variable $V_{fg} = V_f/V_g$. This new set of equations is no longer dependent on the gel thickness. For 0X and 1X crosslinkings, lysozyme uptake data from experiments with various thicknesses and lysozyme concentrations was fitted to Eqs. 5-11 to 5-16 to determine the best-fit values of the parameter D_{eff}. The uptake at higher crosslinks was considered negligible and thus diffusivity estimates could not be obtained. The differential equations were solved numerically using an implicit finite-difference scheme. The best-fit values of the parameters were obtained by minimizing the error defined as $E = \sum_{i=1}^{Ne} (C_{f,i} - C_{model,i})^2$, where Ne is total number of data points, and $C_{f,i}$ and $C_{model,i}$ are the dimensionless experimental and model predicted lysozyme concentrations in PBS, respectively. The minimization was done using the function fminsearch in MATLAB. For 0X gels, D_{eff} was determined to be $1.97 \times 10^{-15} \pm 1.33 \times 10^{-15}$ m^2/s. The best-fit value for D_{eff} was found to be $1.92 \times 10^{-16} \pm 6.3 \times 10^{-17}$ m^2/s for the 1X hydrogels and was independent of lysozyme concentration and hydrogel thickness.

The model fitted the data well in all cases as shown in Figure 5-8 for the 0X gels and in Figure 5-9 and 5-10 for the 1X gels. This suggests that the transport process can indeed be modeled by Fickian diffusion with concentration-independent diffusivity.

To put into perspective the extent to which the diffusion of lysozyme is impeded by the gel, the diffusivity of lysozyme in gel can be compared to diffusivity of lysozyme in free solution. Substituting the hydrodynamic radius (R_h) of 1.89 nm in the following Stokes-Einstein equation,

$$D_0 = \frac{k_B T}{6\pi\eta R_H} \tag{5-17}$$

where k_B is the Boltzmann constant (1.38 x 10^{-23} m^2 kg s^{-2} K^{-1}), T is temperature (300K) and η is the viscosity of solution (9.5 x 10^{-4} Pa-s), we get a lysozyme diffusivity as 1.2 x 10^{-10} m^2/s. Accounting for the increased partition coefficient (K circa 50) we get $D_{0eff} = D_0/K$ = 2.4 x 10^{-12} m^2/s. Thus, the lysozyme diffusivity is reduced by 3-4 orders of magnitude due to the crosslinked polymer chains.

5.2.5 Lysozyme Desorption and Model Validation

To test whether lysozyme binding is reversible, desorption experiments were conducted by replacing the PBS-lysozyme solution with fresh PBS at certain times during the lysozyme uptake experiments. In some cases lysozyme solution was replaced before the equilibrium was achieved and in some cases the uptake experiments were allowed to reach equilibrium. The desorption transients were predicted completely from the uptake data using diffusivity and relationship of partition coefficient and equilibrium concentration.

Eq. 5-16 was solved along with Eq. 5-17 and Eq. 5-19 and the following the initial condition and rest of the boundary conditions:

$$C(y, t=0) = C_{g\infty} \tag{5-18}$$

$$C_f(t=0) = 0 \tag{5-19}$$

$$\frac{\partial C}{\partial y}(t, y=0) = 0 \tag{5-20}$$

where $C_{g\infty}$ is the concentration profile in the gel at the end of the corresponding uptake experiment. The above set of equations were simulated with parameters obtained previously which were D_{eff} = 1.92 x 10^{-16} m^2/s and $1/K = 0.0065C_f + 0.0153$, to predict the concentration transients in the desorption experiments. As in the case of uptake modeling, the equations were made dimensionless and a finite difference scheme was employed. The profiles in Figure 5-11 represent the desorption experiments from gels that were equilibrated during the uptake experiments. The profiles in Figure 5-12 show the results for release of the lysozyme from gels that were soaked in a 0.55 mg/ml lysozyme solution for various durations, and thus equilibrium was not achieved. The predicted profiles are in reasonable agreement with the experimental results proving that lysozyme binding to the polymer is reversible, and suggesting that the model developed above is indeed valid. While these results show that lysozyme can desorb from the gels even after extended periods of adsorption, the desorbed molecules could potentially be denatured. We do not determine the conformation of the desorbed molecules because our main focus here is on the contact lens application where protein desorption is important during cleaning, but the conformation of the desorbed protein is insignificant.

5.3.6. Theoretical Estimation of Lysozyme Diffusivity in P-HEMA Hydrogels

The diffusivity of a solute in a gel can be related to the mesh size, which has been determined through the rheology earlier. According to Stringer et al.[122], the effective diffusivity of a species in a crosslinked hydrogel can be estimated by the equation,

$$\frac{D_i}{D_{i,w}} = (1 - \frac{r}{\xi_r}) e^{(\frac{-1}{Q-1})} \tag{5-21}$$

where D_i is the diffusivity of free solute in hydrogel (earlier referred to as D_f), $D_{i,w}$ is the diffusivity in pure solvent, r is the radius of the solute, ξ_r is gel mesh size equivalent to the radius of a hollow sphere between neighboring polymer chains and Q is the swelling ratio. $D_{i,w}$ can be estimated from Einstein-Stokes equation as:

$$D_{i,w} = \frac{k_B T}{6\pi\mu r} \tag{5-22}$$

where k_B is Boltzmann constant. The swelling ratio Q is defined as

$$Q = \frac{V_{s,gel}}{V_{poly}} = 1/\phi_2 \tag{5-23}$$

where $V_{s,gel}$ is volume of swollen gel, V_{poly} is volume of polymer and ϕ_2 is polymer volume fraction in a swollen gel. Substituting Eqs. 5-22 and 5-23 in Eq. 5-21, we get

$$De^{\frac{\phi_2}{1-\phi_2}} = \frac{kT}{6\pi\mu}(\frac{1}{r} - \frac{1}{\xi_r}) \tag{5-24}$$

Assuming the length between two crosslinks is twice the value of radius of sphere between two polymer chains, i.e., $\xi = 2\xi_r$, Eq. 5-24 can be rewritten as

$$De^{\frac{\phi_2}{1-\phi_2}} = \frac{kT}{3\pi\mu}\left(\frac{1}{d} - \frac{1}{\xi}\right) \quad (5\text{-}25)$$

where d is hydrodynamic diameter of the diffusing solute, which is 37.8 Å [121] for lysozyme. The diffusivity values predicted from Eq. 5-25 for 0X and 1X gels are compared in Table 5-3 with the values obtained by fitting the transport data. The measured values are considerably smaller than the estimated values. A potential reason for the discrepancy could be that the bound lysozyme does not diffuse and thus the effective diffusivity determined from the lysozyme uptake experiments should be f*D/K. For comparison, the predicted diffusivity should be converted to effective predicted diffusivity which is f*D predicted/K. The values of f*D predicted/K which are also listed in Table 5-3 are still significantly larger than the measured values as well.

There could be several reasons that contribute to these differences. The most likely ones are errors in estimation of the mesh size and the lysozyme size. Any errors in sizes lead to very large errors in estimated diffusivities in the limiting case when the mesh size approaches the solute size, which appears to be the case for lysozyme. Lysozyme likely diffuses with a preferred orientation in such tight networks, which is neglected in the theoretical models. Also, in p-HEMA gels, hydrophobic solutes tend to diffuse slower than hydrophilic solutes. Thus, simply taking in account the effect of the partition coefficient due to hydrophobic interactions is not enough. If the mesh size of the gel is close to the size of the diffusing molecule, then there is also a need to account for changes caused in mesh size due to chain fluctuations as well. When soaked in an organic solvent like ethanol, these gels swell to a much larger extent indicating that the gels are more relaxed in an aqueous environment. Thus even if the effective size of the

molecule is larger than the mesh size, fluctuations may allow molecules to diffuse in and not just adsorb on the surface.

5.2.7 Simulated Lysozyme Uptake by Contact Lenses during Day Time Wear and Overnight Cleaning.

The p-HEMA based contact lenses cannot be worn overnight due to the limited oxygen permeability, which will result in severe hypoxia of the cornea if worn overnight. Also, to minimize the deleterious impact of protein and lipid deposits in extended wear contact lenses, the users are expected to take the lenses off during nights and soak the lenses in cleaning solutions to extract the deposited proteins. The duration of lens wear during the day can be expected to be about 12 hours, followed by 12 hours of soaking to extract the proteins. The model developed above can be utilized to simulate the cycle of 12 hour wear and 12 hour extraction to determine whether this regimen is adequate to extract a majority of the lysozyme. The contact lenses are complicated in shape but for this calculation, we assume an average thickness of 80 μm. We also assume infinite source and sink conditions during wear and cleaning respectively. The diffusion equation for the lens was solved with the cyclic boundary conditions at the edges and the concentration profiles in the lens were integrated to yield the mean lysozyme concentration in the lens. If t is real time and t1 and t2 are the individual cycle times in the uptake and release steps respectively (t_1 = 12 hr and t_2 = 12 hr), then for the m^{th} day, the average concentration of lysozyme in contact lens during uptake is given by:

$$\frac{C_{g,avg}}{C_{tear}} = K(1-\sum_{n=0}^{\infty}\frac{8}{(2n+1)^2\pi^2}[\sum_{i=1}^{m-1}(\exp(-(\frac{(2n+1)\pi}{2H})^2 D(t-i(t_1+t_2)))$$
$$-\exp(-(\frac{(2n+1)\pi}{2H})^2 D(t-it_1-(i-1)t_2))) + \exp(-(\frac{(2n+1)\pi}{2H})^2 D(t))]) \quad (5\text{-}26)$$

Similarly, for the mth day, the average concentration of lysozyme in contact lens during release is given by:

$$\frac{C_{g,avg}}{C_{tear}} = -K\sum_{n=0}^{\infty}\frac{8}{(2n+1)^2\pi^2}[\sum_{i=1}^{m-1}(\exp(-(\frac{(2n+1)\pi}{2H})^2 D(t-i(t_1+t_2)))$$
$$-\exp(-(\frac{(2n+1)\pi}{2H})^2 D(t-it_1-(i-1)t_2)))$$
$$-\exp(-(\frac{(2n+1)\pi}{2H})^2 D(t-mt_1-(m-1)t_2)) + \exp(-(\frac{(2n+1)\pi}{2H})^2 D(t))] \quad (5\text{-}27)$$

The ratio of the mean lens concentration to the tear concentration is plotted in Figure 5-13 as a function of time. The results show that in each cycle, a fraction of the lysozyme deposited in the lens is not extracted out during cleaning, and thus there is a net increase in the mass of lysozyme in the lens with each day. This simulation though neglects the presence of the surfactants and other agents in the cleaning solution, which probably diffuse into the lens to increase the rate at which protein diffuse out by causing desorption of the adsorbed protein. The impact of cleaning agents in lens care solutions on the protein desorption will be explored in future. The continuous buildup of protein in the lenses can potentially affect several properties of the lenses including ion and oxygen permeabilities, which in turn may affect the lens comfort and performance.

5.3 Concluding Remarks

Protein binding to hydrogels plays an important role in determining the suitability of such materials in several biomedical applications. In this paper, we have measured lysozyme uptake and release from p-HEMA gels of various thicknesses to understand, quantify, and model the transport of lysozyme in the hydrogel. Lysozyme diffuses into the gels through the water filled pores and binds to the p-HEMA polymer, with a high, concentration dependent partition coefficient. The adsorbed polymer desorbs even after

25 days of continuous adsorption suggesting that the adsorbed lysozyme is not aggregated or denatured irreversibly. The uptake and release dynamics are diffusion controlled, even for very thin gels showing that the time scale for adsorption and desorption are rapid. Theoretical models do not yield accurate values of lysozyme diffusivity mainly because the mesh size of the gel is close to the size of the lysozyme. The results of this study can be applied to understand protein adsorption to contact lenses and to design optimum lens care solutions and protocols. For instance, the experimental results show that p-HEMA lenses with 5X (0.024 mol EGDMA / mol HEMA) crosslinking exhibits negligible protein uptake, but the zero frequency storage modulus of about 2 MPa is far too high for contact lens application. Based on the combined criterion of minimizing protein uptake and optimum modulus, a 2.5X (0.012 mol EGDMA / mol HEMA) crosslinking would seem to be optimal for fabricating p-HEMA contact lenses. Also, applying the transport model to a cycle of wear and cleaning shows that there could be continuous accumulation of protein in the lenses even if the lenses are soaked overnight for cleaning.

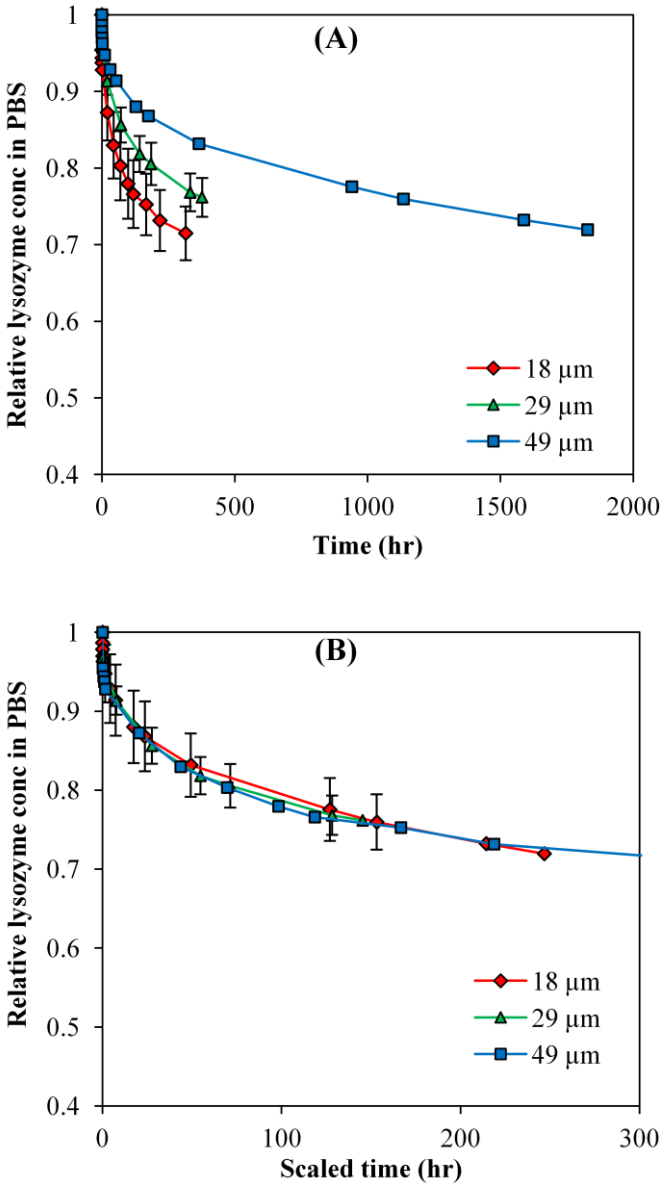

Figure 5-1. Profiles of lysozyme uptake for gels of three different thicknesses at an initial lysozyme concentration of 0.2 mg/ml. A) On normal time scale. The gel thicknesses are indicated in the legend. Data are presented as mean ± S.D. with n = 3. B). Profiles for lysozyme uptake from 5-1A plotted on a scaled time axis.

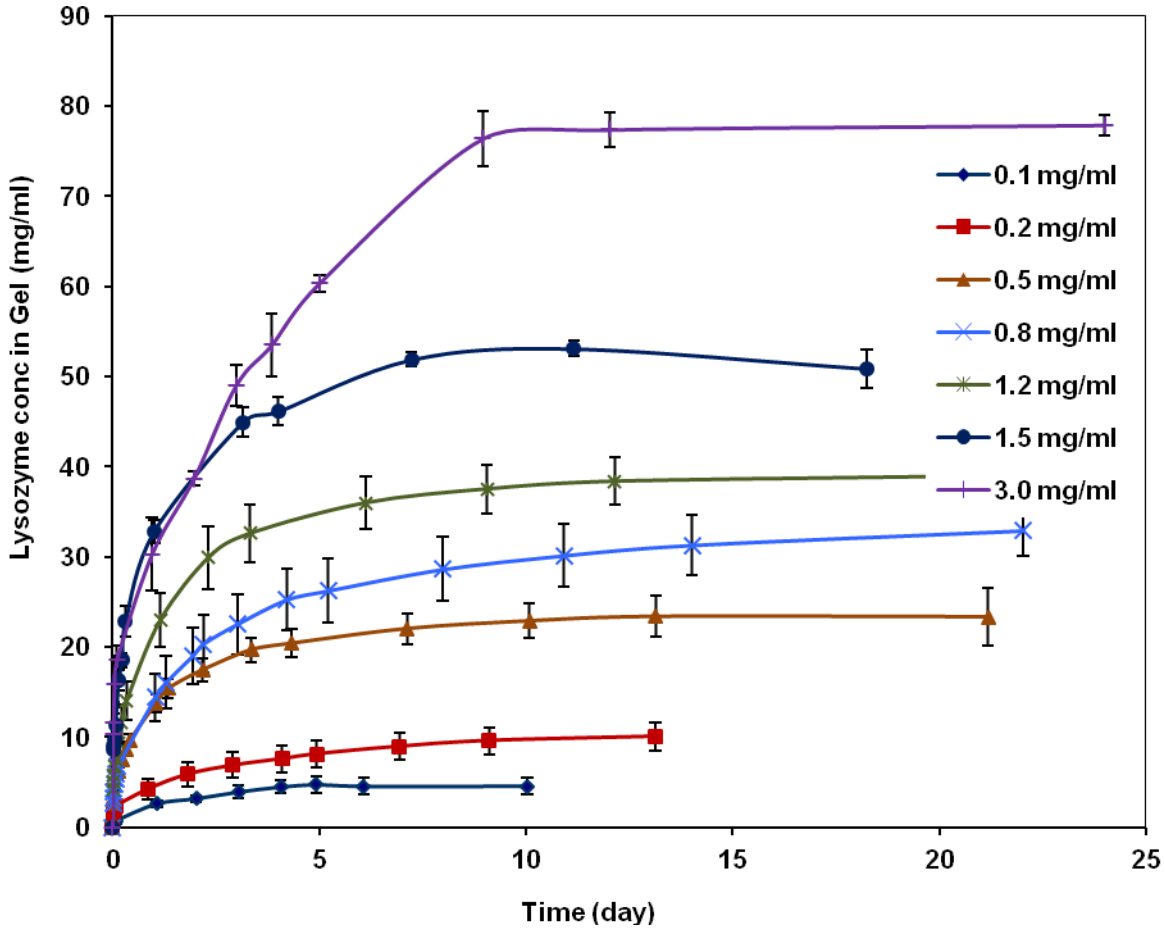

Figure 5-2. The profiles of lysozyme uptake in 18 μm gels for several concentrations of lysozyme-PBS solutions. The initial lysozyme concentrations are indicated in the legend. Data are represented as mean ± S.D. with n = 3.

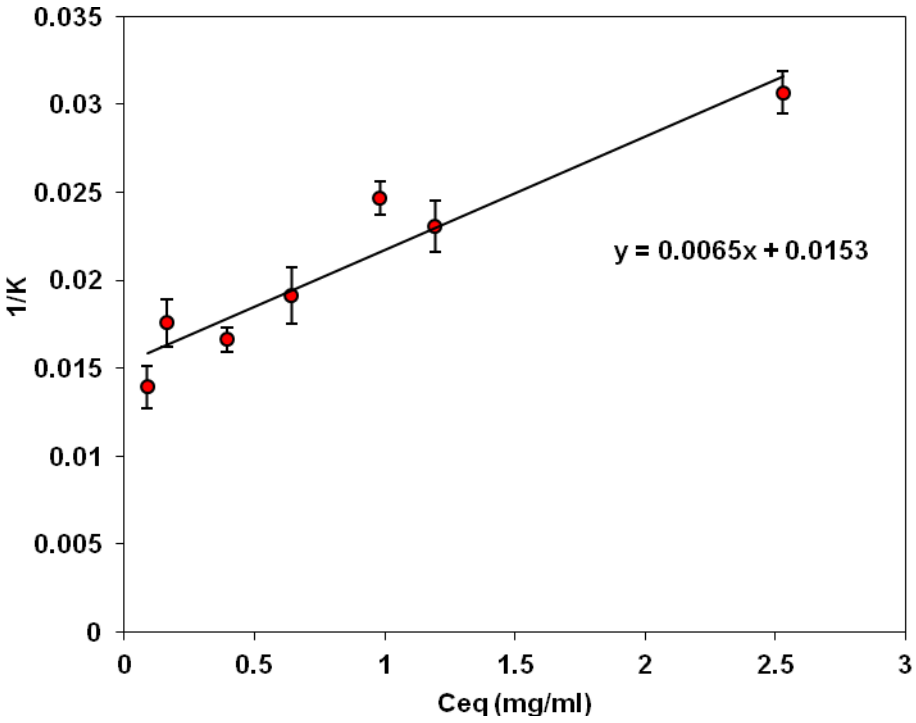

Figure 5-3. Concentration dependence of the partition coefficient for a lysozyme/p-HEMA hydrogel system. Data are represented as mean ± S.D. with n = 3.

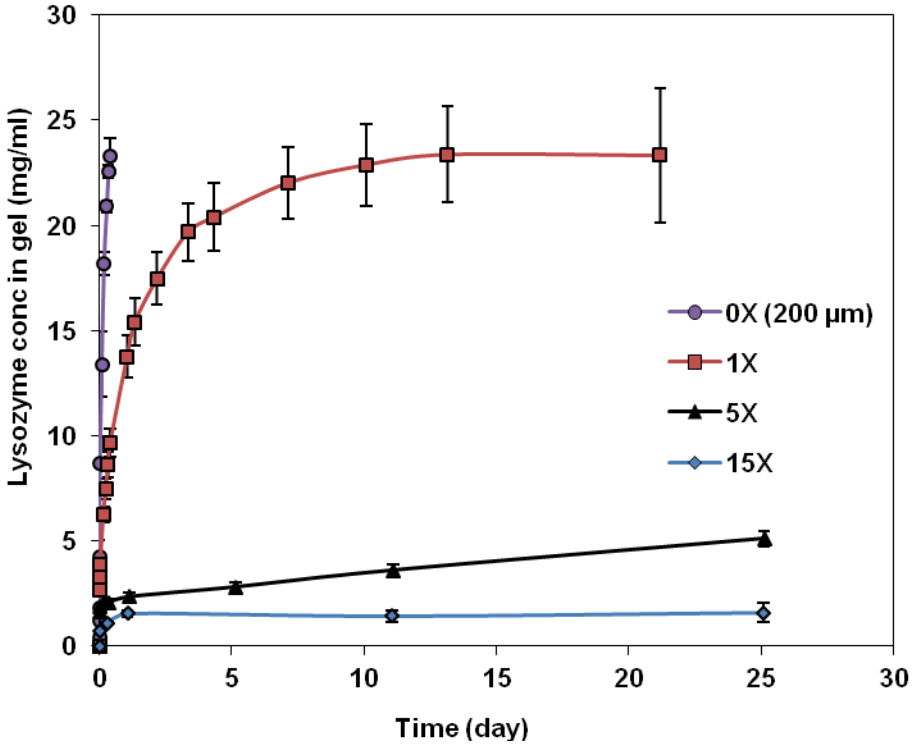

Figure 5-4. Effect of crosslinking on lysozyme uptake in 18 µm (200 µm for 0X) gels for an initial lysozyme concentration of 0.5 mg/ml. The degree of crosslinking is indicated in the legend. Data are represented as mean ± S.D. with n = 3.

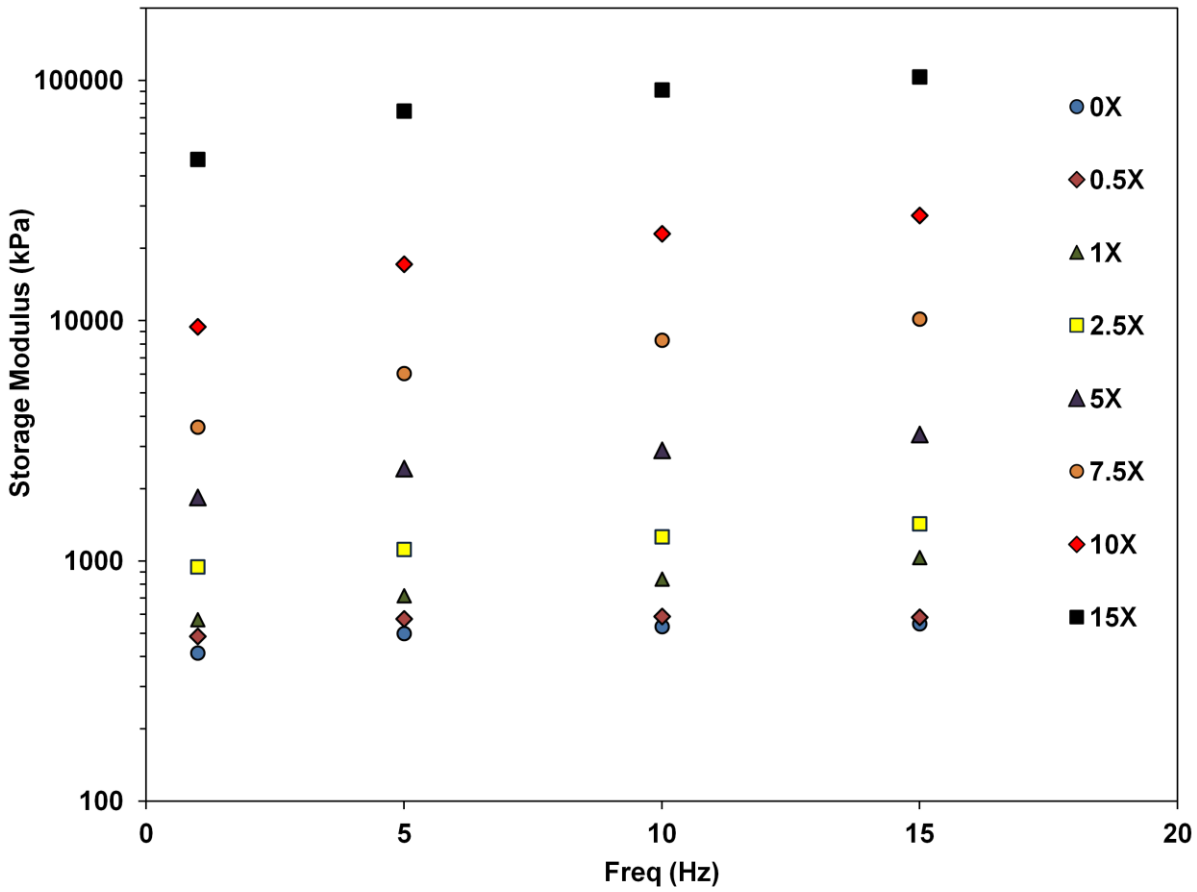

Figure 5-5. Dependence of storage modulus on applied frequency for various crosslinked p-HEMA gels.

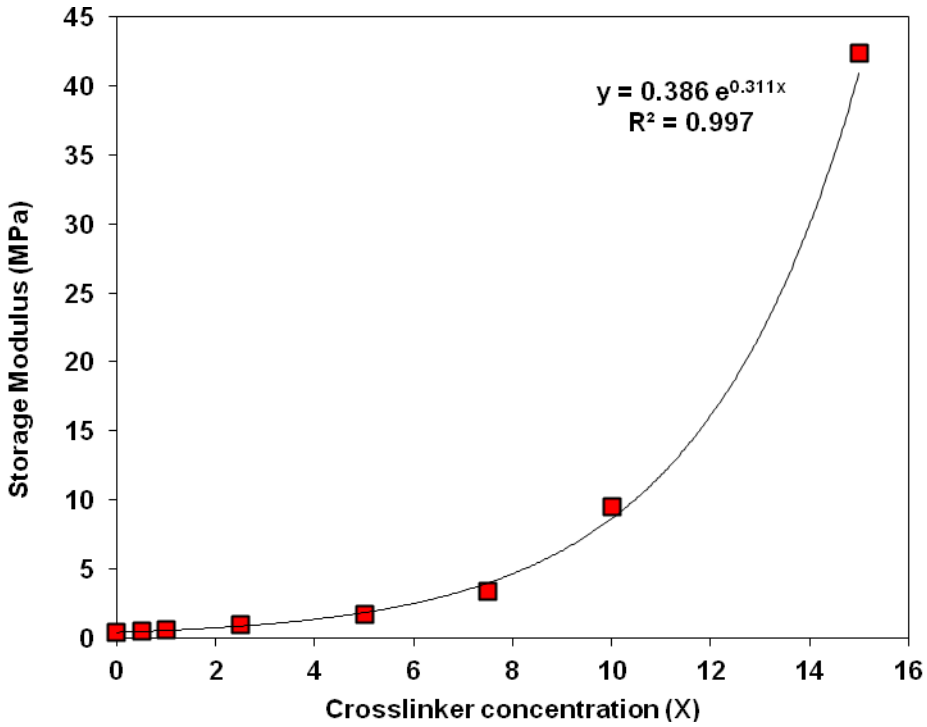

Figure 5-6. Effect of crosslinker concentration on storage modulus

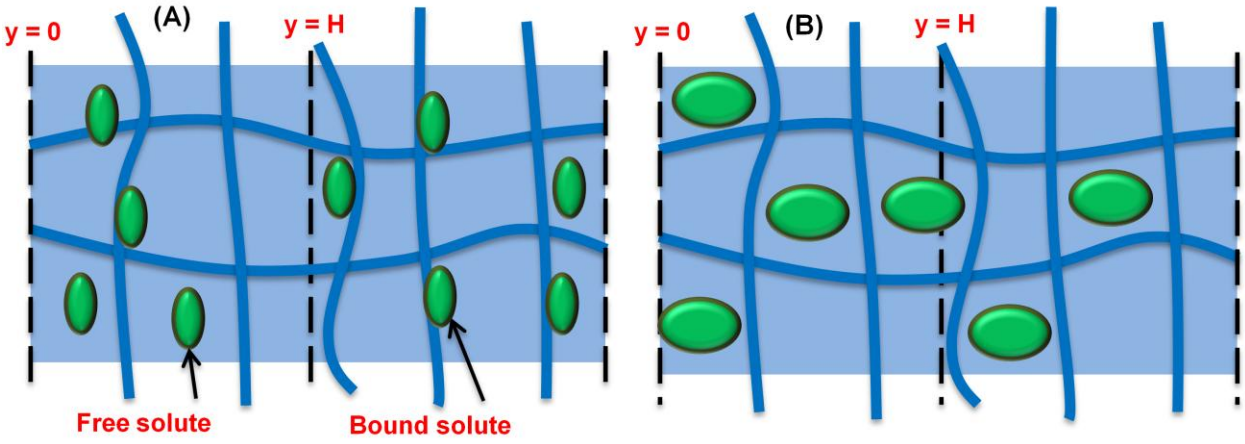

Figure 5-7. (A). Mesh size of hydrogel larger than solute size (B). Mesh of hydrogel similar to solute size

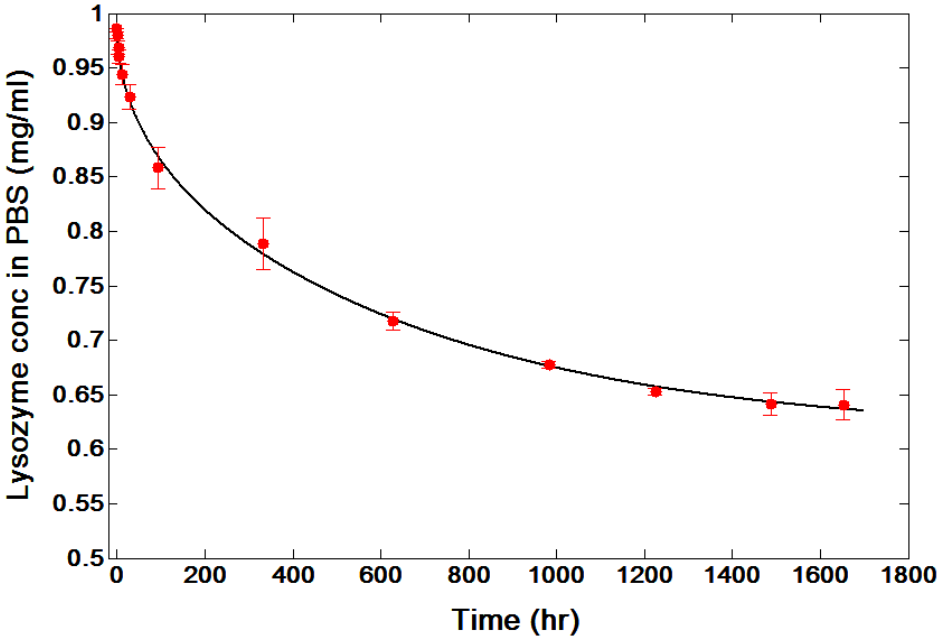

Figure 5-8. Modeling of lysozyme diffusion in 200 μm gels for 0X gel. The model and experimental data are represented by a solid line and points, respectively.

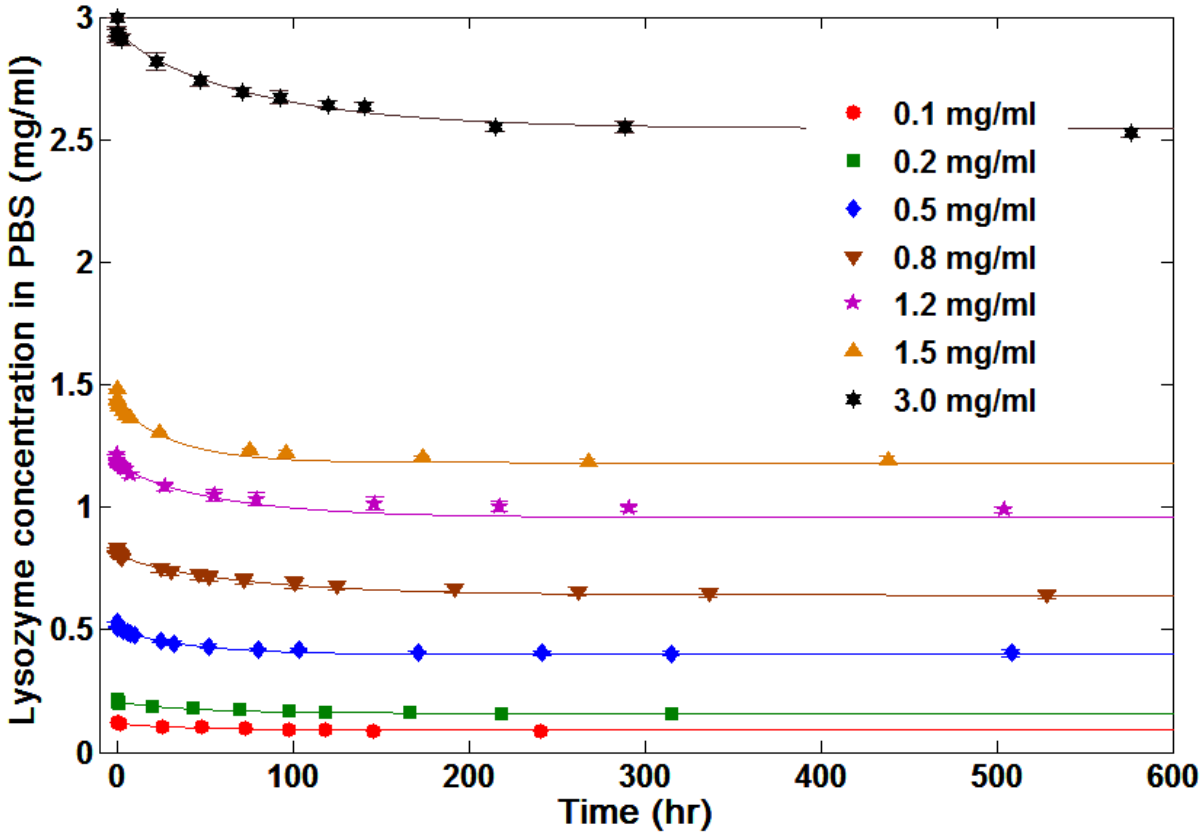

Figure 5-9. Modeling of lysozyme diffusion in 18 μm gels for various lysozyme concentrations for 1X gels. The initial lysozyme concentrations are listed in the legend. The model and experimental data are represented by a solid line and points, respectively.

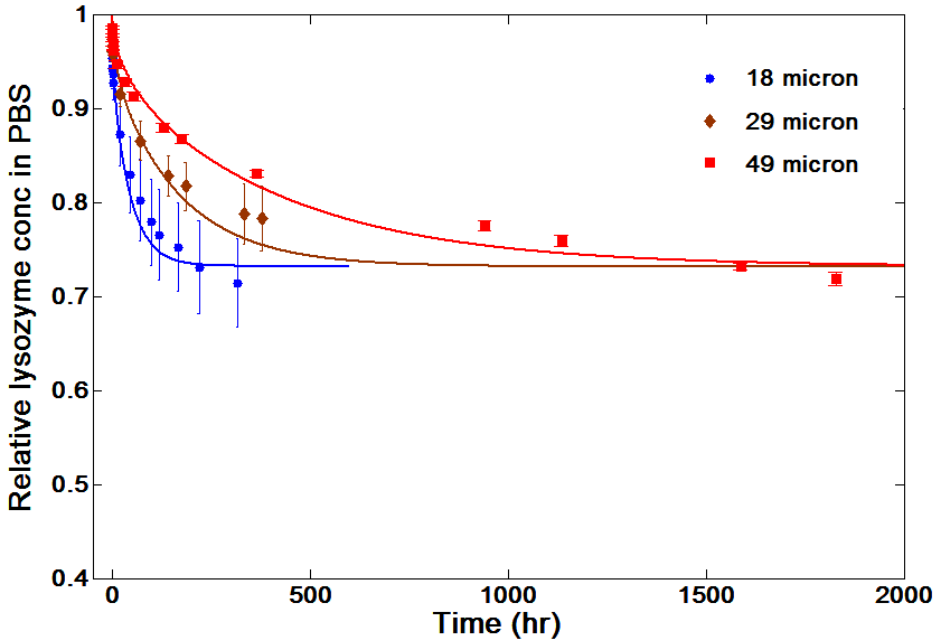

Figure 5-10. Modeling of lysozyme diffusion in 1X gels of various thicknesses at an initial lysozyme concentration of 0.2 mg/ml. The thicknesses are listed in the legend. The model and experimental data are represented by a solid line and points, respectively. Lysozyme concentration has been scaled with initial lysozyme concentration to negate the effect of minor differences in initial concentration.

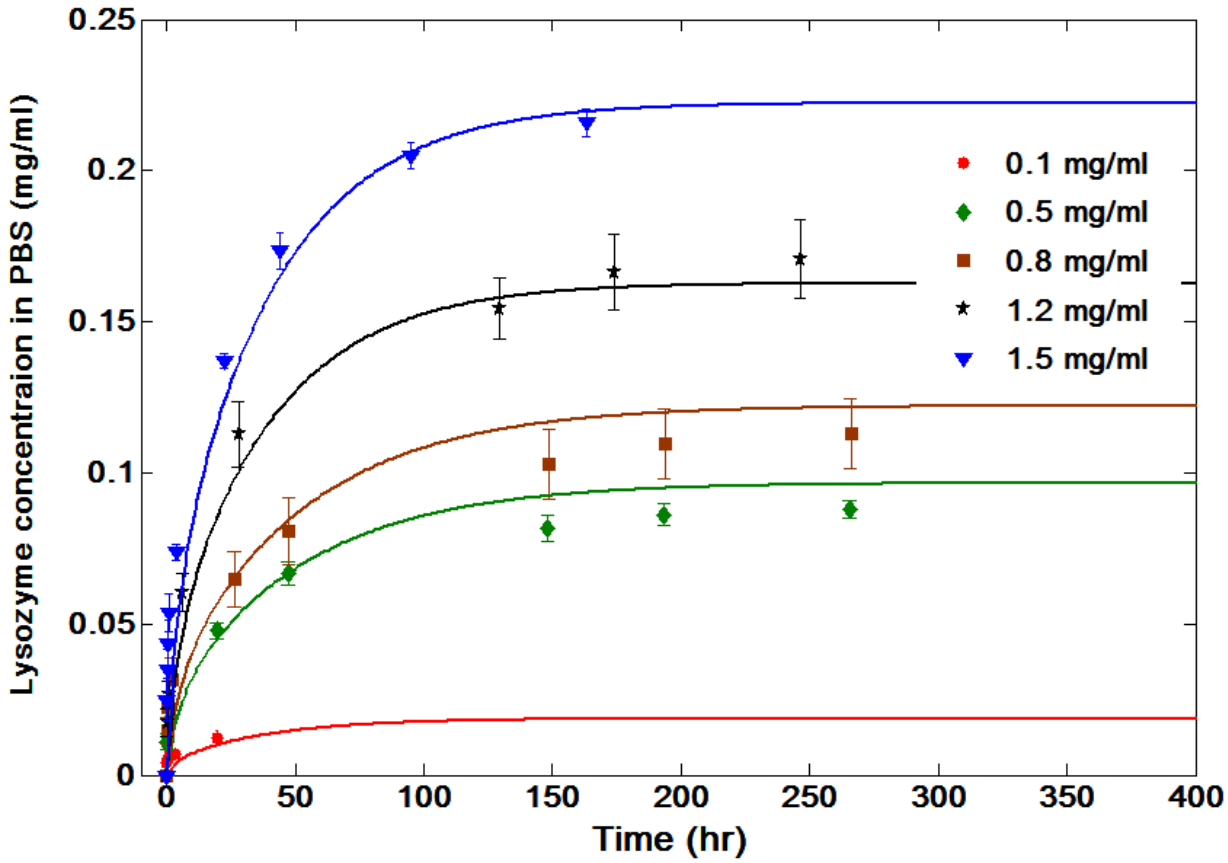

Figure 5-11. Profiles for lysozyme release from 18 µm gels into PBS solutions. The initial lysozyme concentrations for lysozyme uptake are indicated in the legend. The model and experimental data are represented by a solid line and points, respectively. Data are represented as mean ± S.D. with n = 3.

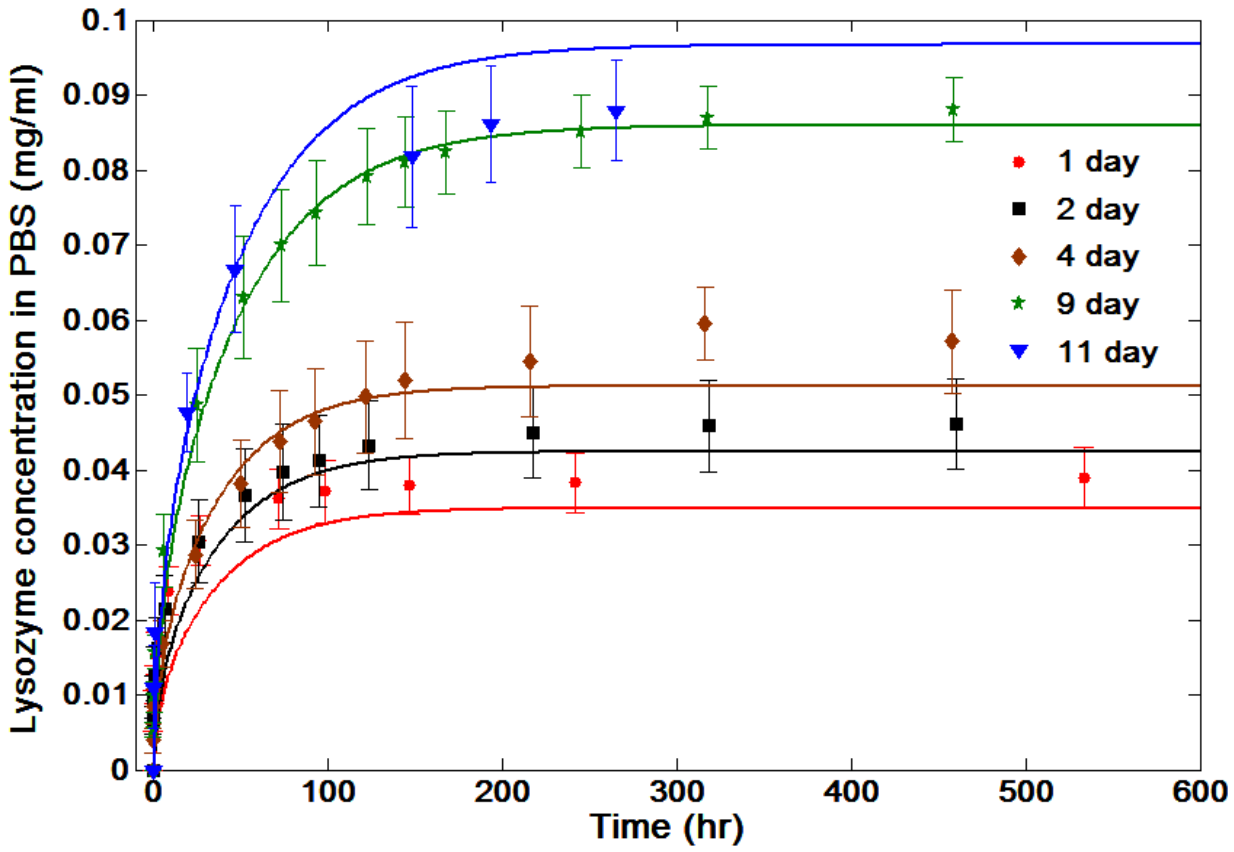

Figure 5-12. Profiles for lysozyme release from 18 µm gels into PBS solutions for varying uptake times at an initial lysozyme uptake concentration of 0.55 mg/ml. The model and experimental data are represented by a solid line and points, respectively. Data are represented as mean ± S.D. with n = 3.

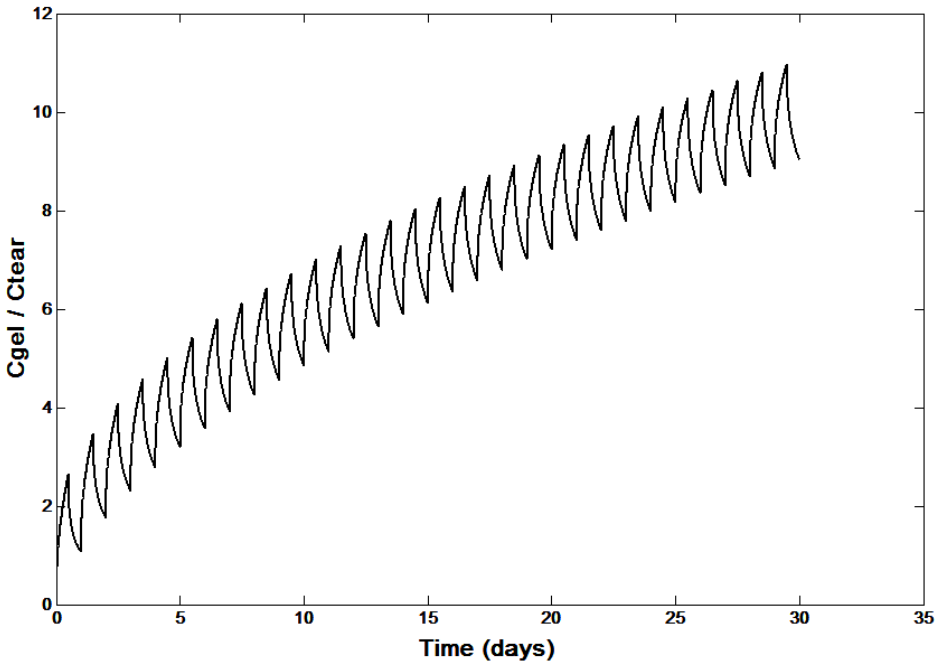

Figure 5-13. Predicted profile for lysozyme concentration in a lens with regular wear and cleaning pattern.

Table 5-1. The effect of increased crosslinking on the partition coefficient

Crosslinking	Partition coefficient
0X	60.7 ± 2.4
1X	60.2 ± 9.5
5X	10.2 ± 0.8
15X	3.0 ± 0.9

Table 5-2. Equilibrium aqueous content (EAC), storage modulus (G') and predicted values of p-HEMA hydrogel mesh sizes (ξ) as a function of crosslinker concentration.

Crosslinking	EAC (%)	G' (ω = 0) (MPa)	ξ (Å)
0X	34.96 ± 0.28	0.38	46.1
0.5X	34.70 ± 0.22	0.47	41.4
1X	33.98 ± 0.30	0.53	38.9
2.5X	32.36 ± 0.08	0.91	29.8
5X	30.83 ± 0.06	1.70	21.8
7.5X	27.70 ± 0.11	3.32	15.6
10X	26.01 ± 0.18	9.50	9.20
15X	25.79 ± 0.38	42.4	4.36

Table 5-3. Comparison between diffusivity predicted and that obtained from modeling experiments (m^2/s)

Crosslink	D predicted	D_{eff}, measured	D_{eff}, predicted (= f*D predicted/K)
0X	2.35×10^{-12}	1.97×10^{-15}	1.27×10^{-14}
1X	6.67×10^{-14}	1.92×10^{-16}	4.54×10^{-16}

CHAPTER 6
CONCLUSIONS

After exhaustive experiments with surfactant and drug loaded p-HEMA gels, we can now create a picture of how they transport and how they interact. BAC and CAC can be loaded in p-HEMA gels by either soaking in surfactant solution in water or PBS or by directly incorporating it in HEMA monomer mixture prior to polymerization. Loading surfactant by soaking in solution is useful to integrate in current manufacturing techniques as it needs just one additional step. Direct addition prior to polymerization is useful as it saves processing time.

The transport of BAC and CAC was diffusion controlled. When loaded by water, the loading reached a maximum or a saturation point when the equilibrium concentration of the solution exceeded CMC. It was hypothesized that the gel in is equilibrium with the free surfactant concentration alone. The partition coefficients while loading from solutions in PBS were significantly higher than while loading from water. In fact, CAC did not elute out of the gels up to a loading of 25%. This could be due to larger Debye length in water compared to PBS. The larger repulsion will reduce the packing of the adsorbed surfactant. Thus, the surfactant – gel structure would like be that CAC was simply adsorbed on the p-HEMA chains creating a charged surface.

This property was utilized to create a contact lens capable of ocular drug delivery. CAC loaded gels had the capability of loading very high quantities of an anionic drug DXP along with imparting extended drug release characteristics. The modified gels were transparent, had good surface wettability and presence of surfactant reduced protein binding significantly. The partition coefficient of the drug increased exponentially with surfactant loading in the gel in at least qualitative agreement with the

Debye-Hückel theory. The drug adsorbed on the surfactant covered polymer, and could also diffuse along the surface with diffusivity lower than that for the free drug, leading to a reduction in the effective diffusivity, which is the weighted combination of the free and surface diffusivities. Drug transport was diffusion controlled even for very thin gels which implied that the rate of adsorption – desorption of the drug was rapid. A Fickian diffusion model was constructed to obtain drug diffusivities. Drug release tests were carried out and the model predictions had good agreement with the release dynamics. The concept was tried in commercial contact lenses as well. CAC loaded 1-Day Acuvue lenses extended the drug release durations to about 50 hrs from less than 2 hrs without any surfactant.

Another important application of such a surfactant loaded lens is to improve the surface wettability. However, the surfactant can release out leading to potential toxicity issues. Thus, 3 types of polymerizable surfactants were incorporated in the gel by addition prior to polymerization. All surfactants were incorporated into the gel structure. The reacted fraction varied from about 30-60% of the loaded surfactant. Incorporation of both surfactants significantly reduced contact angle from 90^0 for p-HEMA gels to about 10^0 for 10% surfactant loading (w/w) in hydrated gel. The coefficient of friction also decreased with surfactant addition from a value of about 0.2 for HEMA gels to 0.05 for the gels with the 10% surfactant loading. The gels were clear and certain compositions also have the capability to block UVC and UVB radiation. The water content increased and the modulus decreased, but these effects were not significant. Both N10 and N30 Noigen surfactants decreased contact angle and friction coefficient, but the N10 surfactant was more suitable because of its higher incorporation into the lens matrix.

The surfactant incorporation did not appear to significantly impact any other critical property and so its incorporation into the lenses could improve surface properties without any adverse effect on the bulk properties. Surfactant addition also led to an increase in water content which is beneficial for p-HEMA lens as it can improve oxygen and ion transport. Based on this study it was concluded that a p-HEMA contact lens with 30% of the N10 surfactant in the formulation is an excellent candidate for further in vitro characterization and in vivo comfort studies.

In order for any lens to function in the actual environment, it is necessary to understand its interaction with tear proteins. The results of such a study could assist in the development of contact lens materials that exhibit minimal protein binding, in designing cleaning regimens for protein removal from contact lenses, and in applications related to protein binding in several other biomaterials. The tear protein lysozyme diffused in p-HEMA hydrogels. Lysozyme uptake experiments with gels of different thicknesses showed a time scale increase as the square of the thickness suggesting diffusion controlled transport. Partition coefficient was found to be dependent on the equilibrium concentration of lysozyme, and also on the degree of crosslinking. Since transport is related to mesh size, gel modulus was obtained for various crosslinkings and utilized to estimate the mesh size. The transport data were fitted to a diffusion model and the fitted diffusivity was compared to diffusivity predicted from a model based on hydrogel mesh size. Both protein absorption and desorption data fitted the diffusion model with the same value of diffusivity, but the experimentally measured diffusivities were significantly smaller than those estimated on the basis of the gel mesh size. Models were modified to take into account protein binding to the

polymer but the modified predictions were still larger than the measured values. The adsorbed polymer desorbs even after 25 days of continuous adsorption suggesting that the adsorbed lysozyme is not aggregated or denatured irreversibly. The experimental results showed that p-HEMA lenses with 5X (0.024 mol EGDMA / mol HEMA) crosslinking exhibits negligible protein uptake, but the zero frequency storage modulus of about 2 MPa is far too high for contact lens application. Based on the combined criterion of minimizing protein uptake and optimum modulus, a 2.5X (0.012 mol EGDMA / mol HEMA) crosslinking would seem to be optimal for fabricating p-HEMA contact lenses. Also, applying the transport model to a cycle of wear and cleaning showed that there could be continuous accumulation of protein in the lenses even if the lenses are soaked overnight for cleaning.

CHAPTER 7
FUTURE WORK

Understanding transport properties of hydrogels is important to utilize them for drug delivery and other biomedical applications. The following are the areas in which the studied above can be pursed

7.1 Ocular Drug Delivery by Silicone Lenses

Among the two types of contact lens materials (p-HEMA based and silicone based), silicone lenses have gained popularity in the recent years [123]. Since silicone lenses are preferred for extended wear, any extended drug delivery lens should ideally be silicone based. Preliminary experiments with commercial silicone contact lenses show that CAC can be loaded the same way as p-HEMA gels. DXP release could be extended from less than 1 hr to almost 15 hrs which is a significant improvement. However, for a truly extended release, the lenses should release drug from at least 1-2 days or more which was the case for p-HEMA lenses (Fig 7-1).It is necessary to understand the differences in the microstructure of the surfactant in silicone lenses and p-HEMA lenses conducting these tests on lab-made silicone gels with varying thicknesses and compositions.

7.2 Hydrophobic Drug Delivery by CAC Loaded Lenses

In this case, only a hydrophilic drug was tested. Thus, the next step is to explore the possibility of utilizing the same CAC-p-HEMA gel system to deliver hydrophobic drugs as well. Formation of surfactant aggregates may be extremely useful for hydrophobic drug delivery. However, one can hypothesize that in a simple p-HEMA gel, the hydrophobic drug transports chiefly by diffusion along the polymer chains. Presence of moieties or obstructions like a long chain surfactant stuck on these polymer chains

can create blocks for drug transport thus potentially retarding drug release. An important application of such an experiment would be to explore multi-drug delivery where the drugs have different characteristics in terms of hydrophobicity.

Another area of exploration is delivery of cationic drugs with anionic surfactant loaded lens.

7.3 Drug Delivery by Combination Lenses

It is possible that the hydrophobic drug release behavior may not be easily controlled by ionic surfactant loaded lenses. However, there are other barrier based techniques like addition of Vitamin E [50,51], addition of nanoparticles [41], addition of non-ionic surfactant (Brij) aggregates [37,38] etc. It may be possible to combine the effect of these nanobarriers with that of ionic surfactants to create lenses capable of sustaining drug release for very long periods of time (1-3 months).

7.4 Polymerizable Surfactants in Silicone Lenses

Since silicone lenses are more popular due to their high oxygen transport, it is logical to try and add pzsurfs to them. Silicone lenses have usually 3-5 different monomers and addition of pzsurfs would require a careful understanding of reaction kinetics of the various monomers.

7.5 Macroporous P-HEMA Hydrogels

Macroporous biocompatible gels like those made from HEMA find several applications such as substrates for enzymes, cellular and tissue engineering [124-126]. They also find application in large molecule delivery for e.g. delivery of proteins [127]. It is not possible to create these macroporous gels simply by adding more diluent (i.e.water). A water content beyond a critical value in the polymerization mixture leads to either creation of mechanically weak gels or leads to phase separation and the final

product is a thick p-HEMA layer. Other methods to create these gels is by addition of particulate porogens [128] or by addition of inert diluents [129]. Here, either sufficient quantity of porogen material is required and the inert diluents are organic in nature and their extraction can be problematic. However, by addition of surfactants (non-polymerizable and polymerizable), it may be possible to create these macroporous gels without utilizing excess surfactants. The phase separation can be enhanced by addition of NaCl [126].

Preliminary experiments with such a system led to creation of macroprous gels with water contents ranging from 62% to 83%. The methodology was as follows: Monomer mixture containing HEMA, salt solution, surfactant, thermal initiator azobisisobutyronitrile (AIBN) and small quantities of ethanol (for complete dissolution of components which checked by making sure that the solution was clear) was mixed thoroughly. The solution was placed in a vial with constant stirring and placed in a heated water bath at a specified temperature. The solution was removed a few minutes after the formation of the gel. Unreacted components were extracted in boiling the gel in water. Two types of surfactant were used namely the polymerizable surfactants (Noigen RN-30 and Hitnol BC-30) and Pluronic® F-127 which is a biocompatible surfactant frequently used in cosmetic applications.

For a fixed water volume (4 ml), there are several variables on which the properties of the gel depend including amount of HEMA, type of surfactant, amount of surfactant, amount of initiator, amount of ethanol, temperature of water bath, salt concentration and speed of rotation. There is also the possibility of addition of EGDMA

for added mechanical strength. Detailed experimentation is required to understand the effect of different variables or properties such as water content.

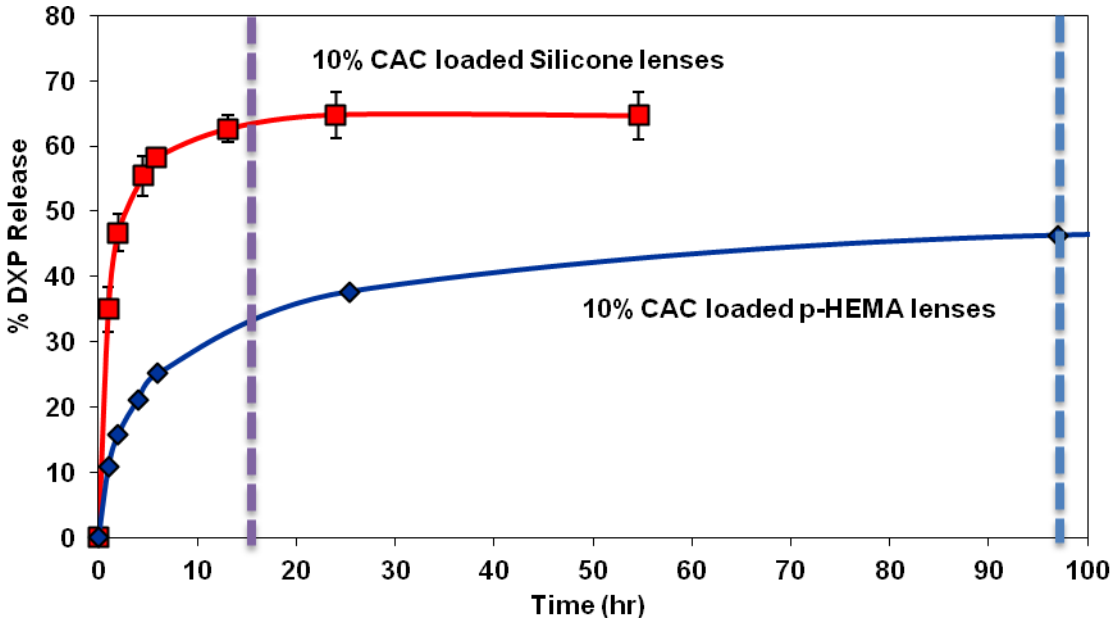

Figure 7-1. Comaprision of DXP release from CAC loaded commercial p-HEMA and silicone lenses

LIST OF REFERENCES

1. Peppas NA. Hydrogels and drug delivery. Curr Opin Colloid In 1997;2:531-37.

2. Kopecek J. Hydrogel biomaterials: a smart future? Biomaterials 2007;28:5185-92.

3. Bourlais CL, Acar L, Zia H, Sado PA, Needham T, Leverge R. Ophthalmic Drug Delivery Systems - Recent Advances. Prog Retin Eye Res 1998;17:33-58.

4. Gaudana R, Ananthula HK, Parenky A, Mitra AK. Ocular Drug Delivery. The AAPS journal 2010;12:348-60.

5. Larke JR. Tears. The Eye in Contact Lens Wear. 2nd ed. : Butterworth Heinemann, 1997. p. 30.

6. Watsky MA, Jablonski MM, Edelhauser HF. Comparison of conjunctival and corneal surface areas in rabbit and human. Curr Eye Res 1988;7:483-86.

7. Prausnitz MR, Noonan JS. Permeability of cornea, sclera, and conjunctiva: A literature analysis for drug delivery to the eye. J Pharm Sci 1998;87:1479-88.

8. Gray C. Systemic toxicity with topical ophthalmic medications in children. Paediatr Perinat Drug Ther 2006;7:23-9.

9. Salminen L. Review: systemic absorption of topically applied ocular drugs in humans. J Ocul Pharmacol 1990;6:243-9.

10. Anti-inflammatory agents. In: Bartlett JD, editor. Ophthalmic Drug Facts: Wolters Kluwer Health, Inc, 2005. p. 93.

11. Gahl WA, Kuehl EM, Iwata F, Lindblad A, Kaiser-Kupfer MI. Corneal crystals in nephropathic cystinosis: natural history and treatment with cysteamine eyedrops. Mol Genet Metab 2000;71:100-20.

12. Chrai SS, Makoid MC, Eriksen SP, Robinson JR. Drop size and initial dosing frequency problems of topically applied ophthalmic drugs. J Pharm Sci 1974;63:333-8.

13. Fechtner RD, Realini T. Fixed combinations of topical glaucoma medications. Curr Opin Ophthalmol 2004;15:132-5.

14. Bourlais CL, Acar L, Zia H, Sado PA, Needham T, Leverge R. Ophthalmic drug delivery systems--recent advances. Prog Retin Eye Res 1998;17:33-58.

15. Ghate D, Edelhauser HF. Ocular drug delivery. Expert Opin Drug Deliv 2006;3:275-87.

16. Kuno N, Fujii S. Recent Advances in Ocular Drug Delivery Systems. Polymers 2011;3:193-221.

17. Al-Kinani AA, Calabrese G, Vangala A, Naughton D, Alany RG. Nanotechnology in ophthalmic drug delivery. In: Souto EB, editor. Patenting Nanomedicines: Legal Aspects, Intellectual Property and Grant Opportunities: Springer-Verlag Berlin Heidelberg, 2012. p. 277-303.

18. Eljarrat-Binstock E, Domb AJ. Iontophoresis: a non-invasive ocular drug delivery. J Controlled Release 2006;110:479-89.

19. Jiang J, Gill HS, Ghate D, McCarey BE, Patel SR, Edelhauser HF, Prausnitz MR. Coated Microneedles for Drug Delivery to the Eye. Invest Ophthalmol Vis Sci 2007;48:4038-43.

20. Wichterle O, LÍM D. Hydrophilic Gels for Biological Use. Nature 1960;185:117-8.

21. Sedlacek J. Possibility of the application of ophthalmic drugs with the use of gel contact lenses. Cesk Oftalmol 1965;21:509-12.

22. Waltman SR, Kaufman HE. Use of hydrophilic contact lenses to increase ocular penetration of topical drugs. Invest Ophthalmol 1970;9:250-5.

23. Hillman JS. Management of acute glaucoma with Pilocarpine-soaked hydrophilic lens. Br J Ophthalmol 1974;58:674-9.

24. Jain MR, Batra V. Steroid pentetration in human aqueous with 'Sauflon 70' lenses. Indian J Ophthalmol 1979;27:26-31.

25. Jain MR. Drug delivery through soft contact lenses. Br J Ophthalmol 1988;72:150-4.

26. Hehl EM, Beck R, Luthard K, Guthoff R, Drewelow B. Improved penetration of aminoglycosides and fluorozuinolones into the aqueous humour of patients by means of Acuvue contact lenses. Eur J Clin Pharmacol 1999;55:317-23.

27. Tian X, Iwatsu M, Kanai A. Disposable 1-day Acuvue contact lenses for the delivery of lomefloxacin to rabbits' eyes. CLAO J 2001;27:212-5.

28. Sieg JW, Robinson JR. Mechanistic studies on transcorneal permeation of pilocarpine. J Pharm Sci 1976;65:1816-22.

29. Maurice DM. Structure and Fluids Invovled in the Penetration of Topically Applied Drugs. Int Ophthalmol Clin 1980;20:7-20.

30. Mindel JS, Smith H, Jacobs M, Kharlamb AB, Friedman AH. Drug reservoirs in topical therapy. Invest Ophthalmol Vis Sci 1984;25:346-50.

31. Karlgard CC, Jones LW, Moresoli C. Ciprofloxacin interaction with silicon-based and conventional hydrogel contact lenses. Eye Contact Lens 2003;29:83-9.

32. Karlgard CC, Wong NS, Jones LW, Moresoli C. In vitro uptake and release studies of ocular pharmaceutical agents by silicon-containing and p-HEMA hydrogel contact lens materials. Int J Pharm 2003;257:141-51.

33. Hui A, Boone A, Jones L. Uptake and Release of Ciprofloxacin-HCl From Conventional and Silicone Hydrogel Contact Lens Materials. Eye Contact Lens 2008;34:266-71.

34. Schultz CL, Poling TR, Mint JO. A medical device/drug delivery system for treatment of glaucoma. Clin Experiment Ophthalmo 2009;92:343-8.

35. Soluri A, Hui A, Jones L. Delivery of Ketotifen Fumarate by Commercial Contact Lens Materials. Optom Vis Sci 2012;89:1140-9.

36. Boone A, Hui A, Jones L. Uptake and Release of Dexamethasone Phosphate From Silicone Hydrogel and Group I, II, and IV Hydrogel Contact Lenses. Eye Contact Lens 2009;35:260-7.

37. Kapoor Y, Chauhan A. Drug and surfactant transport in Cyclosporine A and Brij 98 laden p-HEMA hydrogels. J Colloid Interface Sci 2008;322:624-33.

38. Kapoor Y, Thomas JC, Tan G, John VT, Chauhan A. Surfactant-laden soft contact lenses for extended delivery of ophthalmic drugs. Biomaterials 2009;30:867-78.

39. Gulsen D, Chauhan A. Ophthalmic drug delivery through contact lenses. Invest Ophthalmol Vis Sci 2004;45:2342-7.

40. Li C, Abrahamson M, Kapoor Y, Chauhan A. Timolol transport from microemulsions trapped in HEMA gels. J Colloid Interface Sci 2007;315:297-306.

41. Jung HJ, Chauhan A. Temperature sensitive contact lenses for triggered ophthalmic drug delivery. Biomaterials 2012;33:2289-2300.

42. Alvarez-Lorenzo C, Concheiro A. Molecularly imprinted polymers for drug delivery. J Chromatogr B 2004;804:231-45.

43. Alvarez-Lorenzo C, Yañez F, Barreiro-Iglesias R, Concheiro A. Imprinted soft contact lenses as norfloxacin delivery systems. J Controlled Release 2006;113:236-44.

44. Byrne ME, Park K, Peppas NA. Molecular imprinting within hydrogels. Adv Drug Deliv Rev 2002;54:149-61.

45. Byrne ME, Salian V. Molecular imprinting within hydrogels II: progress and analysis of the field. Int J Pharm 2008;364:188-212.

46. Ribeiro A, Veiga F, Santos D, Torres-Labandeira JJ, Concheiro A, Alvarez-Lorenzo C. Bioinspired imprinted PHEMA-hydrogels for ocular delivery of carbonic anhydrase inhibitor drugs. Biomacromolecules 2011;12:701-9.

47. Tieppo A, White C, Paine A, Voyles M, McBride M, Byrne M. Sustained in vivo release from imprinted therapeutic contact lenses. J Controlled Release 2012;157:391-7.

48. Kim J, Conway A, Chauhan A. Extended delivery of ophthalmic drugs by silicone hydrogel contact lenses. Biomaterials 2008;29:2259-69.

49. Peng C, Kim J, Chauhan A. Extended delivery of hydrophilic drugs from silicone-hydrogel contact lenses containing Vitamin E diffusion barriers. Biomaterials 2010;31:4032-47.

50. Peng C, Burke MT, Chauhan A. Transport of topical anesthetics in vitamin E loaded silicone hydrogel contact lenses. Langmuir 2011;28:1478-87.

51. Peng C, Burke MT, Carbia BE, Plummer C, Chauhan A. Extended drug delivery by contact lenses for glaucoma therapy. J Controlled Release 2012;162:152-8

52. Peng C, Ben-Shlomo A, Mackay EO, Plummer CE, Chauhan A. Drug delivery by contact lens in spontaneously glaucomatous dogs. Curr Eye Res 2012;37:204-11.

53. Safety Study of a contact lens wtih Ketotifen in Healthy, Normal Volunteers by Vistakon Pharmaceuticals at ClinicalTrials.gov. 2011;2013.

54. Alvarez-Lorenzo C, Concheiro A. Effects of surfactants on gel behavior. Am J Drug Deliv 2003;1:77-101.

55. Haglund BO, Sundelöf L, Upadrashta SM, Wurster DE. Effect of SDS Micelles on Rhodamine-B Diffusion in Hydrogels. J Chem Educ 1996;73:889.

56. Barreiro-Iglesias R. Incorporation of small quantities of surfactants as a way to improve the rheological and diffusional behavior of carbopol gels. J Controlled Release 2001;77:59-75.

57. Nichifor M, Zhu XX, Cristea D, Carpov A. Interaction of Hydrophobically Modified Cationic Dextran Hydrogels with Biological Surfactants. The Journal of Physical Chemistry B 2001;105:2314-21.

58. Paulsson M, Edsman K. Controlled drug release from gels using surfactant aggregates: I. Effect of lipophilic interactions for a series of uncharged substances. J Pharm Sci 2001;90:1216-25.

59. Liu J, Li L. SDS-aided immobilization and controlled release of camptothecin from agarose hydrogel Eur J Pharm Sci 2005;25:237-44.

60. Philippova OE, Hourdet D, Audebert R, Khokhlov AR. Interaction of Hydrophobically Modified Poly(acrylic acid) Hydrogels with Ionic Surfactants. Macromolecules 1996;29:2822-30.

61. Hayakawa M, Onda T, Tanaka T, Tsujii K. Hydrogels Containing Immobilized Bilayer Membranes. Langmuir 1997;13:3595-7.

62. Cowie PR, Smith MJ, Hannah F, Cowling MJ, Hodgkeiss T. The prevention of microfouling and macrofouling on hydrogels impregnated with either Arquad 2C-75® or benzalkonium chloride. Biofouling 2006;22:195-207.

63. Smith M. The Effects of Cationic Surfactants on Marine Biofilm Growth on Hydrogels. Estuar Coast Shelf Sci 2002;55:361-7.

64. Kapoor Y, Chauhan A. Drug and surfactant transport in Cyclosporine A and Brij 98 laden p-HEMA hydrogels. J Colloid Interface Sci 2008;322:624-33.

65. Kapoor Y, Thomas JC, Tan G, Jophn VT, Chauhan A. Surfactant-laden soft contact lenses for extended delivery of ophthalmic drugs. Biomaterials 2009;30:867-78.

66. Sato T, Uchida R, Tanigawa H, Uno K, Murakami A. Application of polymer gels containing side-chain phosphate groups to drug-delivery contact lenses. J Appl Polym Sci 2005;98:731-5.

67. Kakisu K, Matsunaga T, Kobayakawa S, Sato T, Tochikubo T. Development and efficacy of a drug-releasing soft contact lens. Invest Ophthalmol Vis Sci 2013;54:2551-61.

68. Yamazaki Y, Matsunaga T, Syohji K, Arakawa T, Sato T. Effect of anionic/siloxy groups on the release of ofloxacin from soft contact lenses. J Appl Polym Sci 2013;127:5022-7.

69. Xu J, Li X, Sun F. Preparation and Evaluation of a Contact Lens Vehicle for Puerarin Delivery. J Biomat Sci-Polym E 2010;21:271-88.

70. Clark AF, Yorio T. Ophthalmic drug discovery Nat Rev Drug Discov 2003;2:448-59.

71. Kim J, Chauhan A. Dexamethasone transport and ocular delivery from poly(hydroxyethyl methacrylate) gels. Int J Pharm 2007;352:205-22.

72. Fonn D. Targeting contact lens induced dryness and discomfort: what properties will make lenses more comfortable Optom Vis Sci 2007;84:279-85.

73. Weed K, Fonn D, Potvin R. Discontinuation of contact lens wear. Optom Vis Sci 1993;70:140.

74. Pritchard N, Fonn D, Brazeau D. Discontinuation of contact lens wear: a survey Int Contact Lens Clin 1999;26:157-62.

75. Thai LC, Tomlinson A, Simmons PA. In vitro and in vivo effects of a lubricant in a contact lens solution Ophthalmic and Physiological Optics 2002;22:319-29.

76. Guillon M, Guillon J. Hydrogel lens wettability during overnight wear Ophthal Physl Opt 1989;9:355-9.

77. Efron N, Brennan NA. A survey of wearers of low water content hydrogel contact lenses Clin Exp Optom 1988;71:86-90.

78. French K. Contact lens material properties. Part 1 - Wettability. Contact lens Monthly, Optician 2005;230:20-8.

79. Holly FJ. Tear film physiology and contact lens wear. II. Contact lens-tear film interaction Am J Optom Physiol Opt 1981;58:331-41.

80. Young G, Bowers R, Hall B, Port M. Six month clinical evaluation of a biomimetic hydrogel contact lens CLAO J 1997;23:226-36.

81. Young G, Bowers R, Hall B, Port M. Clinical comparison of Omafilcon A with four control materials CLAO J 1997;23:249-58.

82. Hall B, Jones S, Young G, Coleman S. The on-eye dehydration of proclear compatibles lenses CLAO J 1999;25:233-7.

83. Menzies KL, Jones L. The impact of contact angle on the biocompatibility of biomaterials Optom Vis Sci 2010;87:387-99.

84. Nick J, Winterton L, Lally J. Enhancing comfort with a lubricating daily disposable. Contact lens Monthly, Optician 2005;229:30-2.

85. Peterson RC, Wolffsohn JS, Nick J, Winterton L, Lally J. Clinical performance of daily disposable soft contact lenses using sustained release technology Cont Lens Anterior Eye 2006;29:127-34.

86. Osborn K, Veys J. A new silicone hydrogel lens for contact lens-related dryness: Material Properties. Contact lens Monthly, Optician 2005;229:39-41.

87. Subbaraman LN, Bayer S, Glasier MA, Lorentz H, Senchyna M, Jones L. Rewetting drops containing surface active agents improve the clinical performance of silicone hydrogel contact lenses Optom Vis Sci 2006;83:143-51.

88. Tonge S, Jones L, Goodall S, Tighe B. The ex vivo wettability of soft contact lenses Curr Eye Res 2001;23:51-9.

89. Doughty MJ. Re-wetting, comfort, lubricant and moisturising solutions for the contact lens wearer Cont Lens Anterior Eye 1999;22:116-26.

90. Choy CK, Cho P, Boost MV. Cytotoxicity and effects on metabolism of contact lens care solutions on human corneal epithelium cells Clin Exp Optom 2012;95:198-206.

91. Kenneth LA. Evaluation of Corneal Staining and Patient Preference With Use of Three Multi-Purpose Solutions and Two Brands of Soft Contact Lenses. Eye Contact Lens 2003;29:213-20.

92. Andrasko G, Ryen K. Corneal staining and comfort observed with traditional and silicone hydrogel lenses and multipurpose solution combinations Optometry 2008;79:444-54.

93. Lievens CW, Hakim NO, Chinn AO. The effect of multipurpose solutions on ocular surface. Eye Contact Lens 2006;32:8-11.

94. Torstensson M, Ranby B, Hult A. Monomeric surfactants for surface modification of polymers Macromolecules 1990;23:126-32.

95. Torstensson M, Hult A. Surface modification of polymers using surfactant monomers Polymer Bulletin 1992;29:549-56.

96. Holmberg K. Polymerizable surfactants Progress in Organic Coatings 1992;20:325-37.

97. Lakshman NS, Glasier MA, Senchyna M, Sheardown H, Jones L. Kinetics of in vitro lysozyme deposition on silicone hydrogel, PMMA, and FDA groups I, II, and IV contact lens materials. Curr Eye Res 2006;31:787-96.

98. Zhang S, Borazjani RN, Salamone JC, Ahearn DG, Crow SA,Jr, Pierce GE. In vitro deposition of lysozyme on etafilcon A and balafilcon A hydrogel contact lenses: effects on adhesion and survival of Pseudomonas aeruginosa and Staphylococcus aureus Cont Lens Anterior Eye 2005;28:113-9.

99. Sassi AP, Lee SH, Park YH, Blanch HW, Prausnitz JM. Sorption of lysozyme by HEMA copolymer hydrogels. J Appl Poly Sci 1996;60:225-34.

100. Senchyna M, Jones L, Louie D, May C, Forbes I, Glasier MA. Quantitave and conformational characterization of lysozyme deposited on balafilcon and etafilcon contact lens material. Curr Eye Res 2004;28:25-36.

101. Lord MS, Stenzel MH, Simmons A, Milthorpe BK. Lysozyme interaction with poly(HEMA)-based hydrogel Biomaterials 2006;27:1341-5.

102. Garrett Q, Garrett RW, Milthorpe BK. Lysozyme sorption in hydrogel contact lenses Invest Ophthalmol Vis Sci 1999;40:897-903.

103. Okada E, Matsuda T, Yokoyama T, Okuda K. Lysozyme penetration in group IV soft contact lenses Eye Contact Lens 2006;32:174-7.

104. Kastl PR, editor. Contact lenses, the CLAO guide to basic science and clinical practice. : Kendall/Hunt Publishing Company, 1995.

105. Subbaraman LN, Glasier MA, Senchyna M, Sheardown H, Jones L. Kinetics of in vitro lysozyme deposition on silicone hydrogel, PMMA, and FDA groups I, II, and IV contact lens materials Curr Eye Res 2006;31:787-96.

106. Jones L, Senchyna M, Glasier MA, Schickler J, Forbes I, Louie D, May C. Lysozyme and lipid deposition on silicone hydrogel contact lens materials Eye Contact Lens 2003;29:S75-9.

107. Wu J, Sassi AP, Blanch HW, Prausnitz JM. Partitioning of proteins between an aqueous solution and a weakly-ionizable polyelectrolyte hydrogel. Polymer 1996;37:4803-8.

108. White JA, Deen WM. Effects of Solute Concentration on Equilibrium Partitioning of Flexible Macromolecules in Fibrous Membranes and Gels Macromolecules 2001;34:8278-85.

109. Lazzara MJ, Deen WM. Effects of concentration on the partitioning of macromolecule mixtures in agarose gels J Colloid Interface Sci 2004;272:288-97.

110. Kosto KB, Deen WM. Diffusivities of macromolecules in composite hydrogels AIChE J 2004;50:2648-58.

111. Peppas NA, Reinhart CT. Solute diffusion in swollen membranes. Part I. A new theory J Membr Sci 1983;15:275-87.

112. Reinhart CT, Peppas NA. Solute diffusion in swollen membranes. Part II. Influence of crosslinking on diffusive properties J Membr Sci 1984;18:227-39.

113. Moynihan HJ, Honey MS, Peppas NA. Solute diffusion in swollen membranes. Part V: Solute diffusion in poly(2-hydroxyethyl methacrylate) Polym Eng Sci 1986;26:1180-5.

114. Amsden B. Solute Diffusion within Hydrogels. Mechanisms and Models Macromolecules 1998;31:8382-95.

115. Brazel CS, Peppas NA. Mechanisms of solute and drug transport in relaxing, swellable, hydrophilic glassy polymers Polymer 1999;40:3383-98.

116. am Ende MT, Peppas NA. Transport of ionizable drugs and proteins in crosslinked poly(acrylic acid) and poly(acrylic acid-co-2-hydroxyethyl methacrylate) hydrogels. II. Diffusion and release studies J Controlled Release 1997;48:47-56.

117. Cheng L, Muller SJ, Radke CJ. Wettability of silicone-hydrogel contact lenses in the presence of tear-film components Curr Eye Res 2004;28:93-108.

118. Lorentz H, Rogers R, Jones L. The impact of lipid on contact angle wettability Optom Vis Sci 2007;84:946-53.

119. Guan L, Gonzalez Jimenez ME, Walowski C, Boushehri A, Prausnitz JM, Radke CJ. Permeability and partition coefficient of aqueous sodium chloride in soft contact lenses J Appl Polym Sci 2011;121:1457-71.

120. Peppas NA, Moynihan HJ, Lucht LM. The structure of highly crosslinked poly(2-hydroxyethyl methacrylate) hydrogels J Biomed Mater Res 1985;19:397-411.

121. Parmar AS, Muschol M. Hydration and hydrodynamic interactions of lysozyme: effects of chaotropic versus kosmotropic ions Biophys J 2009;97:590-8.

122. Stringer JL, Peppas NA. Diffusion of small molecular weight drugs in radiation-crosslinked poly(ethylene oxide) hydrogels. J Controlled Release 1996;42:195-202.

123. Nichols J. Contact Lenses 2011. Contact Lens Spectrum 2012;27:20-5.

124. Haldon RA, Lee BE. Structure and permeability of porous films of poly(hydroxy ethyl methacrylate) Brit Polym J 1972;4:491-501.

125. Chirila TV, Constable IJ, Crawford GJ, Vijayasekaran S, Thompson DE, Chen Y, Fletcher WA, Griffin BJ. Poly(2-hydroxyethyl methacrylate) sponges as implant materials: in vivo and in vitro evaluation of cellular invasion Biomaterials 1993;14:26-38.

126. Liu Q, Hedberg EL, Liu Z, Bahulekar R, Meszlenyi RK, Mikos AG. Preparation of macroporous poly(2-hydroxyethyl methacrylate) hydrogels by enhanced phase separation Biomaterials 2000;21:2163-9.

127. Antonsen KP, Bohnert JL, Nabeshima Y, Sheu M, Wu XS, Hoffman AS. Controlled Release of Proteins from 2-Hydroxyethyl Methacrylate Copolymer Gels Artif Cell Blood Sub 1993;21:1-22.

128. Oxley H, Corkhill P, Fitton J, Tighe B. Macroporous hydrogels for biomedical applications: methodology and morphology Biomaterials 1993;14:1064-72.

129. Horák D, Lednický F, Bleha M. Effect of inert components on the porous structure of 2-hydroxyethyl methacrylate-ethylene dimethacrylate copolymers Polymer 1996;37:4243-9.

BIOGRAPHICAL SKETCH

Lokendrakumar Chainroop Bengani was born in Mumbai, Maharashtra, India in 1986. He did his schooling at Smt. Sulochanadevi Singhania School and junior college in Science at SIES, Mumbai. He joined Institute of Chemical Technology (formerly UDCT or MUICT) in 2004 to pursue his undergraduate degree in Chemical Engineering and graduated in 2008. He joined the Dept. of Chemical Engineering at University of Florida in Fall 2008 to purse MS and continued to stay to complete his doctoral research in Dr. Anuj Chauhan's group.